AD_____

Award Number: DAMD17-98-1-8584

TITLE: Regulation of Hormone Responses in Prostate Cancer by BAGIL

PRINCIPAL INVESTIGATOR: John C. Reed, M.D., Ph.D.

CONTRACTING ORGANIZATION: The Burnham Institute
La Jolla, California 92037

REPORT DATE: September 2003

TYPE OF REPORT: Final, Phase II

PREPARED FOR: U.S. Army Medical Research and Materiel Command
Fort Detrick, Maryland 21702-5012

DISTRIBUTION STATEMENT: Approved for Public Release;
Distribution Unlimited

The views, opinions and/or findings contained in this report are those of the author(s) and should not be construed as an official Department of the Army position, policy or decision unless so designated by other documentation.

REPORT DOCUMENTATION PAGE

Form Approved
OMB No. 074-0188

1. AGENCY USE ONLY (Leave blank)	2. REPORT DATE	3. REPORT TYPE AND DATES COVERED
	September 2003	Final, Phase II (1 Sep 1998 - 15 Sep 2003)

4. TITLE AND SUBTITLE
Regulation of Hormone Responses in Prostate Cancer by BAGIL

5. FUNDING NUMBERS
DAMD17-98-1-8584

6. AUTHOR(S)
John C. Reed, M.D., Ph.D.

7. PERFORMING ORGANIZATION NAME(S) AND ADDRESS(ES)
The Burnham Institute
La Jolla, California 92037

E-Mail: jreed@burnham.org

8. PERFORMING ORGANIZATION REPORT NUMBER

9. SPONSORING / MONITORING AGENCY NAME(S) AND ADDRESS(ES)
U.S. Army Medical Research and Materiel Command
Fort Detrick, Maryland 21702-5012

10. SPONSORING / MONITORING AGENCY REPORT NUMBER

11. SUPPLEMENTARY NOTES
Original contains color plates: All DTIC reproductions will be in black and white.

12a. DISTRIBUTION / AVAILABILITY STATEMENT
Approved for Public Release; Distribution Unlimited

12b. DISTRIBUTION CODE

13. ABSTRACT (Maximum 200 Words)

Androgen ablation therapy represents the principal treatment for metastatic prostate cancer. However, nearly all tumors eventually relapse as hormone-refractory disease, indicating a need to better understand how the androgen receptor (AR) functions. In this project, we studied the expression and function of an AR-binding protein discovered in our laboratory, BAG1L. We showed that BAG1L becomes over-expressed in many prostate cancers. We determined that BAG1L potentiates the actions of AR, lowering concentrations of dihydrotestosterone needed to activate AR and rendering the AR resistant to anti-androgen drugs. We mapped the domains in BAG1L required for this activity, and generated transgenic mice over-expressing BAG1L in the prostate for future use in studying effects of BAG1L on AR in vivo. Finally, we performed work showing that BAG1L also interacts with the Vitamin D Receptor (VDR) and potentiates the growth suppressive and pro-apoptotic effects of VDR-ligands in prostate cancer cell lines in culture. Taken together, these observations suggest that prostate cancers containing high levels of BAG1L are less likely to respond favorably to anti-androgen therapy (due to their decreased sensitivity to anti-androgens), but if these tumors express VDR, then they may be excellent candidates for Vitamin-D-based therapies (due to their increased sensitivity to Vitamin D and synthetic Vitamin D analogs).

14. SUBJECT TERMS
Androgen Receptor; Vitamin D Receptor; Chaperone; Heat Shock; BAG-1

15. NUMBER OF PAGES
46

16. PRICE CODE

17. SECURITY CLASSIFICATION OF REPORT	18. SECURITY CLASSIFICATION OF THIS PAGE	19. SECURITY CLASSIFICATION OF ABSTRACT	20. LIMITATION OF ABSTRACT
Unclassified	Unclassified	Unclassified	Unlimited

FOREWORD

Opinions, interpretations, conclusions and recommendations are those of the author and are not necessarily endorsed by the U.S. Army.

_N/A_ Where copyrighted material is quoted, permission has been obtained to use such material.

_N/A_ Where material from documents designated for limited distribution is quoted, permission has been obtained to use the material.

_N/A_ Citations of commercial organizations and trade names in this report do not constitute an official Department of Army endorsement or approval of the products or services of these organizations.

_√_ In conducting research using animals, the investigator(s) adhered to the "Guide for the Care and Use of Laboratory Animals," prepared by the Committee on Care and use of Laboratory Animals of the Institute of Laboratory Resources, national Research Council (NIH Publication No. 86-23, Revised 1985).

_√_ For the protection of human subjects, the investigator(s) adhered to policies of applicable Federal Law 45 CFR 46.

_√_ In conducting research utilizing recombinant DNA technology, the investigator(s) adhered to current guidelines promulgated by the National Institutes of Health.

_√_ In the conduct of research utilizing recombinant DNA, the investigator(s) adhered to the NIH Guidelines for Research Involving Recombinant DNA Molecules.

_N/A_ In the conduct of research involving hazardous organisms, the investigator(s) adhered to the CDC-NIH Guide for Biosafety in Microbiological and Biomedical Laboratories.

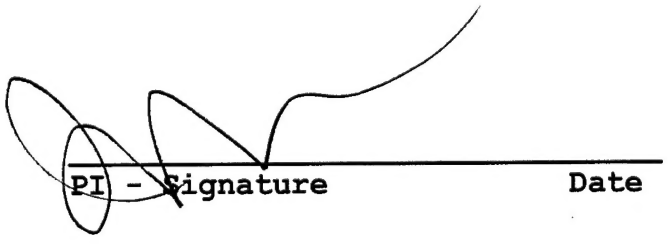

PI - Signature Date

Table of Contents

INTRODUCTION

Prostate cancer is an androgen-driven disease. In the absence of testosterone or related androgens which can serve as ligands for the androgen receptor, the secretory epithelial cells of the prostate undergo rapid programmed cell death (1). Current treatment for metastatic adenocarcinoma of the prostate is predicated on the cell death inducing effects of anti-androgens and hormone ablative measures which reduce endogenous production of androgens. However, nearly all hormone-dependent prostate cancers eventually relapse as fatal hormone-independent disease (2).

Multiple, still largely unidentified mechanisms may account for the complete independence or reduced dependence of prostate cancers on androgens (reviewed in (3-5). AR gene deletion and sequestration of AR in the cytoplasm have been described in some hormone-independent tumors, implying that genetic alterations associated with tumor progression can abrogate the necessity for AR in some cases. However, many tumors may rely on other strategies which allow cancer cells to grow in low concentrations of androgens, including AR gene amplification or over-expression (6, 7) and AR mutations which permit trans-activation of target genes with little or no requirement for steroid hormones (1, 2). Since most hormone-insensitive prostate cancers still retain a wild-type AR, presumably alterations in the factors that control the levels of AR and its function play a major role in resistance to anti-androgen and hormone ablative therapies. Thus, a need exists to understand more about the molecular mechanisms that govern the activity of ARs.

Upon binding steroid ligands, the AR undergoes a conformational change, translocates to the nucleus and binds to specific DNA sequences located near or in promoter regions of target genes. After binding DNA, the receptor interacts with components of the basal transcription machinery and sometimes sequence-specific transcription factors, resulting in positive or negative effects on gene transcription (3, 4). A number of proteins have been identified which associate with hormone-receptor complexes, including several heat shock family proteins and various types of transcription co-activators (reviewed in (5, 6)). However, many details remain unclear as to the molecular mechanisms by which these proteins modulate the activities of steroid hormone receptors and even less is known about whether alterations in their expression or function might contribute to the deregulation of steroid hormone responses in prostate cancer.

In this proposal, we describe experiments designed to explore the biological significance and molecular mechanisms by which AR is regulated by BAG-1 family proteins. BAG-1 is a novel Hsp70-family binding protein cloned in our laboratory. We have discovered that an isoform of this protein, BAG-1L, forms complexes with AR and potentiates the activity of this steroid hormone receptor, allowing it to transactive target genes with 100-1,000 x lower concentrations of dihydrotestosterone. We have also determined that BAG-1 and

BAG-1L are expressed in most prostate cancers. Our goals have been to define the overall significance of BAG-1 family proteins on AR responses in prostate cancers and to delineate the mechanisms by which these Hsp70-binding proteins control the function of AR and other steroid hormone receptors of relevance to prostate cancer cell growth, differentiation, and survival. These studies may reveal new strategies for improving androgen ablation therapy and attacking hormone-refractory metastatic prostate cancer.

1. BODY

1. Funded Objectives:

The original funded objectives of the cycle I and II projects were to:

1. Determine the expression and location of BAG1 and BAG1L in primary and metastatic prostate cancers.
2. Study consequences of ablation of BAG1 and BAG1L expression in prostate cancer cell lines.
3. Examine in vivo effects of BAG1 and BAG1L on the androgen-dependence of the normal prostate gland.
4. Determine whether BAG1L control the sensitivity of human prostate cancer cell lines to anti-androgens and to vitamin D3 analogues.
5. Examine the structural features of BAG1L that are required for its modulation of steroid hormone receptors.

Objective #1. Determine the expression and location of BAG1 and BAG1L in primary and metastatic prostate cancer.

This aim was accomplished. We generated monoclonal antibodies that recognize the BAG1 and the BAG1L proteins. We determined that BAG1 is cytosolic while BAG1L is nuclear. Using these monoclonal antibodies in conjunction with immunohistochemical methods and archival paraffin-embedded prostate cancer specimens, we evaluated the expression of the nuclear (BAG1L) and cytosolic (BAG1) proteins in over 800 cases of prostate cancer. Comparisons were made with BAG1 immunostaining results in normal prostate and benign prostatic hypertrophy. Tissue microarray technology was exploited for much of this analysis, permitting us to analyze large numbers of tumor specimens.

Compared to normal prostate, cytosolic BAG1 immunostaining was elevated in 746 of 876 (85%) of prostate cancers. Nuclear BAG1 immunostaining (BAG1L) was inappropriately increased in 171 of 676 (25%) of prostate cancers, compared to normal prostate gland epithelium. Clinical follow-up data or other types of laboratory information were available for some of these patients, demonstrating a variety of correlations of BAG1 expression with more aggressive tumor phenotypes. For example, in a cohort of 62 patients with early-stage (T1,T2) disease and low Gleason grade (gr 2-6), higher percentages of BAG1 immunopositive tumor cells were associated with higher PSA levels prior to radiation therapy ($p = 0.05$), and with a higher incidence of distant metastases after therapy ($p = 0.05$). Higher intensity BAG1 immunostaining was also associated with a higher incidence of metastatic relapse after radiation therapy (p

< 0.0001). In addition, immunohistochemical analysis of 722 prostate cancer specimens in a microarray format revealed higher percentages of BAG1 immunopositive cells in tumors (n= 722) compared to normal prostate (n=54), mean + SE: 41 $\pm$ 3% normal versus 78 $\pm$ 1 % cancer ($p< 0.0001$). An association was also identified between higher percentages of BAG1 immunopositive tumor cells and locally advanced disease ($p = 0.05$) (n = 625 patients) and with hormone refractory disease ($p<0.001$) (n = 263 patients). Higher percentages of tumor cells with nuclear BAG1-immunostaining (BAG1L) as well as higher intensity nuclear BAG1 staining were also associated with hormone-refractory disease in microarrays: $p<0.001$ and $p<0.0001$, respectively (n=263). Higher intensity BAG1 nuclear immunostaining was also correlated with hormone-refractory (HR) disease in a cohort of 92 prostate cancer patients with locally-advanced disease who were treated with anti-androgen therapy prior to surgery (50% vs 9% HR; $p<0.001$).

From these observations, two conclusions can be reached. First, tumor-specific increases in BAG1 and BAG1L levels commonly occur in prostate cancers. Second, immunohistochemical analysis of BAG1 (cytosolic) and BAG1L (nuclear) expression may provide prognostic information about prostate cancer patients, including information about progression to hormone-refractory disease.

Objective #2. Study consequences of ablation of BAG1 and BAG1L expression in prostate cancer cell lines.

This aim was partially accomplished. We originally proposed to use both antisense methods and expression of dominant-negative mutants to ablate expression or function of BAG1 and BAG1L in prostate cancers.

With respect to antisense experiments, we attempted to ablate expression of BAG1 and BAG1L using antisense methods, including expression plasmids encoding antisense transcripts and synthetic oligonucleotides. However, this proved to be extremely difficult, due to the long half-life of the BAG1 and BAG1L proteins. For example, even if BAG1 mRNA was effectively degraded by synthetic antisense oligonucleotides possessing RNaseH activity, the BAG1 protein survived for at least a day, thus making it difficult to sustain reduction in mRNA long enough to effect a decline in protein.

With respect to dominant-negative mutants, we expressed mutants of BAG1 or BAG1L which lack the C-terminal domain required for Hsc70-binding, so-called ΔC mutants. Our efforts focused on assessing the impact of these trans-dominant inhibitory mutants of BAG1 and BAG1L on function of the Androgen Receptor (AR) and Vitamin D Receptors (VDR) in prostate cancer cell lines. These studies revealed that BAG1L(ΔC) suppresses the functions of the AR and VDR, preventing it from transactivating reporter genes in transient transfection reporter gene assays. These results were published (8-10). (*SEE APPENDIX*).

Thus, we conclude that BAG1L is required for optimal activity of AR and VDR in prostate cancer cell lines.

Objective #3. Examine in vivo effects of BAG1 and BAG1L on the androgen-dependence of the normal prostate gland.

This aim was partially accomplished. We generated transgenic mice expressing BAG1 or BAG1L under the control of a probasin promoter to achieve elevated levels of expression of these proteins in the prostate gland, thus setting the stage for in vivo studies. Expression constructs were prepared and tested by transient transfection in prostate cancer cell lines in vitro before progressing to transgenic mouse production.

The expression constructs were prepared by excising HindIII-SpeI fragments from pcI-NEO-BAG1 and pcI-NEO-BAG1L, thus obtaining human BAG1 and BAG1L cDNAs fused at the 5' end with the 5'untranslated region and an intron from the b-globin gene and at the 3' end with a polyadenylation signal sequence from the SV40 small t antigen gene. These fragments were subcloned into the HindIII and SpeI sites of pBluescript SKII+. The resulting plasmid was digested with HindIII, treated with Calf Alkaline Phosphatase (CIP), and a HindIII fragment containing the rat probasin promoter was inserted, to produce the final constructions (Figure 1).

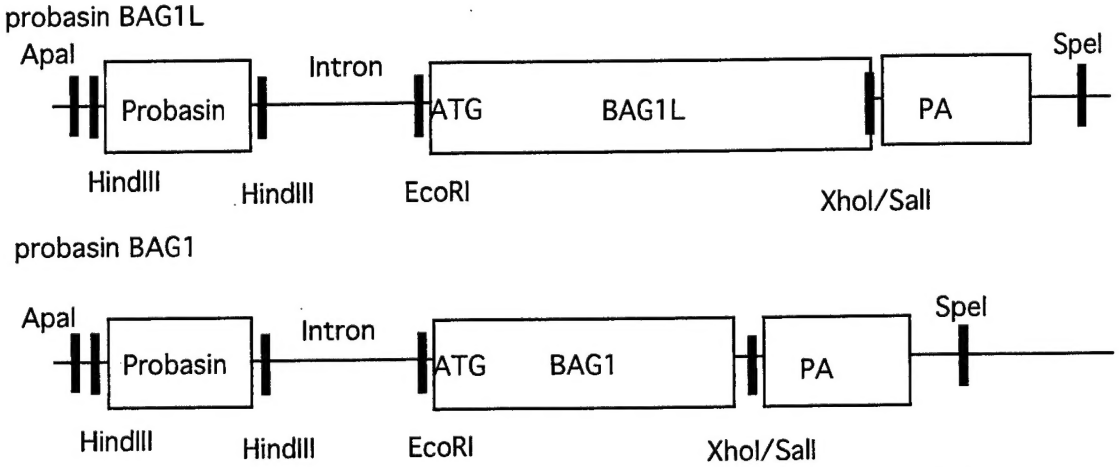

To produce transgenic mice, the probasin-BAG1 and probasin-BAG1L cassettes were excised from the plasmid by digestion with ApaI and SpeI, gel-purified, and microinjected into mouse oocytes, which were then transferred into the oviducts of pseudopregnant female recipient mice. From multiple injections, we obtained four founder lines containing the BAG1L and two founder lines containing the BAG1 constructs, as determined by PCR analysis of tail DNA. For PCRs, DNA was amplified using a forward (5'-AAGCACGACCTTCATGTTACC-3') and a reverse (5'-CCGGCAACCATCTTGTATTCC-3') and 30 cycles of 94°C X 1 minute, 55°C x 1 minute, and 72oC X 2 minutes.

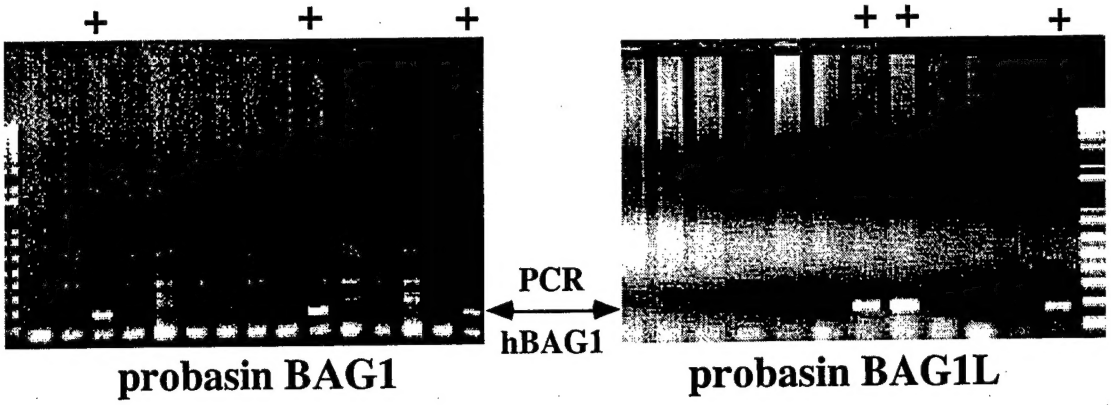

To examine expression of the transgene in the prostate glands of male mice, we sacrificed mice at > 2 months age, dissected out the prostate gland and prepared a tissue homogenate using RIPA buffer. The resulting extracts were normalized for total protein content (20 ug per sample) and analyzed by SDS-PAGE/immunoblotting using our anti-BAG1 monoclonal antibody, KS6C8. Western blotting revealed an endogenous band corresponding to mouse BAG1, which varied widely in levels among male mice. As a control, in vitro translated human BAG1, BAG1M, and BAG1L were run in the same gel, as mobility markers for assessing transgene expression. Elevated levels of BAG1L were found in progeny of two of the four founder lines. Progeny from the two BAG1 founders did not contain elevated levels of BAG1 protein, suggesting that the insertion site of the DNA constructs may have been unfavorable for achieving high levels of prostate expression. Reprobing the blot with an antibody recognizing b-actin confirmed loading of approximately equivalent amounts of protein lysates from each sample.

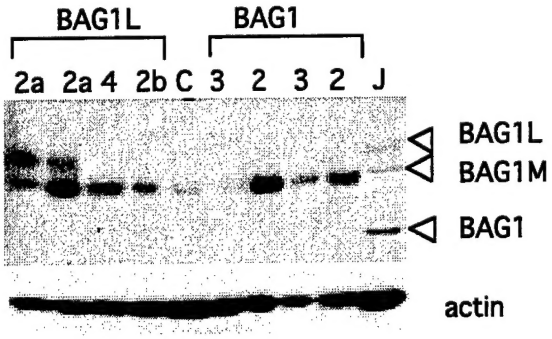

Using the BAG1L over-expressing mice, we are now poised to perform the proposed in vivo experiments. However, it has taken twice as long as anticipated because our original colony of transgenic mice was swiped out by a mouse poxvirus infestation that plagued our institute's vivarium.

Objective #4. Determine whether BAG1L controls the sensitivity of human prostate cancer cell lines to anti-androgens and to vitamin D3 analogues.

We accomplished this aim with respect to vitamin D3 analogues. After achieving stable expression of BAG1L in VDR-expressing prostate cancer cell lines, we then tested the effects on prostate cancer cell proliferation and apoptosis of exposure in culture to 1,25 (OH)2 –Vitamin D3 (VD3) and two synthetic analogs of VD3 that have reduce hypercalcemic effects. We found that elevated levels of BAG1L increased the sensitivity of VDR-expressing prostate cancer cells to the growth inhibitory and proapoptotic effects of VD3 and VD3 analogs. Further, we dissected the apoptotic mechanism, and demonstrated that VD3 triggers a mitochondrial pathway for apoptosis, involving release of cytochrome c from mitochondria, activation of caspases-9 and –3, and cleavage of downstream caspase substrates such as PARP. These events were associated with a decline in levels of three anti-apoptotic Bcl-2 family proteins, Bcl-2, Bcl-XL, and Mcl-1, without reductions in pro-apoptotic proteins Bax and Bak. In contrast to VDR-expressing prostate cancer cell lines, none of these growth inhibitory or pro-apoptotic effects were seen in VDR-negative prostate cancer cells. These findings were published (11) (*SEE APPENDIX*).

Objective #5. Examine the structural features of BAG1L that are required for its modulation of steroid hormone receptors.

This aim was accomplished. We performed a structure-function analysis of the BAG1L protein, mapping the domains necessary for its stimulatory effects on AR. These studies demonstrated that the N-terminal first 50 amino-acids of BAG1L are critical for nuclear targeting of this protein and for its functional collaboration with AR. Fusing an exogenous nuclear targeting sequence onto the shorter BAG1 protein, which lacks this N-terminal unique domain, failed to reconstitute AR-stimulatory activity, though it did result in nuclear targeting of the shorter BAG1 protein. Thus, the N-terminal unique domain of BAG1L appears to be required both for AR co-stimulatory activity and for nuclear targeting. The C-terminal Hsc70-binding domain of BAG1L was also determined to be essential for enhancing AR function. Thus, BAG1L must retain its ability to bind Hsp70 to function as an enhancer of AR function. These results were published (10) (*SEE APPENDIX*). In addition, we collaborated with Dr. K Ely to solve the 3 dimensional structure of the Hsp70-binding domain of BAG1 (12).

2. Key Research Accomplishments

Discovered that approximately one-third of human prostate cancers over-produce the BAG1L protein.

Demonstrated that BAG1L but not BAG1 binds and collaborates with the Androgen Receptor (AR) to induce AR-responsive genes.

Mapped the relevant region of BAG1L to the N-terminal 50 amino-acids, which is uniquely found in BAG1L and not present in BAG1.

Demonstrated that the AR cannot be completely suppressed by anti-androgen drugs if BAG1L levels are high.

Demonstrated that BAG1L collaborates with the Vitamin D Receptor (VDR) to induce VDR-responsive genes.

Showed that VDR-induced cell cycle arrest and apoptosis are enhanced by BAG1L.

Elucidated the mechanism by which VDR-agonists induce apoptosis of prostate cancer cells, showing that a mitochondrial pathway is activated in concert with down-regulation of expression of anti-apoptotic members of the Bcl-2 family.

3. Reportable Outcomes

Publications: Five full-length peer-reviewed publications resulted in whole or part from the funding provided by this grant:

Froesch, B.A., Takayama, S., and Reed, J.C. BAG-1L protein enhances androgen receptor function, J. Biol. Chem. 1273:11660-11666, 1998.

Guzey, M., Takayama, S., and Reed, J.C. Bag1L enhances trans-activation function of the vitamin D receptor, J. Biol. Chem. 275:40749-40756, 2000.

Knee, D.A., Froesch, B.A., Nuber, U., Takayama, S., and Reed, J.C. Structure-function analysis of Bag-1 proteins effects on androgen receptor transcriptional activity, J. Biol. Chem. 276:12718-12724, 2001.

Guzey, M., Kitada, S., and Reed, J.C. Apoptosis induction by $1a_225(OH)_2$ in vitamin-D_3 prostate cancer cell lines. 2002.

Briknarova, K. Takyama, S., Brive, L., Harvert, M.L., Knee, D.A., Velasco, J., Homma, S., Cabezas E., Stuart, J., Hoytt, D.W., Satterthwait, A.C., Llinas, M., Reed, J.C., and Ely, K.R. Structural analysisof interactions between BAG-1 co-chaperone and Hsc70 heat shock protein. Nature Struct. Biol.8:349-352, 2001.

Abstracts describing our work were also accepted for presentation at international meetings, including the annual meeting of the Amer. Assoc. Cancer

Res (AACR) and Endocrinology Society. Some of these were published, as listed below.

Knee, D.A., Krajewski, M., Krajewska, M., Clevenger, C., Reynolds, C., Reed, J.C.: BAG-1 and estrogen receptor function in breast cancers. *Proc. Am. Assc. Cancer Res.* 40:305, 1999.

Takayama, S., Xie, Z., Reed, J.C.: An evolutionarily conserved family of Bag-1-like HSP70/HSC70 molecular chaperone regulators. *Proc. Am. Assc. Cancer Res.* 40:168, 1999.

Knee, D. A., Kudoh, M., Reed, J. C.,: Bag-1 and estrogen receptor (ER) function in breast cancers. *AACR* 41:465, 2000.

Knee, D. A., Froesch, A., Reed, J. C.: Bag-1 and androgen receptor function. *AACR* 41:1514, 2000.

Guzey, M., Takayama, S., Reed, J.C.: BAG-1 family proteins and their relation to Vitamin D receptor (VDR). *The Endocrine Society: ENDO 2000,* 2000.

Takayama S., Homma S., Reed J.C., Götz R., Wiese S., Rossoll W., Schweizer U., Berzaghi M., Jablonka S., Holtmann, B., Rapp U., Sendtner M.: Tissue-specific role of BAG1 and BAG3 in apoptosis suppression in vivo. *AACR,* 44:1399, 2003.

Langer C., Roth W., Kitada S., and Reed J.C.: Identification of genes associated with BAG-1L overexpression in breast cancer cells by cDNA-microarray analysis. *AACR,* 44:1388, 2003.

Research Resources: A variety of research reagents were created with the funding provided by this grant, as listed below.

Hybridomas producing anti-BAG monoclonal antibodies were generated.

Multiple plasmid encoding full-length BAG1L or fragments of the BAG1L protein for expression in mammalian cells were produced.

Stably transfected prostate cancer cell lines over-expressing BAG1L were generated and characterized.

Transgenic mice over-expressing BAG1L in the prostate gland were created.

4. CONCLUSIONS

Understanding the molecular basis for progression of prostate cancers to hormone-refractory disease is critical for designing new therapeutic strategies for

the treatment of advanced prostate cancer. We have discovered a protein, BAG1L, that binds the androgen receptor (AR) and enhances its resistance to anti-androgenic agents. Our findings accomplished with funding from this grant indicate that BAG1L expression is abnormally elevated in ~one-third of prostate cancers. Future studies of the impact of BAG1L expression and BAG1L inhibition in the prostate glands of transgenic mice will reveal the overall significance of BAG1L for regulation of androgen-responses in normal and malignant prostate tissue, and will help contribute to new strategies for overcoming hormone-resistant prostate cancer. In this regard, our discovery that BAG1L also binds VDR, and enhances growth inhibitory and pro-apoptotic effects of VDR-ligands in prostate cancer cell line suggests that, while BAG1L expression may reduce responsiveness to anti-androgens, it may simultaneously increase sensitivity to Vitamin D. Thus, by employing Vitamin D-based therapies, elevated levels of BAG1L could potentially be converted from a asset to a liability for prostate cancer cells.

5. REFERENCES

1. Kyprianou, N. and Isaacs, J. T. Activation of programmed cell death in the rat ventral prostate after castration. Endocrinology, *122:* 552-562, 1988.
2. Crawford, E. D., Eisenberger, M. A., McLeod, D. C., Spaulding, J., Benson, R., Dorr, F. A., Blumenstein, B. A., Davis, M. A., and Goodman, P. J. A control randomized trial of Leuprolide with and without flutamide in prostatic cancer. N. Engl. J. Med., *321:* 419-424, 1989.
3. Marcelli, M., Tilley, W. D., Zoppi, S., Griffin, J. E., Wilson, J. D., and McPhaul, M. J. Molecular basis of androgen resistance. J Endocrinol Invest, *15:* 149-159, 1992.
4. McPhaul, M. J., Marcelli, M., Zoppi, S., Griffin, J. E., and Wilson, J. D. Genetic basis of endocrine disease. 4. The spectrum of mutations in the androgen receptor gene that causes androgen resistance. J Clin Endocrinol Metab, *76:* 17-23, 1993.
5. Coetzee, G. A. and Ross, R. K. Prostate cancer and the androgen receptor. J Natl Cancer Inst, *86:* 872-873, 1994.
6. Koivisto, P., Kononen, J., Palmberg, C., Tammela, T., Hyytinen, E., Isola, J., Trapman, J., Cleutjens, K., Noordzij, A., Visakorpi, T., and Kallioniemi, O.-P. Androgen receptor gene amplification: a possible molecular mechanism for androgen deprivation therapy failure in prostate cancer. Cancer Res, *57:* 314-319, 1997.
7. Visakorpi, T., Hyytinen, E., Koivisto, P., Tanner, M., Keinanen, R., Palmberg, C., Palotie, A., Tammela, T., Isola, J., and Kallioniemi, O. P. In vivo amplification of the androgen receptor gene and progression of human prostate cancer. Nature Genet, *9:* 401-406, 1995.
8. Froesch, B. A., Takayama, S., and Reed, J. C. BAG-1L protein enhances androgen receptor function. J Biol Chem, *273:* 11660-11666, 1998.
9. Guzey, M., Takayama, S., and Reed, J. C. BAG1L enhances trans-activation function of the vitamin D receptor. J Biol Chem, *275:* 40749-40756, 2000.
10. Knee, D. A., Froesch, B. A., Nuber, U., Takayama, S., and Reed, J. C. Structure-function analysis of Bag1 proteins: effects on androgen receptor transcriptional activity. J Biol Chem, *276:* 12718-12724, 2001.
11. Guzey, M., Kitada, S., and Reed, J. C. Apoptosis induction by $1a_2 25(OH)_2$ in vitamin-D_3 prostate cancer cell lines. Mol Cell Therap, *1:* 667-677, 2002.
12. Briknarova, K., Takayama, S., Brive, L., Havert, M. L., Knee, D. A., Velasco, J., Homma, S., Cabezas, E., Stuart, J., Hoytt, D. W., Satterthwait, A. C., Llinas, M., Reed, J. C., and Ely, K. R. Structural analysis of interactions between BAG1 co-chaperone and Hsc70 heat shock protein. Nature Struct Biol, *8:* 359-352, 2001.

6. APPENDIX

Copies of the papers published as a result of this grant are provided as an Appendix to supplement the information provided in the progress report.

Guzey, M., Takayama, S., and Reed, J.C. Bag1L enhances trans-activation function of the vitamin D receptor, J. Biol. Chem. 275:40749-40756, 2000.

Knee, D.A., Froesch, B.A., Nuber, U., Takayama, S., and Reed, J.C. Structure-function analysis of Bag-1 proteins effects on androgen receptor transcriptional activity, J. Biol. Chem. 276:12718-12724, 2001.

Guzey, M., Kitada, S., and Reed, J.C. Apoptosis induction by $1a_225(OH)_2$ in vitamin-D_3 prostate cancer cell lines. 2002.

Briknarova, K. Takyama, S., Brive, L., Harvert, M.L., Knee, D.A., Velasco, J., Homma, S., Cabezas E., Stuart, J., Hoytt, D.W., Satterthwait, A.C., Llinas, M., Reed, J.C., and Ely, K.R. Structural analysisof interactions between BAG-1 co-chaperone and Hsc70 heat shock protein. Nature Struct. Biol.8:349-352, 2001.

THE JOURNAL OF BIOLOGICAL CHEMISTRY
Vol. 275, No. 52, Issue of December 29, pp. 40749–40756, 2000
Printed in U.S.A.

BAG1L Enhances Trans-activation Function of the Vitamin D Receptor*

Received for publication, June 8, 2000, and in revised form, August 30, 2000
Published, JBC Papers in Press, August 30, 2000, DOI 10.1074/jbc.M004977200

Meral Guzey‡§¶, Shinichi Takayama‡, and John C. Reed‡‖

From the ‡Burnham Institute, La Jolla, California 92037 and §RIGEB, MAM-TÜBITAK, P. K. 21 Gebze 41 470, Kocaeli, Turkey

The vitamin D receptor (VDR) is a member of the steroid/retinoid receptor superfamily of nuclear receptors that has potential tumor-suppressive functions. We show here that VDR interacts with and is regulated by BAG1L, a nuclear protein that binds heat shock 70-kDa (Hsp70) family molecular chaperones. Endogenous BAG1L can be co-immunoprecipitated with VDR from prostate cancer cells (ALVA31; LNCaP) in a ligand-dependent manner. BAG1L, but not shorter non-nuclear isoforms of this protein (BAG1; BAG1M/Rap46), markedly enhanced, in a ligand-dependent manner, the ability of VDR to trans-activate reporter gene plasmids containing a vitamin D response element in transient transfection assays. Mutant BAG1L lacking the C-terminal Hsc70-binding domain suppressed (in a concentration-dependent fashion) VDR-mediated trans-activation of vitamin D response element-containing reporter gene plasmids, without altering levels of VDR or endogenous BAG1L protein, suggesting that it operates as a trans-dominant inhibitor of BAG1L. Gene transfer-mediated elevations in BAG1L protein levels in a prostate cancer cell line (PC3), which is moderately responsive to VDR ligands, increased the ability of natural (1α,25(OH)$_2$ vitamin D$_3$) and synthetic (1α,25-dihydroxy-19-nor-22(*E*)-vitamin D$_3$) VDR ligands to induce expression of the VDR target gene, p21^{Waf1}, and suppress DNA synthesis. Thus, BAG1L is a direct regulator of VDR, which enhances its trans-activation function and improves tumor cell responses to growth-suppressive VDR ligands.

1α,25(OH)$_2$ vitamin-D$_3$ is a member of a steroid hormone family which controls calcium homeostasis, and bone formation (reviewed in Refs. 1 and 2). The effects of 1α,25(OH)$_2$ vitamin D$_3$ are largely mediated via interaction with a specific nuclear vitamin D$_3$ receptor (VDR).[1] The VDR is a ligand-dependent transcriptional regulator, belonging to the nuclear receptor (NR) superfamily (reviewed in Ref. 3). VDR primarily interacts with specific DNA sequences composed of a hexanucleotide of direct repeat, binding as either a homodimer or as heterodimer with retinoid X receptors (RXRs) (4).

Known target genes of VDR regulation include the cell cycle inhibitors p21^{Waf1} and p27^{Kip1} (5), perhaps accounting in part for the anti-proliferative effects of VDR ligands on some types of cells. Growth suppressive effects of VDR ligands on epithelial cancer cells *in vitro* have prompted interest in the possibility of applying natural or synthetic VDR ligands for the treatment of cancer (reviewed in Ref. 6). Prostate cancer is among the types of tumor cells with documented sensitivity to VDR ligands. 1α,25(OH)$_2$ vitamin D$_3$ and its less calcemic synthetic analogues have been shown to inhibit *in vitro* growth of established human prostate carcinoma cell lines and primary cultures of normal and prostate cancer cells (7, 8). Depending on the particular cell line tested, VDR ligands can induce cell cycle arrest, differentiation, apoptosis, or combinations of these events (9). Functional VDR is necessary for the growth-inhibitory effect of VDR. However, prostate cancer cell lines vary in their sensitivity to 1α,25(OH)$_2$ vitamin D$_3$ and its synthetic analogues in ways that cannot be explained by differences in VDR protein levels or rates of ligand metabolism, suggesting the existence of mechanisms for modulating VDR function at a post-ligand binding step. This variability in bioresponses to synthetic vitamin D$_3$ analogues has also been observed *in vivo* in clinical trials involving men with advanced prostate cancer (10).

The human *BAG1* gene encodes several proteins, including BAG1, BAG1M (Rap46), and BAG1L, which differ in the length of their N-terminal domains but which all share a conserved C-terminal domain that binds the ATPase domain of heat shock 70-kDa (Hsp70) family molecular chaperones (11). Some of the BAG1 protein isoforms have been shown to interact with and regulate the activity of certain members of the steroid hormone/retinoid superfamily of NRs (12–14). For example, BAG1 binds and suppresses retinoic acid receptors (RARs) (13), BAG1M (Rap46) interacts with and inhibits glucocorticoid receptors (15), and BAG1L associates with and enhances the trans-activation function of androgen receptors (AR) (14). In this report, we examined the relation of BAG1 proteins to VDR. Our findings indicate that the longest of the BAG1 protein isoforms, BAG1L, interacts with VDR in a ligand-inducible manner, enhancing VDR function and improving prostate cancer cellular responses to the growth suppressive effects of vitamin D$_3$ analogues. Thus, levels of BAG1L may be one of the determinants of vitamin D$_3$ responses in normal and malignant tissues.

MATERIALS AND METHODS

VDR Ligands—1α,25(OH)$_2$ vitamin D$_3$ and 1α,25-dihydroxy-19-nor-22(*E*)-vitamin D$_3$ were generously provided by Dr. H. F. DeLuca (Uni-

* This work was supported in part by Department of Defense Prostate Research Program Grant DAMD17-98-1-8584. The costs of publication of this article were defrayed in part by the payment of page charges. This article must therefore be hereby marked "*advertisement*" in accordance with 18 U.S.C. Section 1734 solely to indicate this fact.

¶ Recipient of International Union Against Cancer fellowships from Yamagiwa-Yoshida Memorial and the American Cancer Society Young Investigators.

‖ To whom correspondence should be addressed: Burnham Inst., 10901 N. Torrey Pines Rd., La Jolla, CA 92037. Tel.: 858-646-3140; Fax: 858-646-3194; E-mail: jreed@burnham-inst.org.

[1] The abbreviations used are: VDR, vitamin D receptor; VDRE, vitamin D response element; RXR, retinoid X receptor; RAR, retinoic acid receptor; BSA, bovine serum albumin; PBS, phosphate-buffered saline; CMV, cytomegalovirus; tk, thymidine kinase; CAT, chloramphenicol acetyltransferase; PAGE, polyacrylamide gel electrophoresis; BrdUrd, bromodeoxyuridine; NR, nuclear receptor; AR, androgen receptor.

versity of Wisconsin, Madison, WI) (16). These VDR ligands were prepared as 10^{-3} M stock solutions in ethanol and stored at −20 °C. Stock solution concentrations were confirmed by spectroscopy (Spectra Max 190, Molecular Devices), using an extinction coefficient at 220–290 nm of 18,300 for 1α,25(OH)$_2$ vitamin D$_3$. The spectroscopic confirmation for 1α,25-dihydroxy-19-nor-22(*E*)-vitamin D$_3$ was slightly modified as described previously (16).

Cell Culture—The human prostate cancer cell lines PC-3 and LNCaP, the transformed human embryonal kidney line 293, and monkey kidney COS-7 cell lines were obtained from the American Type Culture Collection (Rockville, MD). The ALVA 31 human prostate cancer cell line was generously provided by Dr. G. Miller (17). Cells were maintained in a humidified atmosphere with 5% CO_2 in RPMI 1640 (PC3, LNCaP, ALVA31) or Dulbecco's modified Eagle's medium (293 and COS-7) supplemented with 10% fetal calf serum, 1 mM glutamine, 100 units/ml penicillin, and 100 μg/ml streptomycin (Life Technologies, Inc.). For most experiments, cells were cultured in medium in which the serum had been preadsorbed with activated charcoal to deplete steroid hormones (14).

Transfections—COS-7 and 293T cells were transiently transfected by a LipofectAMINE method. Cells at ~50% confluence (~2 × 10^5 cells) were seeded per well in six-well (9.4 cm^2) plates (Corning, New York) in 2 ml/well of steroid-depleted medium. The next day, 2.2 μg of DNA was combined with 6 μl of LipofectAMINE in a total volume of 375 μl of Opti-MEM medium (Life Technologies, Inc.) and incubated for ~ 0.5 h. Adherent cells were washed twice with serum-free pre-warmed Opti-MEM, and then DNA/LipofectAMINE mixtures were applied in 750 μl of Opti-MEM. After culturing at 37 °C and 5% CO_2 for 3 h, 1.5 ml of 20% csFBS-containing medium was added per well. The following day, various concentrations of 1α,25(OH)$_2$ vitamin D$_3$ or 1α,25-dihydroxy-19-nor-22(*E*)-vitamin D$_3$ were added and cells were cultured for up to 3 days before preparing lysates for various assays.

For stable transfections, 2.2 μg of either supercoiled or *Sca*I-cleaved pRc/CMV-BAG1L plasmid DNA, encoding BAG1L protein (11) or pRc/CMV parental vector was transfected into PC-3 cells using the LipofectAMINE method, essentially as described above. After 2 days, cells were cultured in medium containing 0.6 mg/ml (active drug) G418 (Life Technologies, Inc.). Medium was replaced twice weekly, until colonies of stably transfected clones arose. Clones were individually recovered and expanded in culture.

Reporter Gene Assays—Transient transfection reporter gene assays were employed for monitoring VDR trans-activation function. Briefly, cells were transiently transfected as described above with various amounts (20, 50, 100, and 150 ng) of pcDNA3 plasmids encoding BAG1L, BAG1L(ΔC), BAG1M, BAG1, BAG1S, or BAG1 (20–800 ng) (11, 14) (see Fig. 1), together with 250 ng of a plasmid encoding one copy of a VDRE upstream of a thymidine kinase minimal promoter and chloramphenicol acetyltransferase (CAT) reporter gene (18, 19), and 400 ng of pCMV-βGal, encoding β-galactosidase under the control of a CMV immediate-early region promoter (14), with or without 100 ng of pcDNA3/VDR, a plasmid encoding the human VDR under the control of a CMV promoter (18). For some experiments, VDRE-tk-CAT was replaced with p21^{Waf1}-CAT, a plasmid containing 2.4 kilobase pairs of the human p21^{Waf1} promoter cloned upstream of a CAT gene (20). After 36–48 h, cell lysates were prepared using Promega reporter lysis buffer (Promega), normalized for total protein content, and relative levels of CAT and β-galactosidase activity were measured as described (14). CAT data were first normalized relative to β-galactosidase, then expressed as -fold activation relative to a defined control, usually cells cultured without VDR ligands or cells transfected without BAG1-encoding plasmids.

Cell Cycle Analysis—The percentage of cells undergoing DNA synthesis was measured by incorporation of bromodeoxyuridine (BrdUrd), essentially as described (21, 22). Stably transfected clones of PC-3 cells containing pRc-CMV control ("Neo") or pRc/CMV-BAG1L plasmids were seeded at 7.5 × 10^3 cells/six-well plate in 2 ml of normal medium for 24 h, then changed to medium in which the serum had been preadsorbed with activated charcoal to deplete steroid hormones. In some cases, VDR ligands were added, as indicated, and cultures were continued for up to 48 h. Cells were then cultured with 10 μM BrdUrd (Sigma) for 1 h, collected by trypsinization, and fixed in 70% ethanol (final concentration ~10^6 cells/100 μl). Fixed cells were then washed in phosphate-buffered saline (pH 7.4) containing 0.5% (w/v) bovine serum albumin (BSA), then exposed to 2 M HCl, 0.5% BSA at room temperature for 20 min before re-washing with PBS/BSA and re-suspending in 0.5 ml of 0.1 M sodium borate ($Na_2B_4O_7$) (pH 8.7) for 2 min at room temperature, and washing a final time with PBS/BSA. Cells were incubated in PBS/BSA with 20 μl/10^6 cells fluorescein isothiocyanate-conjugated anti-BrdUrd antibody (PharMingen) for 20 min in the dark. Finally, propidium iodide (50 μg/ml) was added, and the cells were analyzed using a fluorescence-activated cell sorter (Becton Dickinson FACStar-Plus) using the Cell Quest and Mod-Fit programs.

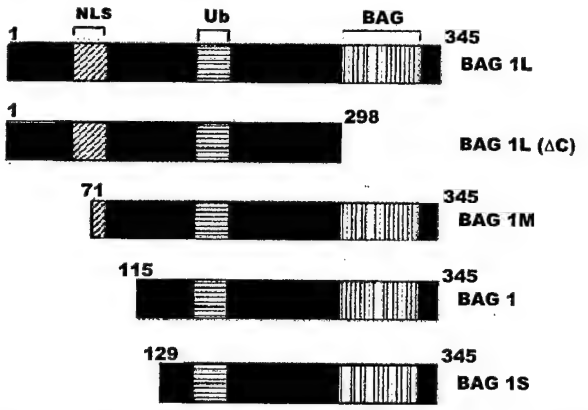

FIG. 1. **Structure of BAG1 protein isoforms.** The structures of the human BAG1 protein isoforms are depicted, showing the conserved BAG domain, as well as other domains found in selected members of the family such as ubiquitin-like domain (*Ub*), and nuclear targeting sequences (*NLS*). The longest of the BAG1L proteins is a predicted 345 amino acids in length. All others are presented relative to BAG1L. The BAG1L(ΔC) mutant is also depicted (14).

Antibodies and Immunoblotting—Cell lysates were prepared using radioimmunoprecipitation assay buffer (10 mM Tris (pH 7.4), 150 mM NaCl, 1% Triton X-100, 1% deoxycholate, 0.1% SDS, 5 mM EDTA), normalized for total protein content (25 μg of protein), and subjected to SDS-PAGE using 12% gels, followed by electrotransfer to 0.45-μm nitrocellulose transfer membranes (Bio-Rad). Blots were incubated as described (11, 14), with the following primary antibodies, including 1:1000 (v/v) of a mouse monoclonal specific for human VDR (IVG8C11) (gift of Dr. H. F. DeLuca) (23), 1:1000 (v/v) of a rabbit polyclonal anti-VDR IgG (Santa Cruz Biotechnology, Inc., Santa Barbara, CA), 1:1000 (v/v) control normal rabbit IgG (Santa Cruz Biotechnology, Inc.), 1:1000 (v/v) control mouse IgG$_1$ (Dako, Inc.), 1:1000 (v/v) of mouse monoclonal (IgG$_1$) specific for human BAG1 (KS6C8) (11, 24), and 1/250 (v/v) of mouse anti-human p21 monoclonal antibody (IgG$_1$) (PharMingen, San Diego, CA). Immunodetection was accomplished essentially as described (11, 14) using horseradish peroxidase-conjugated secondary antibody (Amersham Pharmacia Biotech) and an enhanced chemiluminescence detection method (ECL) (Amersham/Pharmacia Biotech.) with exposure to x-ray film (XAR, Eastman Kodak Co.).

Co-immunoprecipitations—Untransfected ALVA31 and LN-CaP cells or 293T cells transfected with plasmids encoding BAG1L or BAG1L(ΔC) were cultured with or without 5 × 10^{-8} M 1α,25(OH)$_2$ vitamin D$_3$, and collected at 70% confluence. Cells were lysed on ice in HKMEN (10 mM HEPES (pH 7.2), 142 mM KCl, 1 mM EGTA, 1 mM EDTA, 0.2% Nonidet P-40) containing protease inhibitors (Roche Molecular Biochemicals), then either passed several times through a ~21-gauge needle to disrupt nuclei or NE-PER nuclear extraction reagent (Pierce) was added according to the manufacturer's protocol. After centrifugation at 10,000 × *g* for 25 min, the resulting supernatants from equivalent numbers of cells were subjected to immunoprecipitations in HKMEN using the anti-BAG1 monoclonal KS6C8, anti-VDR monoclonal IVG8C11, or anti-VDR polyclonal antiserum, bound to protein G-agarose (Zymed Laboratories Inc., San Francisco, CA). Control immunoprecipitations were performed using mouse IgG$_1$ (Dako) or non-immune rabbit serum (Santa Cruz). Immune-complexes were washed three times with 1 ml of HKMEN and analyzed by SDS-PAGE/immunoblotting, as above.

RESULTS

BAG1L Enhances Trans-activation Function of VDR—We initially explored the effects of BAG1 proteins on the trans-activation function of the VDR using transient transfection reporter gene assays in HEK 293T and COS-7 cells. Several isoforms of the BAG1 protein were compared, as depicted in Fig. 1. These isoforms of BAG1 all contain a conserved C-terminal domain "BAG domain" responsible for high affinity interactions with Hsc70/Hsp70 molecular chaperones and they

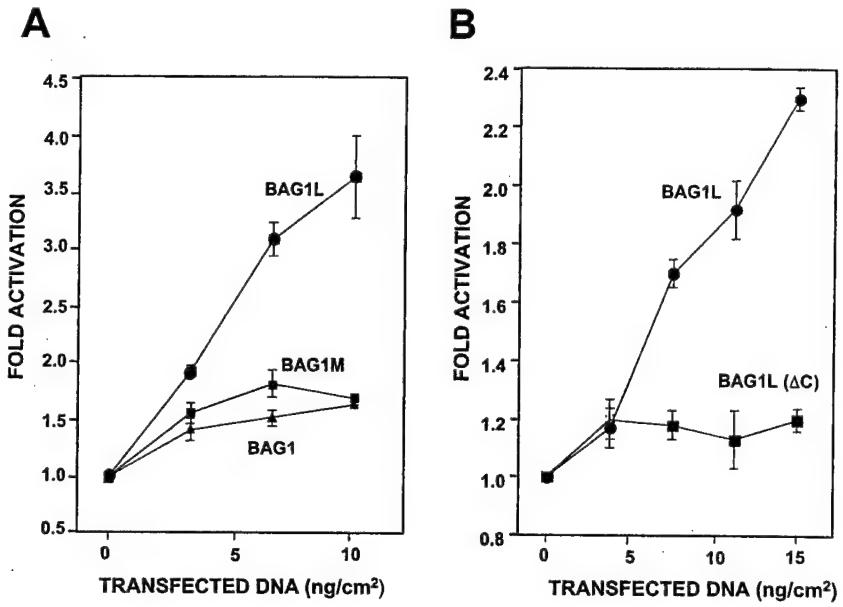

FIG. 2. **BAG1L enhances trans-activation function of VDR.** COS-7 cells at ~50% confluence in six-well plates (area 9.4 cm^2) in steroid-depleted medium were transfected by a LipofectAMINE method with VDR encoding plasmid (100 ng), VDRE-CAT reporter plasmid (250 ng), pCMV-βgal (400 ng), and various amounts of BAG1-encoding plasmids as indicated, normalizing total DNA to 2.2 μg/well. After 1 day, cells were stimulated with 5×10^{-9} M $1\alpha,25(OH)_2$ vitamin D_3. Cell extracts were prepared and assayed for CAT and β-galactosidase activity, expressing normalized data as a ratio relative to transfected cells which received pcDNA3 control DNA instead of a BAG1-expression plasmid (mean ± S.E.; $n = 3$). In *A*, plasmids encoding BAG1 (*triangles*), BAG1M (*squares*), or BAG1L (*circles*) were transfected in amounts of 20, 50, and 100 ng (reported as ng/cm^2). In *B*, plasmids encoding BAG1L (*circles*) or BAG1L(ΔC) mutant (*squares*) were transfected using 20, 50, 100, or 150 ng of these plasmid DNAs, as indicated.

possess an upstream ubiquitin-like domain, but they differ in the length of their N-terminal domains. The various isoforms of BAG1L arise by translation from alternative initiation codons within a common mRNA (11, 25). Among these proteins, only BAG1L contains both nucleoplasmin-like and SV40 large T-like candidate nuclear targeting sequences and is constitutively localized to nuclei (11, 25).

To enforce expression of selected isoforms of BAG1, a cDNA encoding the longest isoform, BAG1L, and various 5′-truncated versions of cDNAs encoding BAG1M, BAG1, and BAG1S were subcloned into an expression plasmid, with additional modifications as described previously (11, 14, 24). These plasmids were then co-transfected in various amounts with a fixed amount of plasmid encoding VDR and a VDRE-CAT reporter gene plasmid. Cells were supplied with physiologically relevant concentrations (5×10^{-9} M) of $1\alpha,25(OH)_2$ vitamin D_3. All data were normalized relative to cells stimulated with $1\alpha,25(OH)_2$ vitamin D_3 in the absence of BAG1 expression plasmids.

As shown in Fig. 2, the longest isoform, BAG1L, enhanced the trans-activation function of VDR in a concentration-dependent manner, resulting in a 2–4-fold increase in VDRE-tk-CAT reporter gene activation under these conditions. In contrast, BAG1M, BAG1, and BAG1S had little effect on VDR activity (Fig. 2 and data not shown). Moreover, although full-length BAG1L effectively enhanced VDR activity, a mutant of BAG1L lacking the C-terminal Hsc70/Hsp70-binding domain did not. This observation confirms the specificity of these finding obtained with full-length BAG1L and also suggests that the C-terminal BAG domain of BAG1L is required for potentiating VDR activity.

Immunoblot analysis was performed to verify production of the BAG1L, BAG1L(ΔC), BAG1M, BAG1, and BAG1S proteins in transfected cells. As shown in Fig. 3, BAG1L, BAG1L(ΔC), BAG1, and BAG1S were produced at comparable levels. The BAG1M protein was also produced, but due to internal translation initiation from the AUG, which normally gives rise to the shorter BAG1 protein, the steady-state levels of BAG1M achieved were only about half the other isoforms. Nevertheless, BAG1M protein was produced at levels far in excess of endogenous BAG1 and BAG1L, which migrate at ~35 and ~55 kDa and which can be seen as faint bands in the immunoblot analysis (Fig. 3). We conclude, therefore, that the selective enhancement of VDR activity seen with BAG1L but not with other BAG1 isoforms in transient transfection reporter gene assays

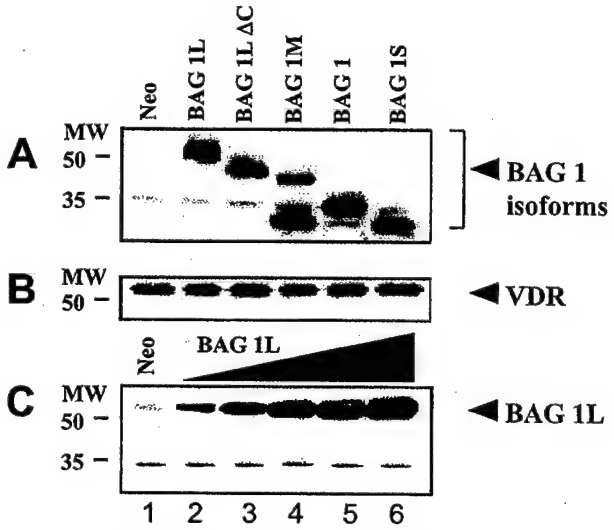

FIG. 3. **Immunoblot analysis of expression of BAG1 isoforms in transfected cells.** COS-7 cell plasmids in 60-mm dishes (growth area; 21 cm^2) were transiently transfected using a LipofectAMINE reagent with 220 ng of VDR and 330 ng of either pcDNA3 (neo) or pcDNA3-plasmids encoding BAG1L, BAG1M, BAG1L(ΔC), BAG1, or BAG1S. After 2 days, whole cell lysates were prepared, normalized for total protein content (25 μg/lane), and subjected to SDS-PAGE/immunoblot assay, using anti-BAG1 (*A*) or anti-VDR (*B*) antibodies in conjunction with an ECL-based detection method. In *C*, 293T cells were transfected with 220 ng of VDR and increasing amounts of pcDNA3-BAG1L DNA (*lanes 2–6*, 44, 110, 220, 330, and 440 ng, respectively) (reported as ng/cm^2 for area of 21 cm^2), normalizing total DNA content (~5 μg in 60-mm dishes) with pcDNA3 (Neo) vector. Lysates were prepared after 2 days and analyzed as above using anti-BAG1 antibody. Molecular size markers are indicated in kilodaltons.

is unlikely to be due to differences in the levels of production of these proteins. Importantly, expression of the various isoforms of BAG1 had no effect on levels of VDR, thus excluding alterations in the receptor for $1\alpha,25(OH)_2$ vitamin D_3 as a trivial explanation for the results obtained in reporter gene assays (Fig. 3*B*). Immunoblotting also confirmed the concentration dependence of BAG1L protein production in response to transfection of various amounts of expression plasmid DNA (Fig. 3*C*), further validating the results obtained by reporter gene assays.

$1\alpha,25(OH)_2$ Vitamin D_3 Induces Association of BAG1L with

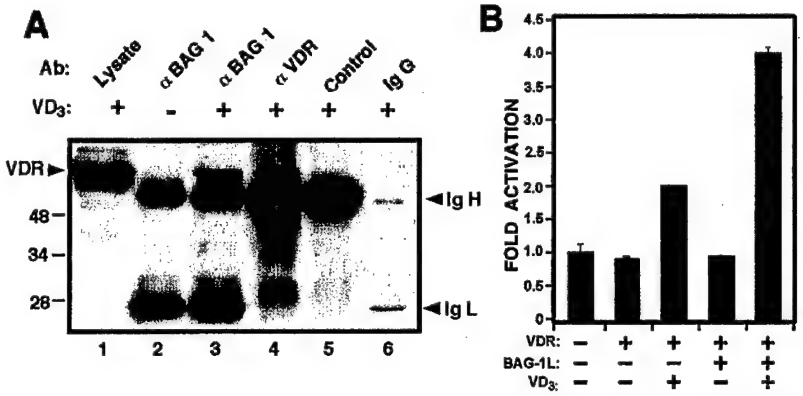

FIG. 4. **BAG1L associates with and modulates function of VDR in a ligand-dependent manner.** In *A*, lysates were prepared using HKMEN solution from ALVA31 prostate cells grown in the absence (−) or presence (+) of 5×10^{-8} M $1\alpha,25(OH)_2$ vitamin D_3. Immunoprecipitations were performed using anti-BAG1 monoclonal (IgG_1) KS6C8 (14) (*lanes 2* and *3*), rabbit polyclonal IgG VDR antibody (Santa Cruz) (*lane 4*), rabbit IgG_1 control (*lane 5*), or mouse IgG control (*lane 6*). Immune complexes were analyzed by SDS-PAGE/immunoblotting using a polyclonal rabbit anti-VDR with ECL-based detection. As a control, lysate (25 μg) from $1\alpha,25(OH)_2$ vitamin D_3-treated cells was also directly loaded in the gel (*lane 1*). The positions of the heavy (*IgH*) and light (*IgL*) chains of the primary antibodies are indicated (*right*), as well as the position of the VDR (*left*). In *B*, COS-7 cells in steroid-depleted medium were transfected as described in Fig. 2, using 100 ng of pcDNA3-BAG1L (+) or pcDNA3 control (−) plasmid DNA. After 1 day, either 5×10^{-9} M $1\alpha,25(OH)_2$ vitamin D_3 (+) or control diluent (−) was added to cultures. Lysates were prepared 48 h later, and relative CAT production from the VDR-CAT reporter gene plasmid was measured, normalizing for β-galactosidase and expressing the data as -fold activation relative to cells that received neither the VDR nor BAG1L plasmids and which were not stimulated with VDR ligand.

VDR—The functional collaboration of BAG1L with VDR prompted us to explore whether these proteins physically interact, particularly given evidence that BAG1L can associate with certain other members of the NR family (13–15). Co-immunoprecipitation assays were performed using lysates from untransfected ALVA-31 (Fig. 4) and LNCaP (data not shown) prostate cancer cells to explore whether the endogenous BAG1L and VDR proteins can form complexes. These lines were chosen because they contain relatively high intrinsic levels of both BAG1L and VDR, and because they are sensitive to $1\alpha,25(OH)_2$ vitamin D_3-induced growth suppression (10).[2] BAG1L was immunoprecipitated from lysates prepared from unstimulated and $1\alpha,25(OH)_2$ vitamin D_3-treated cells, and the resulting immune complexes were analyzed by SDS-PAGE/immunoblotting using an anti-VDR antibody.

Anti-BAG1 immunoprecipitates prepared from lysates of $1\alpha,25(OH)_2$ vitamin D_3 -treated cells contained associated VDR, whereas VDR was not found associated with BAG1L immune complexes derived from unstimulated ALVA31 (Fig. 4) or LNCaP (data not shown) cells. Control immunoprecipitates prepared using mouse IgG_1 instead of anti-BAG1 antibody confirmed the specificity of these results. Comparisons of the levels of VDR and BAG1L proteins in ALVA31 and LNCaP lysates before and after treatment with $1\alpha,25(OH)_2$ vitamin D_3 revealed no demonstrable difference, indicating that the association is not merely secondary to ligand-induced changes in the amounts of these proteins (data not shown). We conclude, therefore, that VDR associates with BAG1L in a ligand-dependent manner.

The ligand-dependent association of BAG1L with VDR predicts that BAG1L should enhance VDR trans-activation function only when appropriate steroid ligand is provided. Accordingly, we performed transient transfection reporter gene assays in which cells were cultured with or without $1\alpha,25(OH)_2$ vitamin D_3 in medium containing steroid-depleted serum. Co-expression of BAG1L with VDR in the absence of ligand did not increase VDR-mediated reporter gene trans-activation (Fig. 4*B*). However, when $1\alpha,25(OH)_2$ vitamin D_3 was provided, BAG1L more than doubled the levels of VDR-mediated induction of the VDRE-CAT reporter gene plasmid compared with COS-7 cells, which received VDR and $1\alpha,25(OH)_2$ vitamin D_3 in the absence of BAG1L. Taken together, these results demonstrate that BAG1L associates with and potentiates the function of VDR complexes in a ligand-dependent manner.

A BAG1L Mutant Lacking the Hsc70/Hsp70-binding Domain Inhibits VDR Activity—It has been shown that the last 47 amino acids of the BAG1 protein are required for binding to the ATPase domain of Hsc70 and Hsp70 chaperones (11, 26). To explore the functional consequences of removing the C-terminal domain from BAG1L on VDR, transient transfection reporter gene assays were performed, assaying VDR-mediated trans-activation of the VDRE-CAT reporter gene plasmid in the presence of increasing amounts of co-transfected pcDNA3-BAG1L (ΔC), which encodes a truncation mutant of BAG1L lacking the Hsp70/Hsc70-binding domain. As shown in Fig. 5*A*, co-transfection of the BAG1L(ΔC) expression plasmid failed to enhance VDR activity and instead inhibited VDR activity in a concentration-dependent manner, reducing trans-activation of the VRE-CAT reporter gene by approximately half. Immunoblot analysis demonstrated dose-dependent production of the BAG1L(ΔC) protein, which reached levels roughly equivalent to full-length BAG1L at the highest concentrations of plasmid DNA transfected (Fig. 5*B*). We conclude, therefore, that the Hsc70/Hsp70-binding domain of BAG1L is necessary for its stimulatory effects on VDR, and that deletion of this domain converts BAG1L from a stimulator to an inhibitor of VDR, presumably functioning as a trans-dominant competitor of the endogenous wild-type BAG1L protein.

To explore the mechanism of the BAG1L(ΔC) protein further, comparisons were made of the ability of BAG1L and BAG1L(ΔC) to associate with VDR, as determined by co-immunoprecipitation experiments (Fig. 5*C*). Although VDR could be readily co-immunoprecipitated with BAG1L from $1\alpha,25(OH)_2$ vitamin D_3-stimulated cells, VDR association with BAG1L(ΔC) was not detected. Immunoblot analysis of the cell lysates derived from transfected 293T cells used for these experiments confirmed production of both the full-length BAG1L and truncated BAG1L(ΔC) proteins (Fig. 5*C*). Thus, deletion of the C-terminal region of BAG1L abrogates its ability to associate with the VDR.

BAG1L Enhances VDR-mediated Trans-activation of the p 21^{Waf1} Promoter—The promoter of the gene encoding the cell cycle regulator, $p21^{Waf1}$, is known to contain a VDRE (27). To extend the analysis of BAG1L effects on VDR to a more natural

[2] M. Guzey, S. Takayama, and J. C. Reed, unpublished observations.

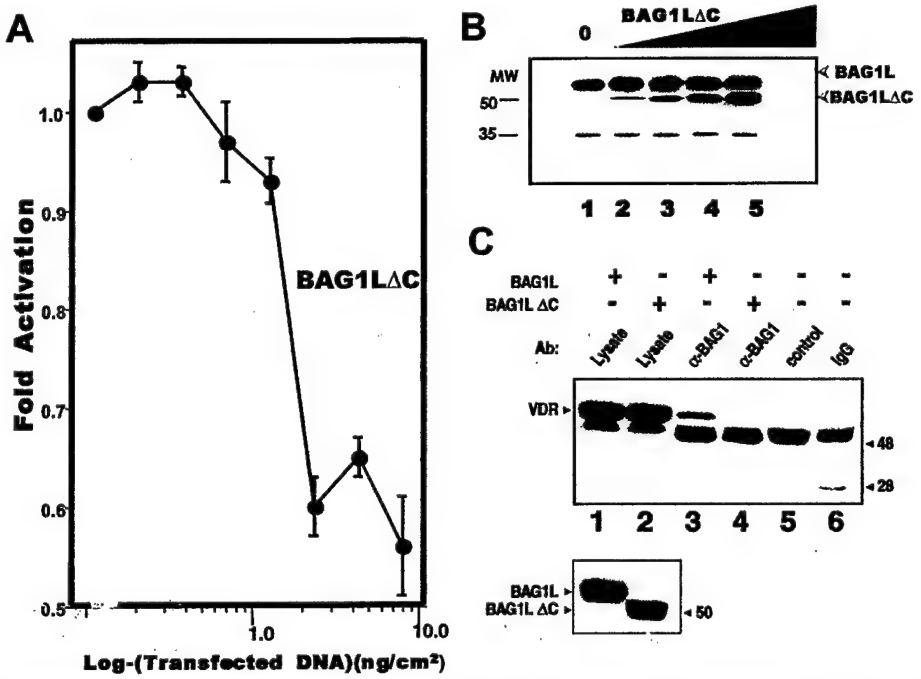

FIG. 5. **BAG1L(ΔC) mutant inhibits VDR function.** *A*, HEK 293T cells were transiently transfected with 200 ng of VDR, 250 ng of the VDRE-CAT, 400 ng of pCMV-βgal, 250 ng of pcDNA3-BAG1L, and various amounts of pcDNA3-BAG1L(ΔC) (20–800 ng, reported as ng/cm^2) or an equal amount of pcDNA3 control plasmid, total DNA normalized to 2.2 μg/well (six-well plates, growth area 9.4 cm^2) by addition of pcDNA3 control plasmid. After 1 day, cells were stimulated with 5×10^{-9} M 1α,25(OH)$_2$ vitamin D$_3$ and cell extracts were prepared 2 days later and assayed for CAT and β-galactosidase activity. Data were normalized using β-galactosidase, and results expressed as -fold activation relative to 1α,25(OH)$_2$ vitamin D$_3$ -stimulated cells, which received the VDR expression vector in combination with pcDNA3 control plasmid. *B*, COS-7 cells in 60-mm dishes (area 21 cm^2) were transiently transfected with 330 ng of pcDNA3-BAG1L, 220 ng of VDR, and increasing amounts of pcDNA3-BAG1L(ΔC) (*lanes 2–5*, 44 , 110, 220, 330, and 440 ng, respectively) (reported as ng/cm^2). After 2 days, whole cell lysates were prepared, normalized for total protein content (25 μg/lane), and subjected to SDS-PAGE/immunoblot assay using anti-BAG1 antibody. The positions of the BAG1L and BAG1L(ΔC) proteins are indicated (*arrowheads*). Molecular size markers are indicated in kilodaltons. *C*, 293T cells in 100-mm dishes were transiently transfected with equivalent amounts of plasmids (~1 μg each) encoding VDR, and either full-length BAG1L or BAG1L(ΔC). Cells were treated 1 day later with 5×10^{-8} M 1α25(OH)$_2$ vitamin D$_3$, then collected at 2 days after transfection, lysed on ice in HKMEN buffer, and immunoprecipitations were performed using either anti-BAG1 monoclonal KS6C8 or mouse IgG control antibody. Immune complexes were analyzed by SDS-PAGE immunoblotting, using a polyclonal rabbit anti-VDR antiserum with ECL-based detection. Lysates (25 μl) were also run directly in the gel for comparison with immunoprecipitates. The blot was reprobed with anti-BAG1 antibody (*lower panel*) to verify production of the BAG1L and BAG1L(ΔC) proteins (indicated by *arrowheads*).

promoter context, we asked whether BAG1L protein could enhance VDR-mediated trans-activation in a CAT reporter gene plasmid containing the p21^{Waf1} promoter. For these experiments, COS-7 or HEK 293T cells were transiently co-transfected with various amounts of plasmid DNA encoding BAG1L, together with fixed amounts of VDR and p21-CAT plasmids. Cells were cultured in the presence of either the natural VDR ligand, 1α,25(OH)$_2$ vitamin D$_3$ (5×10^{-9} M) (Fig. 6, *A* and *B*) or the synthetic vitamin D$_3$ analogue 1α,25-dihydroxy-19-nor-22(*E*)-vitamin D$_3$ (5×10^{-9} M) (Fig. 6, *C* and *D*).

BAG1L induced a dose-dependent increase in VDR-mediated trans-activation of the p21-promoter in these transient transfection reporter gene assays when VDR ligands were supplied (Fig. 6) but not in the absence of ligands (data not shown). The effect of BAG1L appeared to be more pronounced, in terms of -fold enhancement of reporter gene activation, when the vitamin D$_3$ analogue 1α,25-dihydroxy-19-nor-22(*E*)-vitamin D$_3$ was employed, compared with the natural VDR ligand, 1α,25(OH)$_2$ vitamin D$_3$. However, because maximal BAG1L plasmid DNA concentrations (plateau) were not reached in these experiments, quantitative comparisons should be interpreted cautiously.

BAG1L enhances VDR-mediated induction of the endogenous p21^{Waf1} gene. To extend the analysis of BAG1L to an endogenous target of VDR, we explored the effects of VDR ligands on induction of p21^{Waf1} protein production in PC3 cells. PC3 cells contain moderate levels of VDR (800 fmol/mg protein), but express BAG1L at low levels (10).[2] For these experiments, therefore, PC3 cells were stably transfected with either a control plasmid or BAG1L-encoding plasmid and several clones were characterized. Immunoblot analysis revealed several stably transfected clones with elevated levels of BAG1L protein compared with control-transfected or parental PC3 cells. These clones were then cultured with either natural VDR ligand, 1α,25(OH)$_2$ vitamin D$_3$ (5×10^{-8} M) or vitamin D$_3$ analogue 1α,25-dihydroxy-19-nor-22(*E*)-vitamin D$_3$ (5×10^{-8} M) for 1–3 days, and lysates were prepared for immunoblot analysis of p21^{Waf1} protein levels.

Both natural and synthetic VDR ligands induced greater increases in p21^{Waf1} protein levels in BAG1L-overexpressing PC3 cells compared with controls. Increases in p21 were also sometimes more rapid in BAG1L-overexpressing compared with control-transfected cells. Re-probing the blots with an antibody to β-actin verified loading of equivalent amounts of total protein. Although representative data are provided for two clones in Fig. 7, similar findings were obtained with others (data not shown).

BAG1L Sensitizes PC3 Cells to Growth Inhibition by VDR Ligands—The effects of VDR ligands on p21^{Waf1} expression in PC3 cells suggested that BAG1L-overexpressing cells might display greater sensitivity to the growth suppressive effects of vitamin D$_3$ analogues. Accordingly, clones of PC3 control (Neo)-transfected and BAG1L-transfected cells were cultured in steroid-depleted medium with or without 5×10^{-8} M 1α,25(OH)$_2$ vitamin D$_3$ for 2 days, and the percentage of replicating cells was then estimated by labeling with BrdUrd, which is incor-

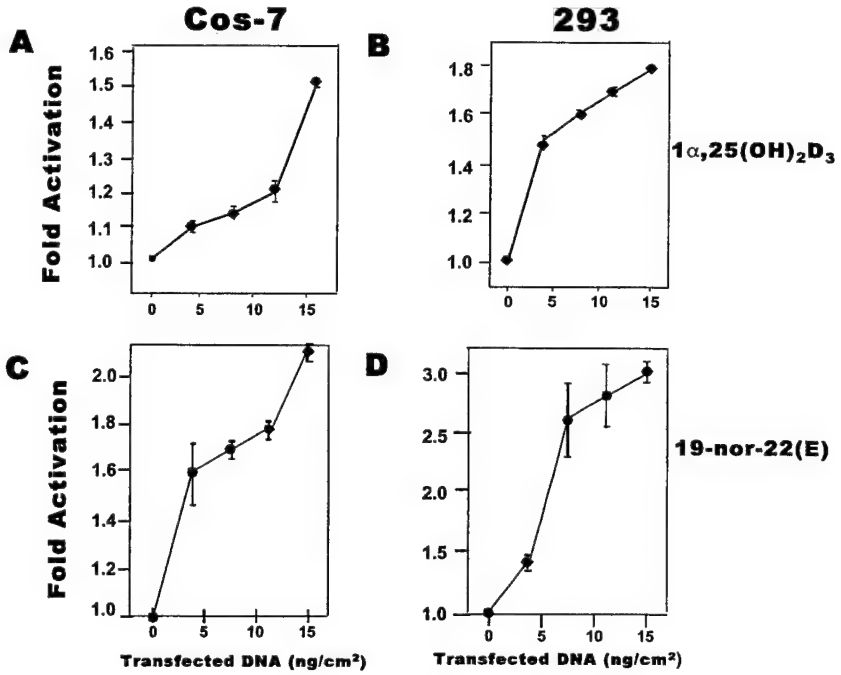

FIG. 6. **BAG1L enhances VDR-mediated trans-activation of p21^{Waf1} promoter.** COS-7 monkey kidney cells (*A* and *C*) and HEK 293T human embryonic kidney cells (*B* and *D*) were transfected by a LipofectAMINE method in 9.4-cm^2 dishes with VDR-encoding plasmid (100 ng), 250 ng of p21-CAT reporter plasmid, 400 ng of pCMV-β-galactosidase, and increasing amounts of pcDNA3-BAG1L expression plasmid, as indicated. One day later, transfected cells were treated with 5×10^{-9} M either 1α,25(OH)$_2$ vitamin D$_3$ (*A* and *B*) or 1α,25-dihydroxy-19-nor-22(*E*)-vitamin D$_3$ (19-nor-22(*E*)) (*C* and *D*) and CAT activity was measured 2 days later, normalizing data relative to β-galactosidase and reporting results as -fold activation relative to cells transfected with pcDNA3 control plasmid instead of pcDNA3-BAG1L. BAG1L did not enhance VDR activity when VDR ligands were omitted from cultures (data not shown).

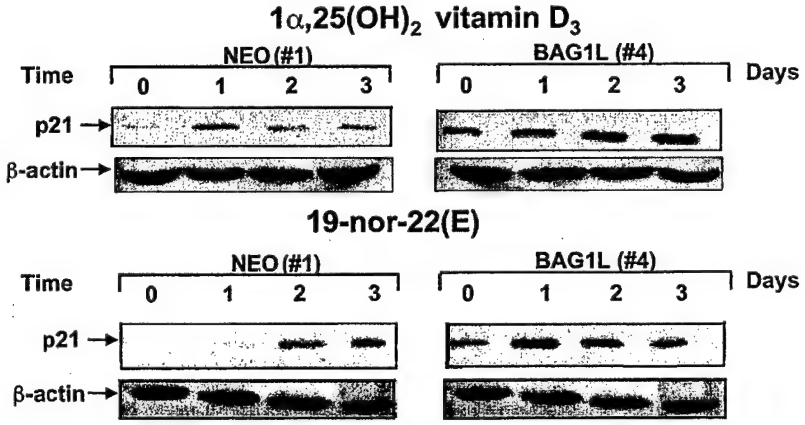

FIG. 7. **BAG1L increases induction of endogenous p21^{Waf1} expression by VDR ligands.** PC-3 cells stably transfected with empty pcDNA3 vector (Neo) or pcDNA3-BAG1L were cultured with 5×10^{-8} M 1α,25(OH)$_2$ vitamin D$_3$ (*top*) or 19-nor-22(*E*) (*bottom*). Cell lysates were prepared after 0, 1, 2, or 3 days of culture, normalized for total protein content (25 μg/lane) and subjected to SDS-PAGE/immunoblot assay using anti-p21 and anti-β-actin antibodies in conjunction with an ECL-based detection method. Data obtained using representative clones (Neo clone 1; BAG1L clone 4) are presented.

porated into the DNA of cells in S-phase. Comparisons were made between two Neo control-transfected clones of PC3 and six BAG1L-transfected clones. The percentage inhibition of cell proliferation induced by VDR ligand was significantly greater for the BAG1L-transfected compared with the Neo-control transfected PC3 cell clones, as determined by contrasting BrdUrd incorporation in each clone when cultured without *versus* with 1α,25(OH)$_2$ vitamin D$_3$ ($p < 0.005$ by unpaired *t* test). Similar results were obtained using the synthetic VDR ligand, 1α,25-dihydroxy-19-nor-22(*E*)-vitamin-D$_3$, and when cell cycle analysis was performed by measuring DNA content of propidium iodide-stained cells instead of by BrdUrd labeling (data not shown). Analysis of cell viability indicated that VDR ligands induced growth arrest without causing a substantial increase in cell death during the time course of these experiments. Immunoblot analysis confirmed that the levels of BAG1L protein were elevated by ~3–10-fold in the BAG1L-transfected clones compared with Neo-control clones of PC3 cells (Fig. 8). In contrast, levels of VDR protein were not different among these clones. Taken together, these data suggest that BAG1L can influence the sensitivity of cells to VDR ligands, with overexpression of BAG1L increasing the sensitivity of prostate cancer cells to the growth-inhibitory effects of VDR ligands.

DISCUSSION

In this report, we provide the first evidence that BAG1L can interact with and regulate the activity of VDR. In contrast, shorter isoforms of BAG1, including BAG1M, BAG1, and BAG1S, lacked the ability to enhance the trans-activation function of VDR. In human cells, at least four BAG1 isoforms can arise from translation-initiation from alternative start codons within a common mRNA, resulting in proteins that all share a common C terminus but that can be distinguished by the length of their N termini: BAG1S, BAG1, BAG1M (previously also termed Rap 46/Hap 46), and BAG1L. Of these, BAG1 and BAG1L are the most abundant *in vivo*, with only scant amounts of BAG1M or BAG1S generally observed (11). Similarly, in mice, BAG1 and BAG1L are the most prevalent isoforms. Moreover, the *bag1* mRNA molecules of mice lack the ATG required for production of BAG1M (11, 25). BAG1 is predominantly, although not exclusively, a cytosolic protein, whereas BAG1L is located entirely in the nucleus of cells (11, 14, 25, 26).

The unique ability of BAG1L to enhance VDR function in cells may be related to the nuclear location of this protein. BAG1L contains candidate nuclear localization sequences, which are not found in other BAG1 isoforms, including nucleoplasmin-like and SV40 large-T antigen-like basic amino acid

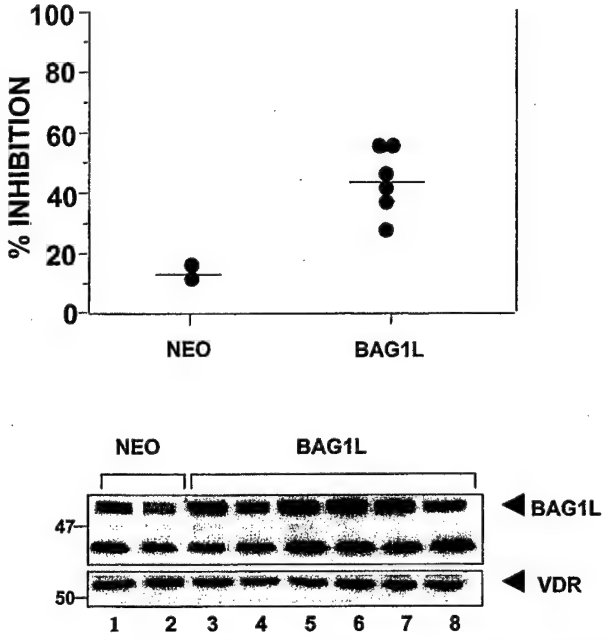

FIG. 8. **BAG1L overexpression increases sensitivity of PC3 cells to growth suppression by 1α,25(OH)$_2$ vitamin D$_3$.** *A*, various clones of control (Neo) or BAG1L-transfected PC3 cells were cultured with or without 5×10^{-8} M 1α,25(OH)$_2$ vitamin D$_3$. BrdUrd was then added to the cultures for 1 h, and cells were recovered, fixed, and stained with anti-BrdUrd antibody, determining the percentage of cells that incorporated BrdUrd into DNA by a flow cytometry method. Data are presented as percentage inhibition based on comparison of untreated and vitamin D$_3$-treated cells. Mean values are indicated by *bars*. *B*, immunoblot data are presented for each of the stably transfected PC3 clones, using lysates normalized for total protein content and probing blots with antibodies specific for BAG1 (*top*) or VDR (*bottom*). The position of BAG1L is indicated by an *arrowhead*. The endogenous BAG1 protein is also seen in the gel (not labeled). Molecular size markers are indicated in kilodaltons.

motifs commonly associated with nuclear import. In contrast, BAG1M contains only a portion of one of these candidate nuclear localization sequences and has been shown to reside in the cytosol unless stimulated to traffic into the nucleus by associating with other proteins, such as glucocorticoid receptors. However, the unique ~50-amino acid N-terminal domain of BAG1L also contains several additional copies of (EEX_4) repeat sequences, which conceivably may have relevance to the ability of this protein to associate with and enhance the function of VDR. In this regard, it has been suggested that these EEX_4 repeats in the BAG1M protein allow it to associate with DNA (28). Thus, the presence of additional copies of this repeating motif in the longer BAG1L protein conceivably could improve its ability targeting to DNA, indirectly enhancing its functional interactions with nuclear hormone receptors. However, other sequences found in the unique N-terminal region of BAG1L might account for its ability to collaborate with VDR, independently of possible DNA binding activity, such as through interactions with co-activator proteins.

The VDR binds its cognate response elements in target genes as either a homodimer (VDR/VDR) or heterodimer (VDR/RXR), leading to activation or repression of transcription via interaction with transcriptional co-factors and the basal transcriptional machinery. Moreover, VDR also can form heterodimers with RAR (29). Previously, we reported that the shorter BAG1 isoform can antagonize RAR activity through what appears to be a direct interaction with RAR, inhibiting binding of RAR/RXR heterodimers to retinoid response elements *in vitro* and suppressing RAR function in cells (13). In contrast, BAG1 does not interact with RXR and does not interfere with RXR signaling in cells. Since the shorter BAG1 protein had no detectable effect on VDR trans-activation function, we consider it unlikely that the observed effects of the longer BAG1L protein on VDR can be attributed to an indirect interaction with this steroid hormone receptor caused by its heterodimerization with RAR.

Association of BAG1L with VDR in co-immunoprecipitation assays was found to be ligand-dependent. Similarly, BAG1L-mediated enhancement of VDR transcriptional activity was also dependent on the presence of VDR ligands. Ligand-dependent effects of BAG1L have also been reported for the AR, where BAG1L likewise enhances trans-activation function of AR in a ligand-dependent manner (14). All members of the NR family of transcription factors contain a ligand-independent and ligand-dependent trans-activation domain: AF1 and AF2, respectively (reviewed in Refs. 29–31). We presume, therefore, that interaction of BAG1L with VDR depends upon the ligand-binding AF2 domain. However, it is unknown at present whether BAG1L binds directly to VDR *versus* associating indirectly through interactions with other VDR-binding proteins whose interactions with VDR are ligand-dependent.

One protein that conceivably could mediate BAG1L interactions with VDR is Hsp70 or Hsc70. All known isoforms of BAG1 contain a conserved C-terminal ~45 amino acid domain (the "BAG domain") that binds the ATPase domain of Hsp70/Hsc70 molecular chaperones with high affinity (11, 26). Thus, if ligand binding to steroid hormone receptors causes conformational changes that permit stable Hsp70/Hsc70 binding, then this could possibly provide a mechanism by which Hsp70/Hsc70 bridges BAG1L to VDR and other members of the NR family. Indeed, deletion of the C-terminal Hsp70/Hsc70-binding domain from BAG1L abrogated its ability to associate with VDR, as determined by co-immunoprecipitation experiments. In this regard, it has been reported that Hsp70 can be found complexed to ligand-activated steroid hormone receptors (*i.e.* estrogen receptor, glucocorticoid receptor, and prolactin receptor) bound to DNA (32–35), further supporting this idea. However, analysis of a mutant of BAG1L lacking the C-terminal Hsc70/Hsp70-binding domain revealed a trans-dominant inhibitory function for this protein, where it suppressed rather than enhanced VDR trans-activation function. A similar trans-dominant inhibitory effect of BAG1L(ΔC) has also been reported previously for AR (14). If the only mechanism for functional interaction of BAG1L with VDR were through association with VDR/Hsp70 complexes, then we would expect deletion of the Hsp70-binding domain to nullify BAG1L effects on VDR but not to interfere with VDR in a trans-dominant manner. Since physiochemical analysis of recombinant BAG1 protein has revealed it to be a monomer (36), it also seems unlikely that the BAG1L(ΔC) mutant interfered with endogenous BAG1L by forming heterodimers/hetero-oligomers with the wild-type BAG1L protein. Thus, we favor the interpretation that BAG1L requires both the Hsc70-binding domain and other upstream regions of this protein for regulating VDR. The purpose of the upstream regions of BAG1L in this context remains to be clarified, but could include interactions with DNA, chromatin, co-activator proteins, or other types of proteins that influence nuclear hormone receptor function.

The mechanism by which BAG1L enhances the trans-activation function of VDR is currently unknown. Given the ability of this protein to bind Hsp70/Hsc70 molecular chaperones, it seems reasonable to speculate that BAG1L may act in collaboration with Hsp70/Hsc70 to produce conformational changes in VDR or VDR-associated proteins such as co-activators that result in a net enhancement of ligand-dependent transcription. However, alternative models are possible. For example, all BAG1 isoforms contain a conserved ubiquitin-like domain,

which has been suggested based on circumstantial evidence to mediate interactions with the 26 S proteosome (37). Accordingly, BAG1L conceivably could facilitate the turnover of proteins within VDR transcription complexes. Although no effect of BAG1L on the steady-state levels of VDR was observed, we cannot exclude the possibility of effects on the turnover of VDR-associated proteins not examined here.

1α,25(OH)$_2$ vitamin D$_3$ and its synthetic analogues can have growth-suppressive effects on certain types of tumor cells, including adenocarcinomas of the prostate (10). However, responses to natural and synthetic VDR ligands vary widely among tumor lines, despite their expression of functional VDR, suggesting that a variety of factors may modulate sensitivity to VDR ligands. The evidence presented here suggests that BAG1L protein levels may represent one determinant of sensitivity to growth inhibition by VDR ligands. Using a prostate cancer cell line, which expresses moderate levels of VDR (800 fmol/mg) but which contains little BAG1L and which displays little responsiveness to VDR ligands, we found that gene transfer-mediated overexpression of BAG1L increased cell cycle arrest induced by VDR ligands. This enhanced sensitivity to growth arrest induced by VDR ligands was associated with increased expression of p21^{Waf1}, a known target gene of VDR (27). However, it remains to be determined whether VDR-mediated growth repression is directly attributable to p21^{Waf1} gene induction by this steroid hormone receptor, and it should be recognized that VDR is likely to affect expression of a wide variety of target genes in cells. Although it cannot be excluded that the down-regulation of p21^{Waf1} seen in PC3 cells treated with natural or synthetic VDR ligands is a consequence rather than a cause of the growth suppressive effects of these compounds, our studies of the p21^{Waf1} promoter in transient transfection reporter gene assays demonstrated that BAG1L is capable of augmenting VDR-mediated transcription of this promoter.

Prostate cancer is the most common lethal form of cancer currently diagnosed in American men, second only to lung cancer as the leading cause of malignancy-associated death among males (38). The primary therapy for men with metastatic disease entails use of anti-androgens and androgen ablation. Hormonal therapy, however, has a limited time of efficacy, and essentially all patients eventually relapse with hormone-refractory disease (10). Androgen ablation therapy also decreases the quality of life as it causes "hot flashes," muscle wasting, and impotence in many men, as well as increasing the risk of osteoporosis. As a result, many physicians prefer to observe rather than treat asymptomatic patients, particularly elderly patients whose PSA levels are rising slowly. An effective, relatively nontoxic agent such as 1α,25(OH)$_2$ vitamin D$_3$ thus could be an ideal type of therapy for use in palliative treatment of metastatic prostate cancer. However, variability in responses to 1α,25(OH)$_2$ vitamin D$_3$-based therapies limits opportunities for clinical applications. Improved understanding of the role of BAG1L and other factors in the regulation of VDR activity and tumor suppression by VDR ligands may contribute to more rational selection of patients for therapy with 1α,25(OH)$_2$ vitamin D$_3$ or its synthetic analogues.

Acknowledgments— We thank H. F. DeLuca for providing vitamin D$_3$ analogues and antibodies, S. Kitada for assistance with fluorescence-activated cell sorter assays, B. Froesch for plasmids, X. Zhang for helpful discussions and reagents, and R. Cornell for manuscript preparation.

REFERENCES

1. Feldman, D. (1997) *Vitamin D* (Feldman, D., Glorieux, F. H., and Pike, J. W., eds.) pp. 3–11, Academic Press, San Diego
2. DeLuca, H. F. (1988) *FASEB J* **2,** 224–236
3. Darwish, H. M., and DeLuca, H. F. (1996) *Prog. Nucleic Acid Res. Mol. Biol.* **53,** 321–344
4. Glass, C. K. (1994) *Endocrine Rev.* **15,** 391–407
5. Silberstein, G. B., and Daniel, C. W. (1987) *Science* **237,** 291–293
6. van Leeuwen, J. P. T. M., and Pols, H. A. P. P. (1997) in *Vitamin D* (Feldman, D., Glorieux, F. H., and Pike, J. W., eds) pp. 1089–1105, Academic Press, San Diego
7. Ly, L. H., Zhao, X.-Y., Holloway, L., and Feldman, D. (1999) *Endocrinology* **140,** 2071
8. Zhao, X. Y., Ly, L. H., Peehl, D. M., and Feldman, D. (1999) *Endocrinology* **140,** 1205–1212
9. Guzey, M., and DeLuca, H. (1997) *Res. Commun. Mol. Pathol. Pharmacol.* **98,** 3–18
10. Gross, C., Peehl, D. M., and Feldman, D. (1997) in *Vitamin D* (Feldman, D., Glorieux, F. H., and Pike, W. P., eds) pp. 1125–1200, Academic Press, San Diego
11. Takayama, S., Krajewski, S., Krajewska, M., Kitada, S., Zapata, J. M., Kochel, K., Knee, D., Scudiero, D., Tudor, G., Miller, G. J., Miyashita, T., Yamada, M., and Reed, J. C. (1998) *Cancer Res.* **58,** 3116–3131
12. Zeiner, M., Gebauer, M., and Gehring, U. (1997) *EMBO J.* **16,** 5483–5490
13. Liu, R., Takayama, S., Zheng, Y., Froesch, B., Chen, G.-q., Zhang, X., Reed, J. C., and Zhang, X.-K. (1998) *J. Biol. Chem.* **273,** 16985–16992
14. Froesch, B. A., Takayama, S., and Reed, J. C. (1998) *J. Biol. Chem.* **273,** 11660–11666
15. Kullmann, M., Schneikert, J., Moll, J., Heck, S., Zeiner, M., Gehring, U., and Cato, A. C. B. (1998) *J. Biol. Chem.* **273,** 14620–14625
16. Perlman, K. L., Sicinski, R. R., Schnoes, H. K., and DeLuca, H. F. (1990) *Tetrahedron Lett.* **31,** 1823–1824
17. Hedlund, T. E., Duke, R. C., and Miller, G. J. (1999) *Prostate* **41,** 154–165
18. Agadir, A., Lazzaro, G., Zheng, Y., Zhang, X.-K., and Mehta, R. (1999) *Carcinogenesis* **20,** 577–582
19. Wu, Q., Li, Y., Liu, R., Agadir, A., Lee, M. O., Liu, Y., and Zhang, X. (1997) *EMBO J.* **16,** 1658–1669
20. El-Deiry, W. S., Tokino, T., Velculescu, V. E., Levy, D. B., Parsons, R., Trent, J. M., Lin, D., Mercer, W. E., Kinzler, K. W., and Vogelstein, B. (1993) *Cell* **75,** 817–825
21. Aladjem, M., Spike, B., Rodewald, L., Hope, T., Klemm, M., Jaenisch, R., and Wahl, G. (1998) *Curr. Biol.* **8,** 145–155
22. Prost, S., Bellamy, C. O., Clarke, A. R., Wyllie, A. H., and Harrison, D. J. (1998) *FEBS Lett.* **425,** 499–504
23. Dame, M. C., Pierce, E. A., Prahl, J. M., Hayes, C. E., and DeLuca, H. F. (1986) *Biochemistry* **25,** 4523–4534
24. Takayama, S., Kochel, K., Irie, S., Inazawa, J., Abe, T., Sato, T., Druck, T., Huebner, K., and Reed, J. C. (1996) *Genomics* **35,** 494–498
25. Packham, G., Brimmell, M., and Cleveland, J. L. (1997) *Biochem. J.* **328,** 807–813
26. Takayama, S., Bimston, D. N., Matsuzawa, S., Freeman, B. C., Aime-Sempe, C., Xie, Z., Morimoto, R. J., and Reed, J. C. (1997) *EMBO J.* **16,** 4887–4896
27. Cohen, M., Padarathsingh, M., and Hendrix, M. (2000) *Am. J. Pathol.* **156,** 355–358
28. Zeiner, M., Niyaz, Y., and Gehring, U. (1999) *Proc. Natl. Acad. Sci. U. S. A.* **96,** 10194–10199
29. Schräder, M., Bendik, I., Becker-André, M., and Carlberg, C. (1993) *J. Biol. Chem.* **268,** 17830–17836
30. Glass, C. K. (2000) in *Introduction to Molecular & Cellular Research,* pp. 83–96, CMRC Endocrine Society Meeting, March 2000, San Diego, CA
31. Rochel, N., Wurtz, J. M., Mitschler, A., Klaholz, B., and Moras, D. (2000) *Mol. Cell* **5,** 173–179
32. Graumann, K., and Jungbauer, A. (2000) *Biochem. J.* **345,** 627–636
33. Koshiyama, M., Konishi, I., Nanbu, K., Nanbu, Y., Mandai, M., Komatsu, T., Yamamoto, S., Mori, T., and Fujii, S. (1995) *J. Clin. Endocrinol. Metab.* **80,** 1106–1112
34. Landel, C. C., Kushner, P. J., and Greene, G. L. (1994) *Mol. Endocrinol.* **8,** 1407–1419
35. Srinivasan, G., Patel, N. T., and Thompson, E. B. (1994) *Mol. Endocrinol.* **8,** 189–196
36. Stuart, J. K., Myszka, D. G., Joss, L., Mitchell, R. S., McDonald, S. M., Takayama, S., Xie, Z., Reed, J. C., and Ely, K. R. (1998) *J. Biol. Chem.* **273,** 22506–22514
37. Lüders, J., Demand, J., and Höhfeld, J. (2000) *J. Biol. Chem.* **275,** 4613–4617
38. Landis, S. H., Murray, T., Bolden, S., and Wingo, P. A. (1999) *Cancer J. Clin.* **49,** 8–31

THE JOURNAL OF BIOLOGICAL CHEMISTRY
Vol. 276, No. 16, Issue of April 20, pp. 12718–12724, 2001
Printed in U.S.A.

Structure-Function Analysis of Bag1 Proteins

EFFECTS ON ANDROGEN RECEPTOR TRANSCRIPTIONAL ACTIVITY*

Received for publication, November 30, 2000, and in revised form, January 19, 2001
Published, JBC Papers in Press, January 19, 2001, DOI 10.1074/jbc.M010841200

Deborah A. Knee‡, Barbara A. Froesch‡§, Ulrike Nuber, Shinichi Takayama, and John C. Reed¶

From The Burnham Institute, La Jolla, California 92037

Bag1 is a regulator of heat shock protein 70 kDa (Hsp70/Hsc70) family proteins that interacts with steroid hormone receptors. Four isoforms of Bag1 have been recognized: Bag1, Bag1S, Bag1M (RAP46/HAP46), and Bag1L. Although Bag1L, Bag1M, and Bag1 can bind the androgen receptor (AR) *in vitro*, only Bag1L enhanced AR transcriptional activity. Bag1L was determined to be a nuclear protein by immunofluorescence microscopy, whereas Bag1, Bag1S, and Bag1M were predominantly cytoplasmic. Forced nuclear targeting of Bag1M, but not Bag1 or Bag1S, resulted in potent AR coactivation, indicating that Bag1M possesses the necessary structural features provided it is expressed within the nucleus. The ability of Bag1L to enhance AR activity was reduced with the removal of an NH_2-terminal domain of Bag1L, which was found to be required for efficient nuclear localization and/or retention. In contrast, deletion of a conserved ubiquitin-like domain from Bag1L did not interfere with its nuclear targeting or AR regulatory activity. Thus, both the unique NH_2-terminal domain and the COOH-terminal Hsc70-binding domain of Bag1L are simultaneously required for its function as an AR regulator, whereas the conserved ubiquitin-like domain is expendable.

Steroid receptors play a crucial role in the development and maintenance of many organs. The androgen receptor (AR)[1] is a ligand-activated transcription factor that is a member of the nuclear receptor superfamily (1). One tissue that exhibits profound dependence on the ligand for this nuclear hormone receptor is the prostate gland. In normal prostate, androgens induce production of growth factors in the stromal cells that cause growth of the luminal secretory epithelial cells (reviewed in Ref. 2). The AR controls gene expression programs in these epithelial cells, resulting in the expression of various proteins characteristic of the differentiated state including prostate-specific antigen (3). Tumors develop from the prostatic epithelial cells and ultimately become independent of the androgenic hormones. Endocrine therapy, either by reducing the levels of androgen or by blockading androgens at the level of the AR, usually results in a favorable clinical response and a dramatic regression of prostate cancer due to apoptotic cell death (4). However, after an initial response to androgen ablation, the prostate cancers eventually become unresponsive if endocrine therapy is continued long term (5).

It remains an open question whether the AR continues to play a role in hormone-independent prostate cancers. Many hormone-insensitive tumors have been found to retain a wild-type AR gene. Moreover, the AR gene is sometimes amplified, or its transcriptional activity may be increased in advanced prostate cancer (6). Therefore, a need exists to understand more about the factors that control the functions of the AR so that the mechanisms responsible for resistance to endocrine therapy can be revealed and eventually alleviated.

In the absence of the ligand, AR and most steroid hormone receptors are maintained in an inactive state complexed with heat shock proteins. Upon binding of the cognate ligand, the receptor dissociates from the inactive complex and translocates to the nucleus in which it binds specific response elements in the promoter and/or enhancer regions of responsive genes (reviewed in Ref. 7). Once bound to the nuclear response element, the nuclear receptor up-regulates or down-regulates transcription by transmitting signals directly to the transcriptional machinery via direct protein-protein interactions. In addition, another class of proteins called coactivators is recruited and serves as bridging molecules between the transcription initiation complex and the nuclear receptor (reviewed in Ref. 8).

Recently, an isoform of the human Bag1 protein (known as Bag1L) has been reported to bind the AR and enhance transcriptional activity in the presence of the ligand (9). Bag1 contains a COOH-terminal "BAG" domain that binds the ATPase domain of heat shock protein 70 kDa (Hsp70/Hsc70) family proteins (10–14) and modulates the activity of Hsc70/Hsp70 family chaperones *in vitro* and *in vivo*. Through this interaction with Hsc70, Bag1 is able to interact with a variety of intracellular proteins and regulate diverse cellular processes relevant to cancer including cell division, cell survival, and cell migration (15–20). However, it is also possible that other non-Hsc70-binding domains in the NH_2-terminal portion of Bag1 mediate interactions with target proteins, thus providing a mechanism for directing Hsc70 family chaperones to specific proteins in the cells. For example, Bag1 contains a ubiquitin-like (UBL) domain, which has been proposed to permit its direct binding to the 26 S proteosome (21). However, the significance of this and other NH_2-terminal regions in Bag1 for

* This work was supported in part by the United States Army Department of Defense Prostate Cancer Research Program Grant DAMD17-98-1-8584, the National Institutes of Health/National Cancer Institute Grant CA-67329, the Susan G. Komen Breast Cancer Foundation (to D. A. K.), The Schweizerische Stiftung fuer medizinisch-biologische Stipendien (to B. A. F.), and the State of California Cancer Research Program Grant CCRP99-00567V-10110). The costs of publication of this article were defrayed in part by the payment of page charges. This article must therefore be hereby marked "*advertisement*" in accordance with 18 U.S.C. Section 1734 solely to indicate this fact.

‡ Both authors contributed equally to the work.

§ Current address: Dept. of Molecular Biology, University of Zurich, Winterthurerstrasse 190, 857 Zurich, Switzerland.

¶ To whom correspondence should be addressed: The Burnham Inst., 10901 N. Torrey Pines Rd., La Jolla, CA 92037. Tel.: 858-646-3140; Fax: 858-646-3194; E-mail: jreed@burnham-inst.org.

[1] The abbreviations used are: AR, androgen receptor; Hsp, heat shock protein; UBL, ubiquitin-like; NLS, nuclear localization sequences; CAT, chloramphenicol acetyltransferase; CT-FBS, charcoal-treated fetal bovine serum; GST, glutathione *S*-transferase; PAGE, polyacrylamide gel electrophoresis; ARE, androgen response element.

transactivation of AR or other steroid hormone receptors is unknown.

It has been shown that at least four isoforms of Bag1 protein can arise from alternative initiation of translation within a common mRNA: Bag1S, Bag1, Bag1M (RAP46/HAP46), and Bag1L (22, 23). These isoforms all contain the Hsc70-binding BAG domain near the COOH terminus as well as the upstream UBL domain, but they differ in the lengths of their amino-terminal regions. Additional motifs have been recognized within the NH_2-terminal segment of the Bag1 proteins including candidate nuclear localization sequences (NLS) and variable numbers of TXSEEX repeat sequences (23, 24). Bag1L, the longest isoform, contains both an SV40-LargeT-like and nucleoplasmin-like candidate NLS preceded by a unique ~50 amino acid-domain. This Bag1 isoform is predominantly nuclear (23). Bag1M (RAP46/HAP46) contains only a portion of the candidate NLS and has been shown to reside in the cytosol unless stimulated to traffic into the nucleus by associating with other proteins, such as the glucocorticoid receptor (24). Bag1 and the shorter and rarer isoform of Bag1S are predominantly found in the cytosol (23).

Bag1 proteins have been reported to interact with and regulate the activity of several members of the nuclear receptor superfamily. For example, Bag1M and Bag1L have been found to repress the activity of the glucocorticoid receptor (24, 25), and Bag1 represses the transcriptional activity of retinoic acid receptors (27). Conversely, Bag1L but not Bag1M or Bag1 can potentiate the transcriptional activity of the AR (9). In this report, we have extended structure-function analysis of Bag1 protein with respect to their regulation of the AR.

MATERIALS AND METHODS

Plasmids—The plasmids pcDNA3-Bag1L, pcDNA3-Bag1L_C, and pcDNA3-Bag1 have been described previously (9). pcDNA3-Bag1M was generated from pcDNA3-Bag1/Bag1M (9) by mutating the initiation codon that gave rise to Bag1 from an ATG to an ATC so that this construct now can give rise only to Bag1M.

The cDNAs encoding various fragments of Bag1 were generated by polymerase chain reaction from the plasmid pcDNA3-Bag1L (9) using the following forward (F) and reverse (R) primers containing *Eco*RI and *Xho*I sites: Bag1S, 5′-GGGAATTCGCCACCATGGCGGCA-3′ (F1) and 5′-CCCTCGAGTCACTCGGCCAGGGCAAAG-3′ (R1); Bag1LΔ1–50, primer 5′-GCGGAATTCGCCACCATGACTGCCAGC-3′ (F2) and R1; Bag1LΔ1–16, 5′-GGGAATTCGAGCGGATGGGTTCCCG-3′ (F3) and R1; Bag1MΔC83, 5′-GGGAATTCATGAAGAAGAAAACCCGGCGCC-3′ (F4) and 5′-CCCCTCGAGTCAAAAACCCTGCTGGATTCCAG-3′ (R2); and Bag1C83 5′-GGGAATTCCTGCCCAAGGATTTGCAAGCTG-3′ and R1.

The polymerase chain reaction products were digested with *Eco*RI and *Xho*I and then directly cloned into the *Eco*RI and *Xho*I sites of the mammalian expression vector pcDNA3 (Bag1S and Bag1LΔ1–50) or pcDNA3-Myc (Bag1LΔ1–16, Bag1MΔC83, and Bag1C83).

The GST-Bag1 fusion proteins were generated from pGEX-4T-Bag1L, pGEX-4T-Bag1LΔC, pGEX-4T-Bag1, pGEX-4T-Bag1ΔC, pGEX-4T-Bag1M, pGEX-4T-Bag1MΔC83, and pGEX-4T-1-Bag1C83. These plasmids were all generated by subcloning the appropriate cDNAs from pcDNA3 clone into the *Eco*RI and *Xho*I sites of pGEX-4T-1 (Amersham Pharmacia Biotech). To generate the nuclear-targeted Bag1 proteins, the appropriate cDNA was subcloned from pcDNA3 clone into the *Eco*RI and *Xho*I sites of pcDNA3-NLS (generated by the insertion of an oligonucleotide containing the SV40-LargeT-like NLS into the *Hin*dIII-*Eco*RI sites of pcDNA3.1).

The reporter pLCI plasmid contains the full-length mouse mammary tumor virus long terminal repeat sequence linked with the chloramphenicol acetyltransferase (CAT) gene (28, 29). The pSG5-AR plasmid contains the cDNA for the wild-type AR (28).

Cell Culture—The monkey kidney COS-7 cell line was obtained from the American Type Culture Collection (Manassas, VA). Cells were maintained in a humidified atmosphere with 5% CO_2 in Dulbecco's modified Eagle's medium supplemented with 10% fetal calf serum, 3 mM glutamine, 100 units/ml penicillin, and 100 μg/ml streptomycin (Life Technologies, Inc.). One day prior to experiments, cells were transferred into charcoal-treated fetal bovine serum (CT-FBS) and Dulbecco's modified Eagle's medium minus Phenol Red to reduce background levels of steroids. R1881 (PerkinElmer Life Sciences) was dissolved in ethanol and added to the cultures at a minimum dilution of 0.0001% (v/v). Control cells received an equivalent amount of solvent only.

Transfections and Enzyme Assays—COS-7 cells at 60% confluency in 12-well plates (Nunc) were transfected by a lipofection method. 1.1 μg of DNA was diluted into 176.5 μl of Opti-MEM (Life Technologies, Inc.) and combined with 3 μl of LipofectAMINE (Life Technologies, Inc.) in 185.5 μl of Opti-MEM. After incubation for 20 min, 0.375 ml of Opti-MEM was added, and the mixtures were overlaid onto monolayers of cells. After culturing with 5% CO_2 for 5 h at 37 °C, 0.75 ml of Opti-MEM containing 20% CT-FBS was added to the cultures. At 32–36 h after transfection, cells were stimulated with 0.1 nM R1881. Cell extracts were prepared 48 h after transfection. For reporter gene assays, cell lysates were made as described previously (30), and assays for β-galactosidase and CAT activity were performed. All transfection experiments were carried out in duplicate, repeated at least three times, and normalized for β-galactosidase activity.

In Vitro Binding Assays—The AR was *in vitro* translated in reticulocyte lysates (TNT lysates, Promega) containing [^{35}S]methionine and then preincubated with 10 nM R1881 for 30 min. Glutathione *S*-transferase (GST) fusion proteins were immobilized on glutathione-Sepharose and blocked in NET-N buffer (20 mM Tris, pH 8.0, 20 mM NaCl, 1 mM EDTA) containing 0.1% Nonidet P-40 and 15% milk for 30 min. The immobilized GST proteins (10 μg) were incubated for 2 h with 10 μl of R1881 treated *in vitro* translated AR in NET-N buffer containing 0.1% Nonidet P-40, proteinase inhibitors, and 10 nM R1881. The beads were washed three times in NET-N buffer containing 0.5% Nonidet P-40 and then boiled in Laemmli SDS sample buffer. The use of equivalent amounts of intact GST fusion proteins and successful *in vitro* translated of the AR was confirmed by SDS-PAGE analysis using Coomassie Blue staining or autoradiography, respectively.

Immunofluorescence—Transfected COS-7 cells were fixed with a −20 °C chilled mix of methanol and acetone (1:1) for 2 min at 20 °C. After fixation the cells were blocked with phosphate-buffered saline containing 3% bovine serum albumin, 2% FBS, and 0.1% goat serum and then incubated for 4 h at 20 °C with anti-Bag1 antibody (Dako Corp., Carpinteria, CA) diluted 1:50 in blocking solution (31). After this incubation, cells were rinsed three times for 10 min with phosphate-buffered saline at 20 °C and then incubated with fluorescein isothiocyanate-conjugated anti-mouse IgG (Dako Corp.), diluted 1:50 in blocking solution for 2 h at 37 °C. Excess secondary antibody was thoroughly washed off with phosphate-buffered saline. The slides were then treated with Mowiol containing 1,4-diazabicylo[2.2.2]octane, and glass coverslips were applied. The stained slides were observed using a laser-scanning confocal microscope (Bio-Rad 1024MP).

Hormone Binding Assay—COS-7 cells at 60% confluency in 10-cm^2 plates were transiently transfected either with empty vectors or a combination of expression vectors encoding for AR, Bag1L, or Bag1 by a lipofection procedure. 10 μg of DNA was incubated with 26 μl of LipofectAMINE (Life Technologies, Inc.) for 20 min, and the mixtures were overlaid onto monolayers of cells. After culturing with 5% CO_2 at 37 °C for 5 h, 1 volume of Opti-MEM containing 20% charcoal-stripped fetal bovine serum (CT-FBS) was added to the cultures. Cells were transferred into 24-well plates 1 day later and grown in CT-FBS medium for an additional 24 h. To determine the hormone binding affinities of the transfected AR, cells were incubated for 2 h with increasing concentrations (0.1–10 nM) of [^{3}H]R1881 (86 ΔCi/nmol, PerkinElmer Life Sciences) in the presence or absence of a 100-fold molar excess of cold R1881. Cells were then washed three times with ice cold phosphate-buffered saline, and radioactivity was determined by scintillation counting. Specific binding was calculated by subtracting the counts/min of cells transfected with a control plasmid from the counts/min of samples transfected with the AR expression plasmid that was treated with the same concentration of the hormone. The results represent the means of three independent experiments.

RESULTS

BAG Domain of Bag1 Is Sufficient to Bind AR in Vitro—The human Bag1 protein exists as four isoforms (Fig. 1*A*), which all contain the same COOH-terminal Hsc70-binding domain and an upstream ubiquitin-like domain but differ in the lengths of their NH_2-terminal regions (23). The Bag1L and Bag1M (RAP46) isoforms of the human Bag1 protein have been previously shown to bind the AR *in vitro* (9, 25). To determine

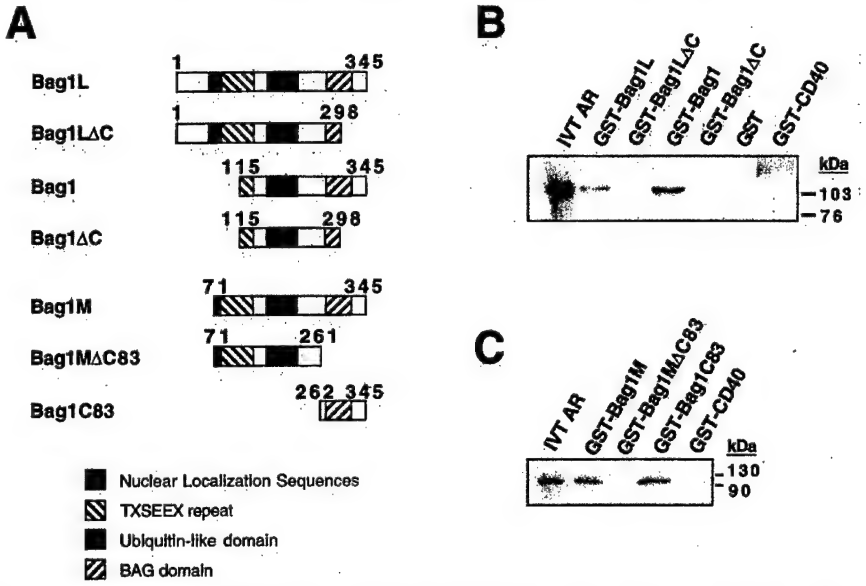

FIG. 1. **The BAG domain is necessary and sufficient for interacting with the AR *in vitro*.** *A*, a *schematic* shows the isoforms of the Bag1 protein, Bag1L, Bag1, Bag1M, and the following deletion mutants: Bag1ΔC and Bag1LΔC, which lack the COOH-terminal last 47 amino acids; Bag1M ΔC83, which lacks the COOH-terminal last 83 amino acids; and Bag1C83, which contains only the last 83 amino acids. The regions encoding the candidate nuclear localization sequences (*black box*), TXSEEX repeat (*downward diagonal striped box*), ubiquitin-like domain (*gray box*), and BAG domain (*upward diagonal striped box*) have been indicated. The *sequence numbers* all refer to the nucleotide numbers of Bag1L and indicate the start codon position for each isoform of Bag1 with respect to Bag1L. *B*, the interaction of the AR with various isoforms of Bag1 or COOH-terminal deletion mutants of these Bag1 proteins was tested by *in vitro* binding assays. The Bag1 isoforms and COOH-terminal mutants were expressed as GST fusion proteins and incubated with AR *in vitro* translated in the presence of [^{35}S]methionine. GST and GST fused to the cytoplasmic domain of CD40 were included as negative controls. GST-Bag1S failed to fold properly and could not be tested. *C*, the interaction of the AR with deletion mutants of Bag1 was tested by *in vitro* binding assays. The Bag1MΔC83 and Bag1C83 were expressed as GST fusion proteins and incubated with AR that was prepared by *in vitro* translation in the presence of [^{35}S]methionine.

whether other isoforms of the human Bag1 protein could interact with the AR, we performed *in vitro* protein interaction assays. The Bag1 isoforms were fused to GST and incubated with *in vitro* translated radiolabeled AR. As shown in Fig. 1*B*, the AR specifically interacted with Bag1L and Bag1 but not with the control proteins GST and GST-CD40. Mutants of Bag1L and Bag1, which lack the COOH-terminal Hsc70-binding domain (ΔC), were unable to interact with the AR in these assays, indicating that the BAG domain is required for interactions with the AR. Moreover, a GST-fusion protein containing only the last COOH-terminal 83 amino acids, GST-Bag1C83, was sufficient for binding to AR under these conditions (Fig. 1*C*). Therefore, we conclude that the BAG domain of Bag1 protein is necessary and sufficient for associating with the AR.

Nuclear Targeting of the Cytoplasmic Bag1 Is Insufficient for Potentiating AR Activity—Although all isoforms of Bag1 interact with the AR *in vitro*, only the Bag1L protein significantly enhances the transcriptional activity of the AR *in vivo* (9). Because the ligand-bound AR is localized to the nucleus (7), only isoforms of the Bag1 protein that are nuclear would be expected to enhance the transcriptional activity of the AR. Therefore, we checked the compartmentalization of the Bag1 proteins by immunofluorescence. COS-7 cells were transfected with plasmids encoding the various Bag1 isoforms followed by immunostaining with an anti-Bag1 monoclonal antibody and analysis by confocal laser-scanning microscopy. Bag1L is exclusively a nuclear protein, whereas all other Bag1 isoforms are predominantly cytosolic (Fig. 2, *left panels*). These findings are consistent with the presence of both nucleoplasmin-like and SV40-LargeT-like nuclear-targeting sequence in the Bag1L protein (22, 23) but not Bag1M, Bag1, or Bag1S. Although the Bag1M (RAP46/HAP46) isoform contains a region of basic residues suggestive of a nuclear targeting sequence (25), it is evidently transported inefficiently into the nucleus. Interestingly, the Bag1L protein may be associated with nuclear substructures given the speckled pattern of the immunofluorescence observed (Fig. 2).

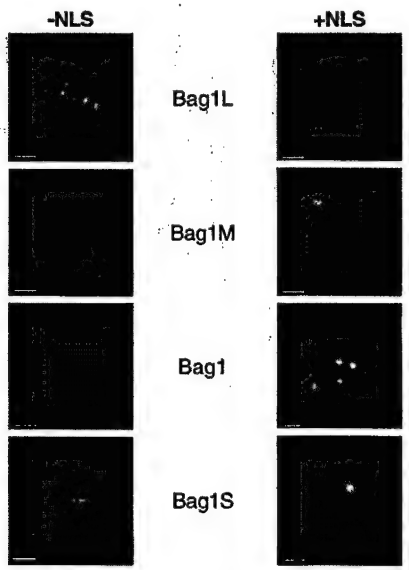

FIG. 2. **Bag1L is the only isoform of Bag1 that is nuclear.** COS-7 cells were transfected with 0.5 μg of pcDNA3-Bag1L, pcDNA3-Bag1M, pcDNA3-Bag1, pcDNA3-Bag1S, pcDNA3-NLS-Bag1L, pcDNA3-NLS-Bag1M, pcDNA3-NLS-Bag1, or pcDNA3-NLS-Bag1S. At 30 h post-transfection, cells were fixed, stained with a monoclonal antibody recognizing Bag1, and visualized using a laser confocal microscope. The nucleus and nucleoli are immunopositive in all transfectants involving NLS-targeted proteins (*right column*).

The difference in cellular distribution of the Bag1 proteins represents a possible explanation for the inability of the cytosolic Bag1 isoforms to enhance the transcriptional activity of the AR. To address this issue, we constructed plasmids that express Bag1L, Bag1M, Bag1, or Bag1S fused to SV40-LargeT-like nuclear-targeting sequences. Nuclear localization of these

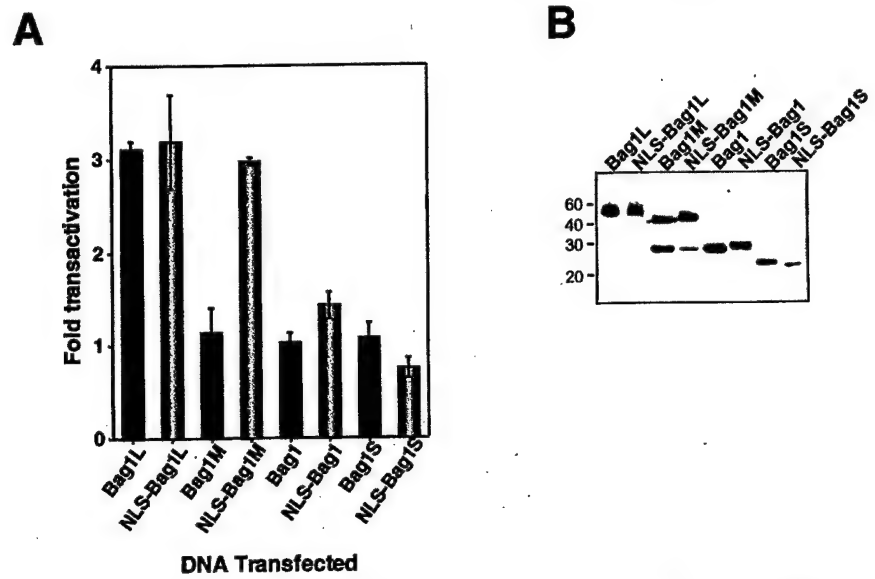

FIG. 3. **Targeting of Bag1M but not the shorter Bag1 isoforms to the nucleus confers the ability to enhance AR-mediated transactivation.** *A*, COS-7 cells were transfected with 0.06 μg of pSG5-AR, 0.5 μg of pLCI, 0.04 μg of pCMV-β-galactosidase, and various amounts of one of the following Bag1 expression plasmids: pcDNA3-Bag1L, pcDNA3-Bag1M, pcDNA3-Bag1, pcDNA3-Bag1S, pcDNA3-NLS-Bag1L, pcDNA3-NLS-Bag1M, pcDNA3-NLS-Bag1, or pcDNA3-NLS-Bag1S. Total DNA was maintained at 1.1 μg by the addition of pcDNA3 control plasmid. At 30 h after transfections, cells were stimulated with 1 nM R1881. Cell extracts were prepared and assayed for CAT and β-galactosidase activity at 40 h after transfection (mean ± S.E., $n = 2$). *B*, COS-7 cells were transfected with one of the following Bag1 expression plasmids: pcDNA3-Bag1L, pcDNA3-Bag1M, pcDNA3-Bag1, pcDNA3-Bag1S, pcDNA3-NLS-Bag1L, pcDNA3-NLS-Bag1M, pcDNA3-NLS-Bag1, or pcDNA3-NLS-Bag1S. At 30 h after transfection, cells were lysed in radioimmune precipitation buffer. Cell extracts (25 μg of total protein) were subjected to SDS-PAGE/immunoblot assay and probed with an antibody to Bag1. The Bag1 expression plasmid pcDNA3-Bag1M produces both the Bag1M and Bag1 proteins due to translational initiation from an internal AUG in Bag1M.

NLS-Bag1 proteins was verified by transfecting COS-7 cells with plasmids expressing the nuclear-targeting Bag1 isoforms and then immunostaining with an antibody that recognizes Bag1 (Fig. 2, *right panels*). Confocal laser-scanning microscopy analysis revealed that all the Bag1 isoforms are located exclusively in the nucleus of transfected cells.

The effects of these nuclear-targeted Bag1 isoforms on AR transcriptional activity were then tested by transfection into COS-7 cells together with an AR-expressing plasmid and an ARE-containing reporter gene. The cells were stimulated with R1881 to activate AR. As shown in Fig. 3*A*, the fusion of heterologous nuclear-targeting sequences to the 5′ end of Bag1L did not alter its ability to enhance the transcriptional activity of the AR. Targeting of Bag1M to the nucleus but not Bag1 or Bag1S was sufficient to enhance the transcriptional activity of the AR. Taken together, these results suggest that the first 70 amino acids of Bag1L are expendable for AR coactivation, whereas the NH_2-terminal region of Bag1M corresponding to amino acids 71–115 of Bag1L is required in conjunction with nuclear localization for enhancing AR function.

Immunoblot analysis showed that the levels of all Bag1 isoforms produced in cells (except Bag1S) were comparable to the nuclear-targeted isoforms, excluding quantitative differences in the levels of these proteins as a trivial explanation for the results (Fig. 3*B*). The difference in the level of expression of Bag1S and NLS-Bag1S makes it difficult to conclude that NLS-Bag1S is without effect on AR-mediated transactivation. The absence of Bag1S from the nucleus would argue against its role in transactivation.

The NH_2-terminal Region of Bag1L Is Required for Efficient Nuclear Localization—The observation that Bag1L is the only isoform that is nuclear suggests that the unique NH_2-terminal domain of Bag1L might perform a role in nuclear targeting or retention. We therefore generated two NH_2-terminal truncation mutants of Bag1L lacking either the first 16 amino acids of Bag1L (Bag1LΔ1–16) or retaining the nuclear-targeting sequences of Bag1L but lacking the NH_2-terminal 50 amino acids that differentiate it from the Bag1M protein (Bag1LΔ1–50).

Both the Bag1LΔ1–16 and Bag1LΔ1–50 proteins retain the candidate nuclear-targeting sequences of Bag1L and therefore should target to nuclei similar to Bag1L. To explore this option, COS-7 cells were transfected with plasmids encoding Bag1LΔ1–16, Bag1LΔ1–50, or Bag1L, and the localization of the resulting proteins was determined by immunofluorescence confocal microscopy. Bag1L and Bag1LΔ1–16 exhibited essentially the same compartmentalization pattern within the cell (Fig. 4*B*, *upper panels*), demonstrating a nuclear speckled pattern of immunostaining. In contrast, the Bag1LΔ1–50 protein was more promiscuous in its subcellular localization. Whereas Bag1LΔ1–50 was found in the same nuclear substructures as Bag1L, the protein was also found in a diffuse cytosolic staining pattern in transfected cells. This finding suggests that amino acids 17–50 of Bag1L may contain sequences necessary for optimal retention of Bag1L in the nucleus.

To contrast these subcellular localization results with coactivation function, COS-7 cells were cotransfected with the AR, an ARE-containing reporter gene, and plasmids encoding Bag1L, Bag1LΔ1–16, or Bag1LΔ1–50. The transfected cells were then stimulated with the synthetic androgen R1881. Bag1LΔ1–50 but not Bag1LΔ1–16 exhibited a decreased ability to enhance the transcriptional activity of the AR (Fig. 4*D*). Taken together, these observations suggest that the correct nuclear targeting/retention of Bag1L is required for optimal functional interactions of Bag1L and the AR.

To confirm this finding, we fused a nuclear-targeting sequence to Bag1L, Bag1LΔ1–16, and Bag1LΔ1–50 and transiently transfected the NLS-fusion constructs into COS-7 cells. Confocal immunofluorescence analysis revealed that NLS-Bag1L, NLS-Bag1LΔ1–16, and NLS-Bag1LΔ1–50 exhibit essentially the same nuclear pattern within the cell (Fig. 4*B*, *lower panels*). Targeting of Bag1L and Bag1LΔ1–16 to the nucleus did not significantly alter their effect on the AR, however, nuclear-targeting of Bag1LΔ1–50 markedly improved its ability to enhance AR transcriptional activity (Fig. 4*D*). Immu-

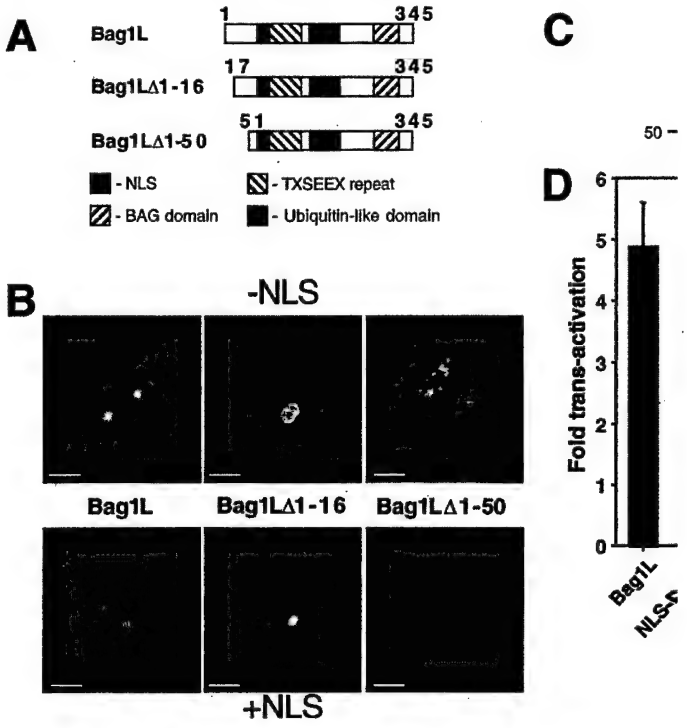

FIG. 4. **The NH_2 terminus of Bag1L is required for its targeting/retention in the nucleus.** *A*, a *schematic* is presented showing deletion mutants of Bag1L, which are lacking the NH_2-terminal 16 (*Bag1LΔ1–16*) or 50 amino acids (*Bag1LΔ1–50*). *B*, COS-7 cells were translated with the following Bag1 expression plasmids: pcDNA3-Bag1L, pcDNA3-Bag1LΔ1–16, pcDNA3-Bag-1LΔ1–50, pcDNA3-NLS-Bag1L, pcDNA3-NLS-Bag1LΔ1–16, or pcDNA3-NLS-Bag-1LΔ1–50. At 30 h post-transfection, cells were fixed, stained, and examined by laser confocal microscopy. *C*, COS-7 cells were transfected as in *A*, and after 30 h the cells were lysed in radioimmune precipitation buffer. Cell extracts (25 μg of total protein) were subjected to SDS-PAGE/immunoblot assay and probed with an antibody to Bag1. *D*, COS-7 cells were transfected with 0.06 μg of pSG5-AR, 0.5 μg of pLCI, 0.04 μg of pCMV-β-galactosidase, and various amounts of the Bag1 expression plasmids used in *B*. Total DNA was maintained at 1.1 μg by the addition of pcDNA3 control plasmid. At 30 h after transfection, cells were stimulated with 1 nM R1881. Cell extracts were prepared and assayed for CAT and β-galactosidase activity at 40 h after transfection (mean ± S.E., $n = 2$).

noblot analysis revealed that all Bag1 isoforms were expressed at similar levels (Fig. 4*C*).

The Ubiquitin-like Domain of Bag1L Is Not Required for Enhancing Transcriptional Activity of AR—The Bag1 protein contains a UBL domain that is conserved within the Bag1 homologues of *Caenorhabditis elegans* and *Schizosaccharomyces pombe* (32). To explore whether this region has functional significance in the enhancement of AR-mediated transcription, we constructed a deletion mutant of Bag1L lacking this region (Bag1LΔUBL) (Fig. 5*A*). COS-7 cells were cotransfected with plasmids expressing Bag1LΔUBL, AR, and an ARE-containing reporter gene plasmid and then stimulated with R1881. As illustrated in Fig. 5*B*, deletion of the UBL domain from Bag1L did not alter its ability to enhance AR-mediated transcription in reporter gene assays, suggesting that this region of Bag1L is not required for functional interactions of Bag1L and the AR. Immunoblot analysis showed that the levels of Bag1LΔUBL produced in cells was comparable to Bag1L (Fig. 5*C*). COS-7 cells were transfected with plasmids encoding Bag1LΔUBL or Bag1L, and the localization of the resulting proteins was determined by immunofluorescence confocal microscopy. Bag1L and Bag1LΔUBL exhibited essentially the same compartmentalization pattern within the cell (Fig. 5*D*), demonstrating a nuclear speckled pattern of immunostaining.

Bag1 Proteins Do Not Alter the Affinity of the AR for Its Ligand—Heat shock proteins and other molecular chaperones are required for placing steroid hormone receptors into a state that is competent to bind steroid ligands (33, 34). The ability of Bag1 proteins to bind and modulate the function of Hsp70/Hsc70 family molecular chaperones (10), therefore, could conceivably alter the ability of AR to bind androgenic hormones. Therefore, we determined the hormone binding affinity of the AR in whole cells in the absence or presence of overexpressed Bag1 or Bag1L. As depicted in Fig. 6*A*, the presence of elevated levels of either Bag1 or Bag1L did not significantly influence the amount of hormone bound to the receptors at any of the hormone concentrations tested. In addition, as revealed by Scatchard analysis (Fig. 6, *B–D*), neither Bag1 nor Bag1L significantly altered the apparent equili (K_d) for R1881. Therefore, Bag1L exe mediated transcription at a stage othe

DISCUSSION

The data presented here confirm isoform of Bag1 capable of enhancing t ity of the AR (9). Thus, despite eviden can interact with the AR *in vitro*, only in cells (9) and alters its transactiv Bag1L is the only isoform that is cons nucleus, one possible explanation is levels of Bag1L may be responsible fc tional interactions with AR complexes shown that Bag1L does not alter the li translocation of the AR (9).

The appendage of an exogenous nucl Bag1M, Bag1, and Bag1S is sufficient t the nucleus. This forced nuclear targeti but not Bag1 or Bag1S the ability to coa it appears that additional structural c Bag1M compared with Bag1 and Bag1S the differential effects of these proteins have suggested that the TXSEEX rep copies, respectively, in Bag1L, Bag1M, repression of the transcriptional activ receptor (24). Thus, these TXSEEX mo functional collaboration of Bag1 with Bag1M are effective at potentiating AR within the nucleus, whereas Bag1 is n

By deleting the NH_2-terminal regic strated a function for this unique pro first time. Subcellular localization ex although Bag1L and Bag1LΔ1–16 w substructures, Bag1LΔ1–50 protein throughout the cells. Therefore, the acids 17 and 50 of Bag1L was foun efficient import into nuclei or retentio speculate that this NH_2-terminal regi

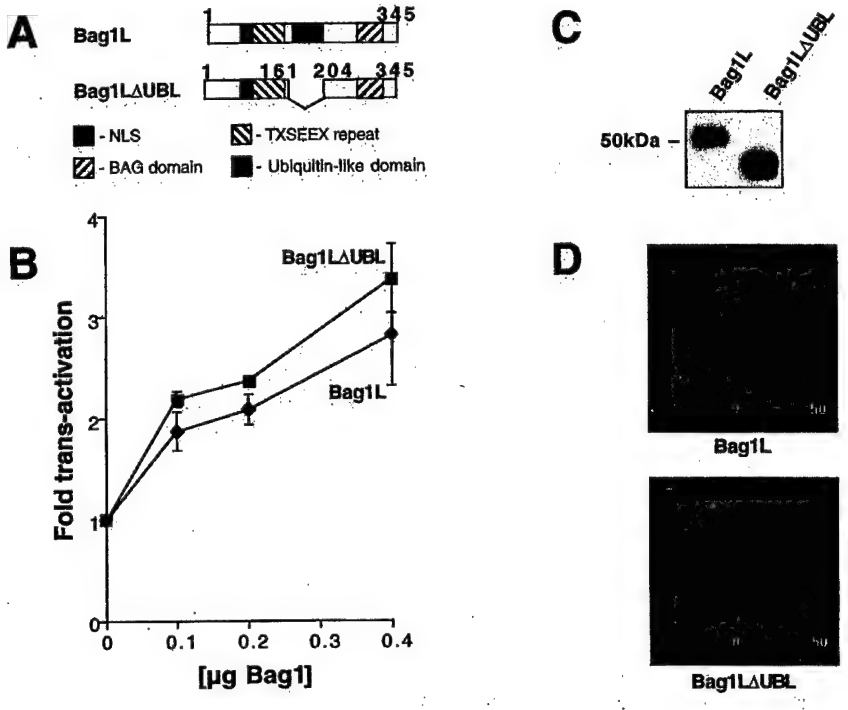

FIG. 5. **Deletion of the ubiquitin-like domain of Bag1L does not alter its ability to enhance AR-mediated transactivation of an ARE-containing reporter.** *A*, a *schematic* is presented showing a deletion mutants of Bag1L that lacks the ubiquitin-like domain. *B*, COS-7 cells were transfected with 0.06 μg of pSG5-AR, 0.5 μg of pLCI, 0.04 μg of pCMV-β-galactosidase, and various amounts of pcDNA3-Bag1L or pcDNA3-Bag1LΔUb. Total DNA was maintained at 1.1 μg by the addition of pcDNA3 control plasmid. At 30 h after transfection, cells were stimulated with 1 nM R1881. Cell extracts were prepared and assayed for CAT and β-galactosidase activity at 40 h after transfection (mean ± S.E., $n = 2$). *C*, COS-7 cells were transfected as in *B*, and after 30 h the cells were lysed in radioimmune precipitation buffer. Cell extracts (25 μg of total protein) were subjected to SDS-PAGE/immunoblot assay and probed with an antibody to Bag1. *D*, COS-7 cells were transfected as in *B*, and at 30 h post-transfection, cells were fixed, stained with a monoclonal antibody recognizing Bag1, and visualized under a laser confocal microscope.

in interactions with the nuclear proteins that serve to anchor Bag1L firmly in the nucleus.

In contrast, deletion of the UBL domain from Bag1L did not impair subcellular targeting or functional collaboration with the AR. A wide variety of proteins have been shown to contain UBLs (reviewed in Ref. 35). These domains can mediate direct interactions with subunits of the proteosome that recognize polyubiquitin chains on proteins that have been targeted for destruction. Recently, Bag1 was reported to bind the 26 S proteosome *in vitro*. The UBL domain is found within all four Bag1 isoforms and is conserved in the Bag1 homologues of other species including the yeast *S. pombe* and the nematode *C. elegans* (32), implying an evolutionarily conserved role for this domain in some aspect of Bag1 function. However, deletion of the UBL domain did not abrogate the stimulatory effect of Bag1L on AR function. Thus, whatever the function of the conserved UBL domain of Bag1 may be, it is expendable for coactivation of steroid hormone receptors.

Similar to the NH_2-terminal unique domain, the COOH-terminal region of Bag1 that is required for Hsc70 binding was found to be essential for potentiation of AR activity. The data reported here and elsewhere indicate that the COOH-terminal Hsc70-binding domain of Bag1 and Bag1L is required for interactions with AR *in vitro* and for coimmunoprecipitation of Bag1L with AR from cell lysates (9). Moreover, we presented novel evidence here that the BAG domain of Bag1 is sufficient for association with the AR *in vitro*. It has therefore been postulated that the interaction of Bag1L with the AR may involve Hsp70. Hsp70/Hsc70 along with Hsp90 and Hsp56 are involved in maintaining nuclear receptors in an inactive conformation in the cytoplasm. Thus, it is possible that Hsc70/Hsp70 family molecular chaperones provide a bridge between the AR and Bag1L. Alternatively, Hsp70 and AR may compete for binding to the BAG domain as has been determined recently for Hsp70 and Raf-1 (36).

Molecular chaperones perform several important functions in the regulation of steroid hormone receptors. For example, a variety of chaperones including Hsc70/Hsp70 is required to achieve receptor conformations that are competent to bind steroid ligands. Thus, enhanced ligand binding represents one possible explanation for the mechanism by which Bag1L poten-

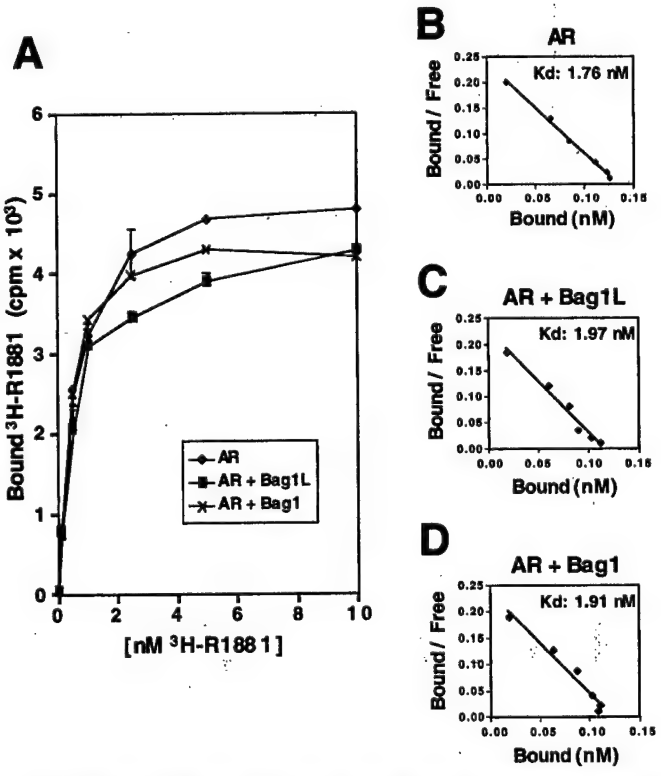

FIG. 6. **Effect of Bag1 and Bag1L on R1881 binding affinity of the AR.** COS-7 cells were transfected with either an empty vector or with expression vectors encoding AR and Bag1 or Bag1L. At 2 days after transfection, cells were incubated in the indicated concentration of [^{3}H]R1881 in the presence or absence of a 100-fold molar excess of cold R1881. The bound radioactivity was calculated by subtracting the amount of radioactivity incorporated in the presence of competitor from the amount incorporated in the absence of competitor. *A*, bound [^{3}H]R1881 as a function of hormone concentration in cells transfected with AR alone (*diamonds*) or in combination with either Bag1 (*crosses*) or Bag1L (*squares*). *B–D*, Scatchard analyses of the data represented in *A*, indicating the calculated K_d for R1881 of AR in the presence or absence of Bag1 and Bag1L. Data represent the mean ± S.E. of three independent experiments.

tiates AR function. If true, however, we would have expected the other isoforms of Bag1 also to potentiate AR activity, given that translation and folding of the AR occurs in the cytosol where the unliganded AR resides in a complex with Hsp90 and other chaperones. Thus, the data reported here demonstrating a lack of effect of Bag1 on the ligand binding affinity of the AR are consistent with the observed differences in the ability of nuclear and cytosolic isoforms of Bag1 to enhance AR activity. In addition, because heat shock proteins sequester AR in the cytosol in an inactive state until bound by specific steroid ligands, it was also possible that Bag1 proteins might regulate cytosol to nuclear translocation of AR, however, we previously demonstrated that this is not the case (9).

Given that Bag1L does not alter the affinity of AR for steroid ligands and does not modulate nuclear translocation of AR, we speculate that it potentiates AR function either by affecting coactivator binding to AR or by altering AR affinity for DNA-binding sites. Interestingly, it has been reported that Bag1M is able to bind to DNA and stimulate basal transcription machinery directly *in vitro* (25). Thus, Bag1L interactions with AR could conceivably increase the affinity of AR-containing transcription complexes for DNA, thereby enhancing transcriptional output of AR-responsive genes. However, given that we failed to see any affect of Bag1L on the binding of the AR to an ARE in gel retardation assays (data not shown), this observation alone cannot account for the unique effects of Bag1L on AR.

Taken together, the data reported here imply that at least two domains within Bag1L are important for its functional collaboration with the AR, namely the TXSEEX repeats and the COOH-terminal BAG domain, which binds Hsp70/Hsc70 family molecular chaperones. Multiple explanations can be envisioned for how these two domains might participate in the regulation of AR. For example, both of these domains might directly or indirectly bind AR. In this regard, it may be relevant that several coactivators of nuclear receptors, such as GRIP-1 and SRC-1, make multiple interactions with nuclear receptors through different domains (26, 37). However, it is equally probable that the BAG domain alone mediates interactions of Bag1L with AR, whereas the TXSEEX repeats associate with other proteins such as coactivators. Difficulties in producing soluble stable TXSEEX repeats alone have precluded us from distinguishing these two mechanisms to date. Another aspect of Bag1L effects on AR is that they may be indirect, involving Bag1L/Hsc70-induced conformational changes in AR that enhance its interactions with coactivators or reduce interactions with corepressors.

Given that only the Bag1L isoform of Bag1 collaborates functionally with the AR, one mechanism by which tissues could alter their responsiveness to androgens is by adjusting the levels of the Bag1L protein produced. The human *bag1* mRNA can generate up to four protein products through alternative mRNA translation from various canonical AUG or non-canonical CUG codons (22, 23). The mouse *bag1* mRNA similarly can produce up to three protein products but lack the AUG that is responsible for generating Bag1M (RAP46) (23). In human tissues and tumor cell lines, it has also been shown that Bag1 and Bag1L are by far the most abundant isoforms of Bag1 produced with little or no Bag1M or Bag1S present (23). Interestingly, whereas Bag1 is ubiquitously expressed throughout the organs of mice and humans, Bag1L production is tissue-specific and found predominantly in hormone-sensitive tissues, such as the testis, ovary, breast, and prostate. Also, in human tumor cell lines, levels of Bag1L tend to be highest in hormone-dependent cancers, such as prostate (AR), breast (estrogen receptor (ER), progesterone receptor (PR), and lymphoid (glucocorticoid receptor) malignancies in which steroid hormones are known to play major roles in the regulation of cell growth, differentiation, and death. Given that Bag1L enhances the transactivation function of AR and that it has been shown to render AR less inhibitable by anti-androgenic drugs (9), it will be interesting to determine whether the levels of Bag1L change during the progression of prostate cancers as they undergo conversion from hormone-responsive to hormone-refractory disease.

Acknowledgments—We thank Dr. Chawnshang Chang for AR and ARE-CAT plasmids and Rachel Cornell for manuscript preparation.

REFERENCES

1. Evans, R. M. (1988) *Science* **240,** 889–895
2. Thompson, T. C. (1990) *Cancer Cells* **2,** 345–354
3. Wolf, D. A., Schulz, P., and Fittler, F. (1992) *Mol. Endocrinol.* **6,** 753–762
4. Westin, P., Stattin, P., Damber, J. E., and Bergh, A. (1995) *Am. J. Pathol.* **146,** 1368–1375
5. Lepor, H., Ross, A., and Walsh, P. C. (1982) *J. Urol.* **128,** 335–340
6. de Vere, W. R., White, R., Meyers, F., Chi, S. G., Chamberlain, S., Siders, D., Lee, F., Stewart, S., and Gumerlock, P. H. (1997) *Cancer Res.* **57,** 314–319
7. Tsai, M. J., and O'Malley, B. W. (1994) *Annu. Rev. Biochem.* **63,** 451–486
8. Freedman, L. P. (1999) *Cell* **97,** 5–8
9. Froesch, B. A., Takayama, S., and Reed, J. C. (1998) *J. Biol. Chem.* **273,** 11660–11666
10. Takayama, S., Bimston, D. N., Matsuzawa, S., Freeman, B. C., Aime-Sempe, C., Xie, Z., Morimoto, R. J., and Reed, J. C. (1997) *EMBO J.* **16,** 4887–4896
11. Zeiner, M., Gebauer, M., and Gehring, U. (1997) *EMBO J.* **16,** 5483–5490
12. Höhfeld, J., and Jentsch, S. (1997) *EMBO J.* **16,** 6209–6216
13. Bimston, D., Song, J., Winchester, D., Takayama, S., Reed, J. C., and Morimoto, R. I. (1998) *EMBO J.* **17,** 6871–6878
14. Nollen, E. A., Brunsting, J. F., Song, J., Kampinga, H. H., and Morimoto, R. I. (2000) *Mol. Cell. Biol.* **20,** 1083–1088
15. Takayama, S., Sato, T., Krajewski, S., Kochel, K., Irie, S., Millan, J. A., and Reed, J. C. (1995) *Cell* **80,** 279–284
16. Wang, H.-G., Takayama, S., Rapp, U. R., and Reed, J. C. (1996) *Proc. Natl. Acad. Sci. U. S. A.* **93,** 7063–7068
17. Bardelli, A., Longati, P., Albero, D., Goruppi, S., Schneider, C., Ponzetto, C., and Comoglio, P. M. (1996) *EMBO J.* **15,** 6205–6212
18. Clevenger, C. V., Thickman, K., Ngo, W., Chang, W.-P., Takayama, S., and Reed, J. C. (1997) *Mol. Endocrinol.* **11,** 608–618
19. Matsuzawa, S., Takayama, S., Froesch, B. A., Zapata, J. M., and Reed, J. C. (1998) *EMBO J.* **17,** 2736–2747
20. Naishiro, Y., Adachi, M., Okuda, H., Yawata, A., Mitaka, T., Takayama, S., Reed, J., Hinoda, Y., and Imai, K. (1999) *Oncogene* **18,** 3244–3251
21. Luders, J., Demand, J., and Höhfeld, J. (2000) *J. Biol. Chem.* **275,** 4613–4617
22. Packham, G., Brimmell, M., and Cleveland, J. L. (1997) *Biochem. J.* **328,** 807–813
23. Takayama, S., Krajewski, S., Krajewska, M., Kitada, S., Zapata, J. M., Kochel, K., Knee, D., Scudiero, D., Tudor, G., Miller, G. J., Miyashita, T., Yamada, M., and Reed, J. C. (1998) *Cancer Res.* **58,** 3116–3131
24. Schneikert, J., Hübner, S., Martin, E., and Cato, A. C. B. (1999) *J. Cell Biol.* **146,** 929–940
25. Zeiner, M., and Gehring, U. (1995) *Proc. Natl. Acad. Sci. U. S. A.* **92,** 11465–11469
26. Ma, H., Hong, H., Huang, S. M., Irvine, R. A., Webb, P., Kushner, P. J., Coetzee, G. A., and Stallcup, M. R. (1999) *Mol. Cell. Biol.* **19,** 6164–6173
27. Liu, R., Takayama, S., Zheng, Y., Froesch, B., Chen, G.-Q., Zhang, X., Reed, J. C., and Zhang, X.-K. (1998) *J. Biol. Chem.* **273,** 16985–16992
28. Lee, H. J., Kokontis, J., Wang, K. C., and Chang, C. (1993) *Biochem. Biophys. Res. Commun.* **194,** 97–103
29. Mowszowicz, I., Lee, H. J., Chen, H. T., Mestayer, C., Portois, M. C., Cabrol, S., Mauvais-Jarvis, P., and Chang, C. (1993) *Mol. Endocrinol.* **7,** 861–869
30. Nielsen, D. A., Chang, T. C., and Shapiro, D. J. (1989) *Anal. Biochem.* **179,** 19–23
31. Takayama, S., Kochel, K., Irie, S., Inazawa, J., Abe, T., Sato, T., Druck, T., Huebner, K., and Reed, J. C. (1996) *Genomics* **35,** 494–498
32. Takayama, S., Xie, Z., and Reed, J. (1999) *J. Biol. Chem.* **274,** 781–786
33. Veldscholte, J., Berrevoets, C. A., Brinkmann, A. O., Grootegoed, J. A., and Mulder, E. (1992) *Biochemistry* **31,** 2393–2399
34. Fang, Y., Fliss, A. E., Robins, D. M., and Caplan, A. J. (1996) *J. Biol. Chem.* **271,** 28697–28702
35. Jentsch, S., and Pyrowolakis, G. (2000) *Trends Cell Biol.* **10,** 335–342
36. Beere, H. M., Wolf, B. B., Cain, K., Mosser, D. D., Mahboubi, A., Kuwana, T., Tailor, P., Morimoto, R. I., Cohen, G. M., and Green, D. R. (2000) *Nat. Cell Biol.* **2,** 469–475
37. Onate, S. A., Boonyaratanakornkit, V., Spencer, T. E., Tsai, S. Y., Tsai, M.-J., Edwards, D. P., and O'Malley, B. W. (1998) *J. Biol. Chem.* **273,** 12101–12108

Apoptosis Induction by 1α,25-Dihydroxyvitamin D_3 in Prostate Cancer[1]

Meral Guzey, Shinichi Kitada, and John C. Reed

Cancer Research Center, The Burnham Institute, La Jolla, California 92037 [M. G., S. K., J. C. R.], and Rigeb, Mam-Tübitak, Gebze 41 470, Kocaeli, Turkey [M. G.]

Abstract

Calcitriol [1α,25-dihydroxyvitamin D_3] is the natural ligand of the vitamin D receptor (VDR). Using cultured prostate cancer (PC) cell lines, LN-CaP and ALVA-31, we studied the effects of 1α,25(OH)$_2$-Vitamin D_3 (VD_3) on expression of several apoptosis-regulating proteins including: (*a*) Bcl-2 family proteins (Bcl-2, Bcl-X_L, Mcl-1, Bax, and Bak); (*b*) the heat shock protein 70-binding protein BAG1L; and (*c*) IAP family proteins (XIAP, cIAP1, and cIAP2). VD_3 induced decreases in levels of antiapoptotic proteins Bcl-2, Bcl-X_L, and Mcl-1, BAG1L, XIAP, cIAP1, and cIAP2 (without altering proapoptotic Bax and Bak) in association with increases in apoptosis. In contrast to VDR-expressing LN-CaP and ALVA-31 cells, VDR-deficient prostate cancer line Du-145 demonstrated no changes in apoptosis protein expression after treatment with VD_3. In sensitive PC cell lines, VD_3 activates downstream effector protease, caspase-3, and upstream initiator protease caspase-9, the apical protease in the mitochondrial ("intrinsic") pathway for apoptosis, but not caspase-8, an initiator caspase linked to an alternative ("extrinsic") apoptosis pathway triggered by cytokine receptors. VD_3 induced declines in antiapoptotic proteins and also stimulated cytochrome *c* release from mitochondria by a caspase-independent mechanism. Moreover, apoptosis induction by VD_3 was suppressed by overexpressing Bcl-2, a known blocker of cytochrome *c* release, whereas the caspase-8 suppressor CrmA afforded little protection. Thus, VD_3 is capable of inhibiting expression of multiple antiapoptotic proteins in VDR-expressing prostate cancer cells, leading to activation of the mitochondrial pathway for apoptosis.

Introduction

Prostate cancer is the most common lethal form of malignancy in North American men and is responsible currently for >200,000 new cancer cases and >31,000 deaths annually in the United States alone. Although adenocarcinoma of the prostate is generally a slow-growing malignancy, morbidity from the disease is nonetheless considerably high because of urological impairment and painful bone metastases. Because prostate cancer incidence increases with advancing age, it is expected that this malignancy will become an increasingly greater problem as worldwide life expectancy improves. The elderly and often debilitated status of many patients with metastatic prostate cancer has raised the need for well-tolerated palliative regimens that slow progression and improve quality of life. Biological response modifiers represent a class of agents with potential utility in this clinical context.

Calcitriol [1α,25(OH)$_2$-Vitamin D_3] is a member of a steroid hormone family that regulates calcium homeostasis and bone formation but which also has been shown to have significant antiproliferative activity when administered to many cancer cell lines *in vitro* (reviewed in Refs. 1, 2). The effects of VD_3[3] are largely mediated via interaction with a specific nuclear VDR. The VDR is a ligand-dependent transcriptional regulator, belonging to the nuclear receptor superfamily (reviewed in Refs. 3, 4). VDR primarily interacts with specific DNA sequences composed of a hexanucleotide direct repeat, binding as either a homodimer or as heterodimer with RXR. Known target genes of VDR include the cell cycle inhibitors $p21^{Waf1}$ and $p27^{Kip1}$, perhaps accounting in part for the antiproliferative effects on VDR ligands on some type of cells.

VDR ligands can also promote apoptosis of some types of tumor cell lines, including the prostate cancer line LN-CaP (5). The target genes relevant to the proapoptotic actions of VDR ligands are largely unknown, but Bcl-2 expression is reportedly down-regulated by treatment of LN-CaP cells with VD_3. Moreover, enforcing Bcl-2 expression by gene transfer sustains survival of these cells in the face of VD_3, implying an important role for this antiapoptotic protein that is known to be overexpressed in many advanced prostate cancers (6).

Bcl-2 is a member of a large family of apoptosis-regulating proteins that target mitochondrial membranes. This protein family includes both antiapoptotic members, such as Bcl-2, Bcl-X_L, and Mcl-1, and proapoptotic members such as Bax and Bak (reviewed in Ref. 7). These proteins govern mitochondrial membrane permeability, either promoting or suppressing release of apoptogenic proteins from these or-

Received 5/10/02; revised 5/20/02; accepted 5/24/02.

[1] Supported by the International Union Against Cancer [International Cancer Technology Transfer (ICRETT) and American Cancer Society Beginning Investigator (ACSBI) awards], the Department of Defense, and Cap-CURE.

[2] To whom requests for reprints should be addressed, at The Burnham Institute, La Jolla, CA 92037. E-mail: jreed@burnham.org.

[3] The abbreviations used are: VD_3, 1α,25(OH)$_2$-vitamin D_3; VDR, vitamin D receptor; RXR, retinoid X receptor; Cyt-c, cytochrome c; PARP, poly(ADP-ribose) polymerase; IAP, inhibitor of apoptosis protein; cRA, 9-*cis*-retinoic acid; DAPI, 4′,6-diamino-2-phenylindole; TUNEL, terminal deoxynucleotidyl transferase-mediated nick end labeling; XTT, sodium 3′-(1-(phenylamino)-carbonyl)-3,4-tetrazolium)-bis-(4-methoxy-6-nitro); Hsp, heat shock protein; zVAD-fmk, benzoyloxycarbonyl-Val-Ala-Asp (OMe)-fluoromethylketone; Ac-DEVD-AFC, benzoyloxycarbonyl-Asp-Glu-Val-Asp-amino-4-trifluoro-methyl-coumarin; Ac-LEHD-AFC, *N*-acetyl-Leu-Glu-His-Asp-AFC; Ac-IETD-AFC, *N*-acetyl-Ile-Glu-Thr-Asp-AFC.

ganelles. Among the mitochondrial proteins released into the cytosol during apoptosis is Cyt-c, which binds and activates Apaf-1, an oligomeric protein that activates the cell death protease, pro-caspase-9. This event triggers a cascade of proteolytic events, with caspase-9 cleaving and activating downstream caspases, which then cleave a variety of substrates responsible for apoptotic demise of the cell.

Additional nonmitochondrial pathways for apoptosis also exist, such as the pathway activated by tumor necrosis factor family death receptors. Upon ligand binding, these death receptors cluster at the plasma membrane, recruiting caspase-binding adapter proteins to their cytosolic domains and triggering protease activation by the induced proximity mechanism (reviewed in Ref. 8). The apical protease in the death receptor pathway is caspase-8, which in turn cleaves and activates directly or indirectly various downstream effector proteases, caspase-3, caspase-6, and caspase-7. Cleavage of specific substrates by effector caspases during apoptosis promotes the degradation of key structural proteins, including PARP and endonuclease regulator ICAD, causing chromatin condensation, DNA fragmentation, and other events typically associated with apoptosis.

The IAPs are a family of antiapoptotic proteins that regulate both the mitochondrial ("intrinsic") and death receptor ("extrinsic") pathways for apoptosis. The antiapoptotic activity of IAPs has been attributed to the conserved baculovirus IAP repeat domain, which is found in all members of this protein family (9). Some of the human IAPs, including XIAPs, c-IAP1, and c-IAP2, have been shown to directly bind procaspase-9 and prevent its activation in response to Cyt-c (10) and to also directly suppress the protease activity of the effector proteases, caspase-3 and caspase-7 (11). Thus, IAPs serve as endogenous antagonists of certain caspases, including downstream proteases that operate at the convergence of the intrinsic and extrinsic pathways for apoptosis. Overexpression of certain IAPs has been documented in cancers, often correlating with adverse clinical outcome (12).

In this report, we characterized the effects on apoptosis gene expression of calcitriol (VD_3) in the VDR-expressing prostate cancer cell lines LN-CaP and ALVA-31. Comparisons were also made with the RXR ligand, cRA, alone and in combination with VD_3. Our findings reveal that VD_3 down-regulates the expression not only of Bcl-2 but also several other antiapoptotic proteins, including Bcl-2 family members, Bcl-X_L and Mcl-1, as well as IAP-family proteins, XIAP, cIAP1, and cIAP2. Dissection of the apoptosis mechanism suggests that VD_3 primarily triggers the mitochondrial pathway for cell death. The findings suggest that VDR ligands could be useful for inducing apoptosis of prostate cancer cells directly or for lowering barriers to apoptosis in prostate cancers before treatment with cytotoxic anticancer drugs or radiation therapy.

Materials and Methods

VDR and RXR Ligands. VD_3 was obtained from Fluka; (Sigma Chemical Co., St. Louis, MO). cRA was obtained from Sigma. These VDR and RXR ligands were prepared as 10^{-3} M stock solutions in ethanol and stored at −20°C. Stock solution concentrations were confirmed by spectroscopy (Spectra Max 190; Molecular Devices), using an extinction coefficient at 220–290 nm of ϵ 18300 for $1\alpha,25(OH)_2D_3$ (13) and 280–388 nm of ϵ 39750 for cRA (14).

Cell Culture and Apoptosis Assays. Human prostate cancer cell lines, Du-145 and LN-CaP, were obtained from American Type Culture Collection (Rockville, MD). The ALVA-31 human prostate cancer cell line was generously provided by Dr. G. Miller (University of Colorado, Denver, CO; Ref. 15). Cells were maintained in humidified atmosphere with 5% CO_2 in RPMI 1640, supplemented with 10% FCS, 1 mM glutamine, 100 units/ml penicillin, and 100 μg/ml streptomycin (Irvine Scientific, Santa Ana, CA). ALVA-31 and LN-CaP cells were cultured with VD_3, cRA, or both of these agents, for up to 4 days. The medium was changed every 2 days, and new hormones were added to the cultures. In some cases, cells were treated with 100 ng/ml of anti-Fas antibody CH-11 (Naka-ku, Nagoya, Japan).

For apoptosis assays, both floating and adherent cells were recovered, and fixed in 3.7% paraformaldehyde in PBS (pH 7.4), and nuclear apoptotic morphology was determined by staining with 2 μg/ml DAPI (mean ± SD; n = 3) with examination by UV microscopy, as described (16). Alternatively, the percentage of cells with fragmented DNA was assayed by the TUNEL method, as described below. In some cases, results were confirmed by labeling of freshly recovered cells with Annexin V-FITC (Biovision, Palo Alto, CA), followed by analysis by flow cytometry (Becton-Dickinson FACScan, San Jose, CA) in the presence of propidium iodide, as described (17). Alternatively, to assess the percentage of cells with fragmented DNA and to monitor cell cycle progression, DNA content analysis was performed by fixing and permeabilizing cells, followed by treatment with RNase and staining with propidium iodide, analyzing cells by flow cytometry essentially as described previously (18). The relative proportion of cells with DNA content indicative of apoptosis (<2N), diploid G_0-G_1 cells (2N), S-phase (>2N but <4N), and G_2-M-phase (4N) was determined.

For cell viability assessments, the trypan blue dye exclusion method was used, counting a minimum of 200 cells/assay and expressing data as a percentage of viable (dye-excluding) cells. Alternatively, relative numbers of viable cells were determined by XTT (Polysciences, Warrington, PA) dye-reduction assays (19). Briefly, cells were seeded at a density of ~2000 cells/well in 96-well, flat-bottomed tissue culture plates (Corning Inc., Corning, NY) in 200 μl of culture medium. The cells were allowed to attach for 24 h, and the medium was replaced with fresh medium containing either ethanol diluent (control), various concentrations of VD_3, cRA, or a combination of these agents. The medium containing vehicle or test compounds was renewed every 2 days during the course of experiments. After incubation, cells were processed by replacing the medium with fresh RPMI 1640 containing XTT reagent (50 μl of 0.025 mM PMS-XTT reagent/well). Plates were incubated 37°C in a humidified atmosphere of 5% CO_2 for ~4 h. Absorbance at 450 nm was read using an automated plate reader (Power Wave 340; Biotechnology Institute, Winooski, VT) using the KC4 program. Pilot assays demonstrated linear production of XTT substrate product for cell densities up to 40,000 cells/well,

which was empirically determined to be within the linear range of the assay under these culture conditions. All experiments were performed in triplicate.

TUNEL Assays. Floating and adherent cells were harvested by trypsinization of cells into culture medium, pelleted by centrifugation, and fixed in 1% formaldehyde in PBS (Sigma) for 15 min on ice. Cells were then recentrifuged at ~200 × *g* for 5 min, washed with PBS, and treated with 70% ethyl alcohol. Then, 5×10^5 cells/sample were centrifuged for 5 min, washed in PBS, and resuspended in 50 μl of a DNA deoxynucleotidyl-transferase (terminal transferase) reaction mixture (Roche Molecular Biochem, Indianapolis, IN), using the manufacturer's protocol for labeling DNA ends with Bio-16-dUTP. After incubation at 37°C for 30 min, 1 ml of PBS was added, followed by centrifugation as before. The cell pellet was suspended in 100 μl of an avidin-FITC buffer consisting of 2.8 μg/ml Avidin-FITC (Sigma), 4× SSC (20× SSC: 3 M NaCl, 0.3 M sodium citrate (pH 7.0), 0.1% Triton X-100, 5% nonfat dried milk (prepared in 0.02% NaN_3; Refs. 20, 21). After incubation at room temperature for 30 min in the dark, the cells were washed once in 1 ml of PBS and then resuspended in 1% formaldehyde/PBS, and propidium iodide was added to a final concentration of 5 μg/ml (Becton-Dickinson) before analysis of samples using a fluorescence-activated cell sorter (Becton-Dickinson FACStar-Plus), using the Cell Quest program data analysis. All experiments were repeated three times.

Antibodies and Immunoblotting. Cell lysates were prepared using RIPA buffer [10 mM Tris (pH 7.4), 150 mM NaCl, 1% Triton X-100, 1% sodium deoxycholate, 0.1% SDS, and 5 mM EDTA], normalized for total protein content (25 μg of protein), and subjected to SDS-PAGE using 12% gels, followed by electrotransfer to 0.45 μm nitrocellulose transfer membranes (Bio-Rad, Hercules, CA). Blots were incubated as described (22) with primary antibodies, including 1:250 (v/v) mouse antihuman p21 monoclonal antibody (IgG1; PharMingen, San Diego, CA), 1:1000 (v/v) mouse anti-PARP monoclonal antibody (PharMingen), 1:1000 (v/v) mouse anti-caspase-8 monoclonal antibody (Alexis Corp., San Diego, CA), 2 μg/ml purified anti-cleaved-caspase-3 rabbit polyclonal antibody (Alexis Corp.), 1:1000 (v/v) anticleaved-caspase-3 (Asp 175) rabbit polyclonal antibody (Cell Signaling, Beverly, MA), 0.05 μg/ml mouse anti-Hsp-60 monoclonal antibody (Stressgen, San Diego, CA), 1 μg/ml purified mouse anti-β-tubulin monoclonal antibody, 1 μg/ml purified mouse anti-Cyt-c monoclonal antibody (PharMingen), 1:2000 (v/v) of rabbit polyclonal antisera recognizing Bcl-2, Bax, or Mcl-1 (23–25), 1:1000 (v/v) of mouse monoclonal (IgG1) specific for human BAG1 (KS6C8; Ref. 26), 1:5000 (v/v) monoclonal anti β-actin clone AC-15 mouse ascites fluid (Sigma), 1:1000 (v/v) GFP rabbit polyclonal antibody (Santa Cruz Biotechnology, Santa Cruz, CA), 1:200 (v/v) cIAP1 rabbit polyclonal antibody (Santa Cruz Biotechnology), 1:250 (v/v) hILP (XIAP) mouse monoclonal antibody, and 1.5 μg/ml affinity-purified rabbit antihuman/mouse cIAP2 (R&D Systems, Minneapolis, MN). Immunodetection was accomplished using horseradish peroxidase-conjugated secondary antibodies (Bio-Rad, Hercules, CA) and an enhanced chemiluminescence detection method (ECL; Amersham/Pharmacia Biotechnology) with exposure to X-ray film (XAR; Eastman Kodak Co., Rochester, NY). Protein bands were quantified by scanning densitometry (low light imaging system, ChemiImager 4000; 4000 × 4.04; Alpha Innotech Corp., San Leandro, CA), and the intensity of each band was calculated as a percentage relative to the band intensity for control (untreated) samples.

Subcellular Fractionation. For Cyt-c release assays, ALVA-31 cells (1.2×10^6 cells/10-cm dish) were treated with 0.1 μM VD_3, with or without 50 μM zVAD-fmk (Biomol, Plymouth Meeting, PA). At various times thereafter, cells were collected for subcellular fractionation analysis, as described previously (27), with slight modifications. Briefly, cells were recovered from cultures by centrifugation, washed with ice-cold PBS, resuspended in 5× volume of buffer A [20 mM HEPES-KOH (pH 7.5), 10 mM KCl, 1.5 mM $MgCl_2$, 1 mM sodium EDTA, and 300 mM sucrose] containing protease inhibitors, and cells were lysed with 30 strokes of a Teflon homogenizer. Nuclei were discarded by centrifugation at 1,200 × *g* for 10 min at 4°C, and the resulting postnuclear lysates were then centrifuged at 7000 × *g* for 25 min at 4°C to obtain a membrane and organelle-enriched fraction (pellet) containing mitochondria. The cytosolic (supernatant) fraction was further clarified by centrifugation at 143,000 × *g* for 60 min at 4°C before analysis. Fractions were normalized for cell equivalents and analyzed by immunoblotting, using antibodies specific for Cyt-c (PharMingen), mitochondrial Hsp-60 (Stressgen), and cytosolic β-tubulin (PharMingen).

Caspase Activity Assays. ALVA-31 cells were stimulated with VD_3, cRA, or the combination of these agents, in the presence or absence of 50 μM zVAD-fmk. At various times thereafter, the cells were lysed on ice in caspase buffer [10 mM Tris (pH 7.3), 25 mM NaCl, 0.25% Triton X-100, and 1 mM EDTA]. Caspase activity in the resulting cell lysates was determined using fluorogenic peptide substrates, including Ac-DEVD-AFC and Ac-LEHD-AFC (Enzyme Systems, Livermore, CA), which had been prepared as stock solutions at 10 mM in DMSO and diluted into caspase buffer immediately before assays. Cell lysates (25 μg protein) were incubated at 30°C with 100 μM LEDH-AFC for caspase-9 activity or DEVD-AFC for caspase-3/caspase-7 activity measurements. For caspase-8 activity assays, 40 μM Ac-IETD-AFC (Biomol, Plymouth Meeting, PA) was used in caspase buffer [50 mM HEPES (pH 7.4), 10% sucrose, 1 mM EDTA, 0.1% 3-[(3-cholamidopropyl)dimethylammonio-1-propanesulfonate, 100 mM NaCl, and 10 mM DTT], measuring substrate cleavage at 37°C. Initial rates of substrate hydrolysis were determined using a Tecan spectroFluor fluorimeter in kinetic mode, with excitation at 400 nm and emission at 500 nm (slit width, 30 nm).

Transfections. ALVA-31 and LN-CaP cells were transiently transfected with various plasmids using LipofectAMINE reagent (Carlsbad, CA). Briefly, cells at ~50% confluence (~2×10^5 cells) in 6-well (9.4-cm^2) plates (Corning, Inc., Corning, NY) in 2 ml/well of steroid-depleted medium were incubated with 1–2.2 μg of plasmid DNA (1 μg pEGFP *versus* pEGFP-Crm A; Refs. 28, 29) or 2.2 μg pRc-CMV *versus* pRcCMV-Bcl-2 (30) combined with 6 μl of LipofectAMINE in a total volume of 375 μl of Opti-MEM medium (Life Technologies, Inc., Grand Island, NY) and

incubated for ~0.5 h. Adherent cells were washed twice with serum-free, prewarmed Opti-MEM, and then DNA/LipofectAMINE mixtures were applied in 750-μl total volume of Opti-MEM. After culturing at 37°C and 5% CO_2 for 3 h, 1.5 ml of 20% charcoal-stripped FCS-containing medium was added per well. After 36 h, medium was changed to fresh RPMI 1640-deficient medium supplied with charcoal-stripped FBS. 0.1 μM VD_3, CH-11 (100 ng/ml), or VP-16 (100 μM) was added, and cells were cultured for various times before performing apoptosis or immunoblot assays. Transfection efficiencies were routinely >70% based on transfecting or cotransfecting a GFP-encoding plasmid. Both floating and adherent cells (after trypsinization) were collected 4 days after addition of VD_3, 1.5 days after VP-16, and 16 h after CH-11 and analyzed by DAPI staining for assessing nuclear morphology.

Statistical Methods and Analysis. All experiments were performed in triplicate, unless otherwise indicated, and mean values were presented as ± SE. A one-way ANOVA was used to statistically analyze the recorded data for XTT assays. When ANOVA indicated significant differences between treatment groups with respect to one of the data sets analyzed, the Dunnett Multiple Comparisons Test was used on that data set to ascertain where the differences occurred. Data on trypan blue exclusion and Annexin V were analyzed by Mann-Whitney *U* Test (31). The software used for these analyses was Graph Pad InStat, v2.02. For all statistical tests, $P < 0.05$ was considered to be significant.

Results

Effects of VD_3 and cRA on Prostate Cancer Cell Growth. The effects of VD_3, cRA, and the combination of these biological response modifiers were tested on the growth of ALVA-31 prostate cancer cells, using an XTT assay for monitoring changes in the relative numbers of viable cells over time in culture. Treatment with concentrations of VD_3 ranging from 1 to 100 nM suppressed the growth of ALVA-31 cells, with ~50% reductions occurring at 6 days after adding VD_3 to cultures (Fig. 1*A*). cRA also suppressed ALVA-31 cell growth but was less potent than VD_3 when tested at similar concentrations. At some concentrations (Fig. 1*A, right panel*), the combination of cRA and VD_3 was superior to VD_3 alone at suppressing growth of ALVA-31 prostate cancer cells *in vitro*. Similar results were obtained either using LNCaP cells instead of ALVA-31 or and when using propidium iodide staining for DNA content analysis as an alternative to XTT assays, providing evidence of G_1 arrest.

The suppression of cell growth seen in cultures of prostate cancer cells treated with VD_3 and cRA was associated with induction of $p21^{Waf1}$, an endogenous inhibitor of cyclin-dependent kinases (Fig. 1*B*). As determined by immunoblotting, levels of $p21^{Waf1}$ increased over time, with higher levels of this cell cycle inhibitor induced in cells treated with VD_3 than cRA, consistent with the differential potency in the growth-suppressing activity of these agents. Loading of equivalent amounts of protein for all samples was confirmed by incubating the same blot with anti-β-tubulin antibody.

The XTT method does not distinguish between suppression of cell growth as a result of proliferation *versus* apoptosis. Thus, to examine the effects of VD_3 and cRA on cell proliferation, we performed cell cycle analysis where cellular DNA content was measured in propidium iodide-stained cells by flow cytometry. As shown in Fig. 1*C*, even after 6 days of culture, either VD_3 or cRA had only a modest effect on prostate cancer cell cycling. In the experiment shown, for example, the ratio of cells with DNA content indicative of G_0-G_1 phase relative to cells in S and G_2-M phases was increased by <15% cRA treatment and by <35% by VD_3. In contrast, the combination of cRA and VD_3 was considerably more potent at inducing G_0-G_1 arrest, causing a >60% increase in the ratio of G_0-G_1:S/G_2-M cells (Fig. 1*C*).

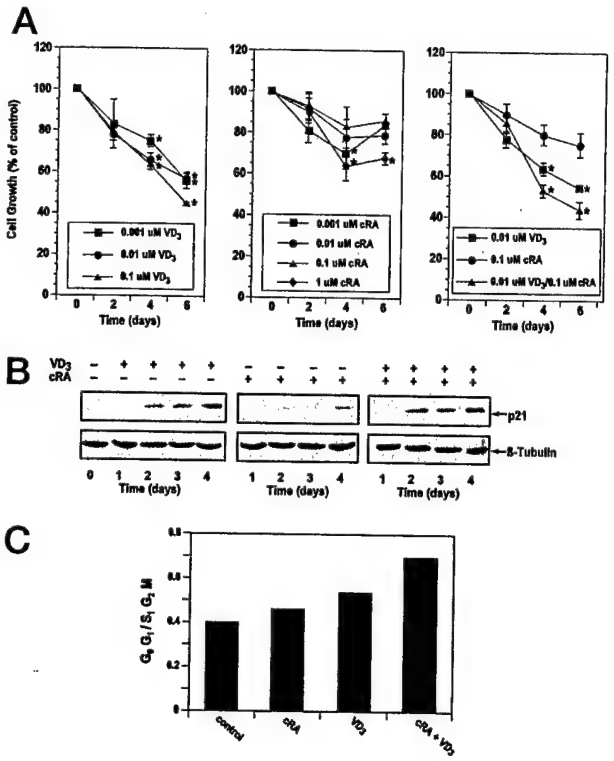

Fig. 1. VD_3 and cRA suppress growth of ALVA-31 prostate cancer cells. *A*, ALVA-31 cells were plated at 2000 cells/well in 96-well plates in 200 μl of medium and cultured for up to 6 days with the indicated concentrations of VD_3 (*left*), cRA (*middle*), or the combination (*right*) of these agents. Medium was changed every 2 days and replaced with fresh medium containing VD_3 and cRA. Relative numbers of viable cells were measured by XTT assay, expressing data as a percentage relative to control (diluent only) treated cells (means; *bars*, SD; $n = 3$). *, statistically significant differences ($P < 0.05$). *B*, ALVA-31 cells were plated at 10^6 cells/10-cm dish in 10 ml of medium with 0.1 μM VD_3, 1 μM cRA, or their combinations. Cell lysates were prepared after 0, 1, 2, 3, or 4 days of culture, normalized for total protein content (25 μg/lane), and subjected to SDS-PAGE immunoblot assay using anti-$p21^{Waf1}$-specific antibody. The same blots were also incubated with an antibody recognizing β-tubulin. *C*, ALVA31 cells were cultured for 6 days with or without 5 nM VD_3, 1 μM cRA, or both of these reagents, as indicated. Cells were recovered from cultured, fixed, permeabilized, treated with RNase, and then stained with propidium iodide. DNA content was analyzed by flow cytometry, and the relative proportion of cells with DNA contents indicative of G_0-G_1 phase was determined relative to cells with DNA content indicative of S or G_2-M-phase cells. A representative experiment is shown.

Effects of VD_3 and cRA on Apoptosis of Prostate Cancer Cell Lines. In addition to suppressing proliferation of prostate cancer cells, we explored whether VD_3, cRA, or the

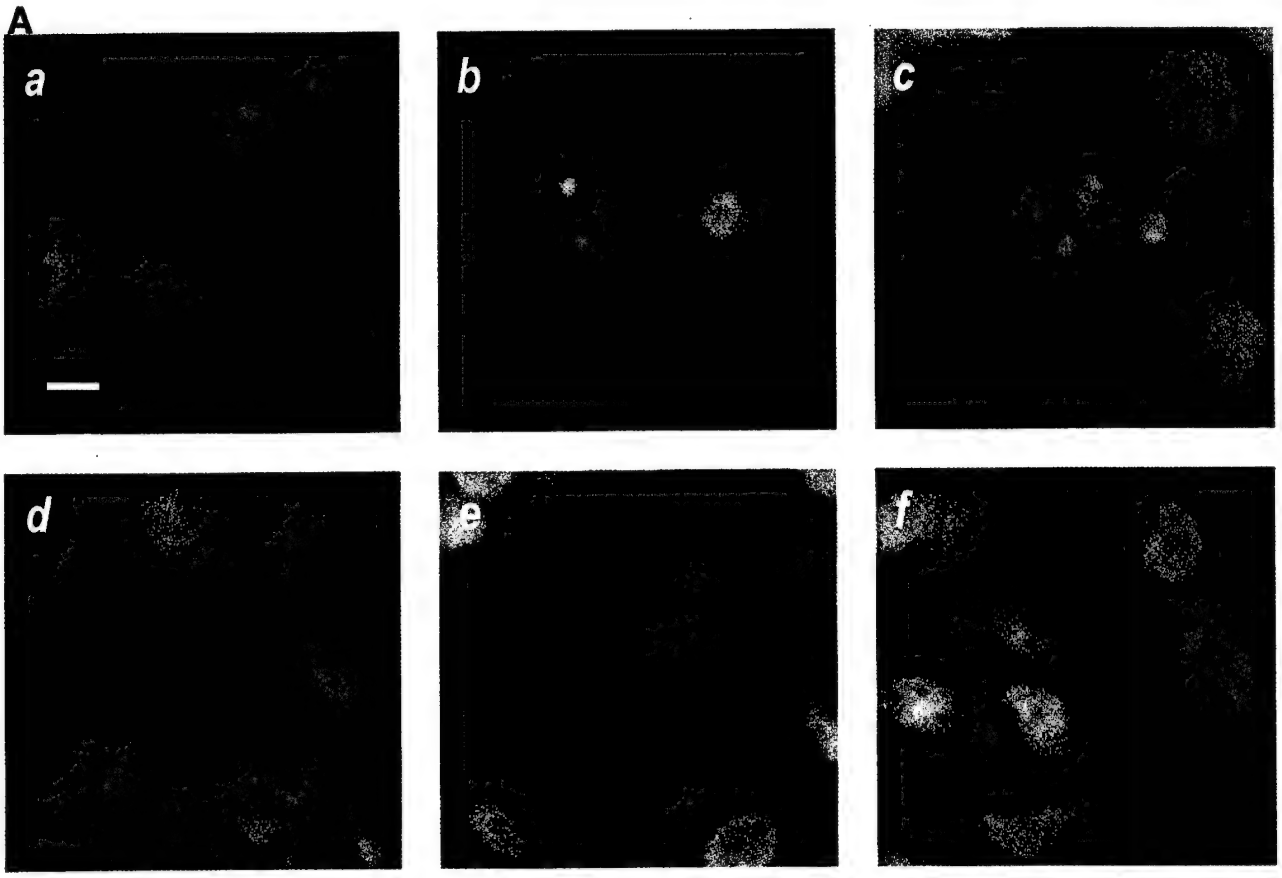

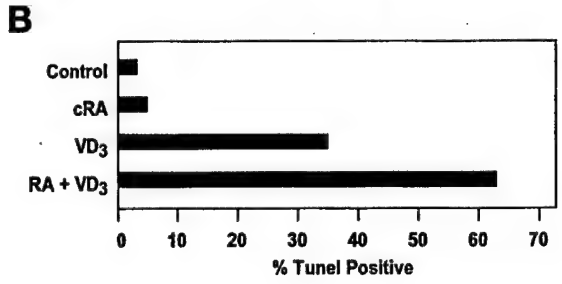

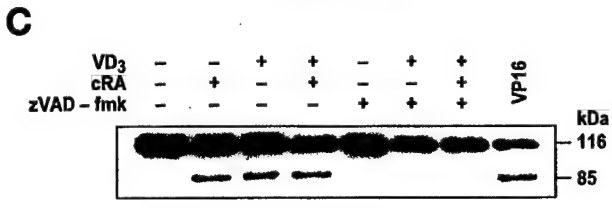

Fig. 2. Induction of apoptosis of prostate cancer cells by VD_3. *A*, ALVA-31 cells were cultured with ethanol diluent (*a* and *d*), 0.1 μM VD_3 (*b* and *e*), or the combination of VD_3 and cRA (*c* and *f*) for 4 days, without (*a–c*) or with (*d–f*) 50 μM zVAD-fmk. Floating and adherent cells were recovered from cultures, pooled, fixed, stained with DAPI, and then examined by UV microscopy (*bar*, 10 μm). *B*, a TUNEL assay was used to determine the percentage of ALVA-31 cells with fragmented DNA, after culture for 4 days with 0.1 μM VD_3, 1 μM cRA, or their combination. Analysis was accomplished by flow cytometry. Data are representative results from a total of three separate experiments. *C*, ALVA cells were cultured for 4 days with 0.1 μM VD_3, 1 μM cRA, or their combination. As a control, cells were also treated with 100 μM of the topoisomerase inhibitor, VP16. Both floating and attached cells were collected after treatment, and cell lysates were prepared, normalized for total protein content (40 μg), and analyzed by SDS-PAGE/immunoblotting using anti-PARP antibody. The positions of the uncleaved M_r 110,000 and cleaved M_r 85,000 PARP bands are indicated.

combination of these agents induces apoptosis of prostate cancer cells. Examination of DAPI-stained cells by UV microscopy showed clear evidence of increased percentages of cells with typical apoptotic morphology in cultures of ALVA-31 and LN-CaP cells treated with VD_3 and to a lesser extent with cRA. Fig. 2 presents some representative results for ALVA-31 cells treated for 4 days with VD_3, cRA, or the combination of these agents. Although precise time-course analysis was not performed, the onset of apoptosis and cell cycle arrest occurred with similar kinetics in cultures of prostate cancer cells treated with VD_3 alone or in combination with cRA.

To confirm that the morphological changes were attributable to apoptosis, the broad-spectrum caspase inhibitor, zVAD-fmk, was included in cultures along with VD_3 and cRA. As shown in Fig. 2*A* (*panels d–f*), 50 μM zVAD-fmk prevented

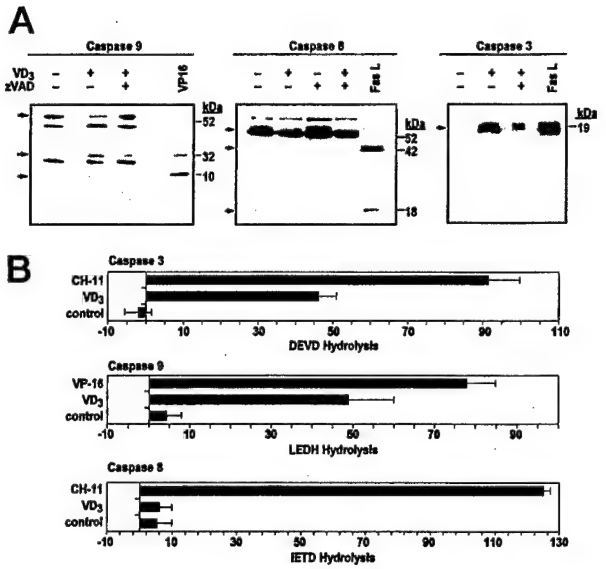

Fig. 3. VD_3 induces caspase-9 processing and activation in prostate cancer cells. *A,* immunoblot analysis was performed using lysates from ALVA-31 cells cultured with 0.1 μM VD_3, 50 μM zVAD-fmk, or a combination of these reagents for 4 days. Alternatively, cells were treated with 100 μM VP16 for 2 days or with 100 ng/ml CH-11 antibody for 16 h before preparing lysates. After normalizing for total protein content (25 μg), lysates were analyzed by SDS-PAGE/immunoblotting using antibodies specific for caspase-9 (*left*), caspase-8 (*middle*), or activate (cleaved) caspase-3 (*right*). *Arrows,* the positions of: *left,* full-length and cleaved large and small subunits of caspase-9; *middle,* full-length pro-caspase-8, a partially processed form of caspase-8, and the fully processed large subunit; and *right,* the processed large subunit of caspase-3. Molecular weight markers are indicated in thousands. *B,* ALVA-31 cells were cultured with 0.1 μM VD_3, 1 μM cRA, or both of these agents, in the absence or presence of 50 μM zVAD-fmk. Cell lysates were prepared, normalized for total protein content, and analyzed for activity of various caspase-family proteases using the AFC-based fluorogenic substrates: *top,* Ac-DEVD-AFC (caspase-3); *middle,* Ac-LEHD-AFC; and *below,* Ac-IETD-AFC (caspase 8). Data represent relative fluorescent units/min (means; *bars,* SD; $n = 3$).

apoptosis, inhibiting chromatin condensation and nuclear fragmentation. Consistent with apoptosis induction, VD_3 also caused DNA fragmentation in cultured ALVA-31 and LN-CaP cells, as determined by TUNEL assays (Fig. 2*B* and data not shown). *c*RA, in contrast, was not effective at inducing significant increases in TUNEL-positive cells, although the combination of *c*RA and VD_3 was slightly more potent than either agent individually (Fig. 2*B*). Similar conclusions were reached by using an Annexin V/propidium iodide staining method to measure percentages of apoptotic cells, as well as based on DNA content analysis where the proportion of cells with subdiploid amounts of DNA were measured (not shown).

During apoptosis, activated caspases cleave various substrate proteins, including the nuclear protein PARP (32). We therefore assessed the effects of VD_3 and *c*RA on PARP cleavage by immunoblot analysis. VD_3, *c*RA, and the combination of these agents induced cleavage of M_r ~110,000 PARP, producing the M_r ~85,000 proteolytic product typical of caspase digestion (Fig. 2*C*). PARP cleavage was blocked by culturing ALVA-31 cells with caspase inhibitor, zVAD-fmk.

Assessment of Caspase Cleavage Patterns in VD_3-treated Prostate Cancer Cells. To preliminarily assess which caspase activation pathway might be responsible for

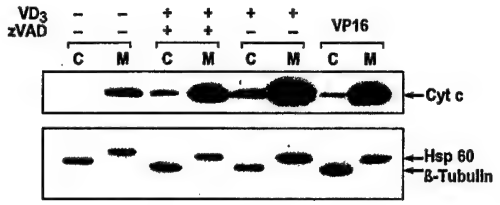

Fig. 4. VD_3 induces caspase-independent release of Cyt-c from mitochondria. ALVA-31 cells were cultured with 0.1 μM VD_3 alone or together with 50 μM caspase inhibitor zVAD-fmk, where zVAD-fmk was added to cultures 12 h before VD_3. Medium was changed every 2 days, replenishing VD_3 and zVAD-fmk. The cells were lysed in isotonic, detergent-free solution 4 days after addition of VD_3. Mitochondria-containing membrane (*M*) and cytosolic (*C*) fractions were prepared, normalized for cell equivalents, and analyzed by SDS-PAGE/immunoblotting using anti-Cyt-c antibody, as well as antibodies recognizing mitochondrial Hsp60 and cytosolic β-tubulin which served as loading controls, and verifying proper fractionation.

VD_3-mediated apoptosis, we analyzed lysates from ALVA-31 cells by immunoblotting using antibodies recognizing either caspase-8 or caspase-9, the apical proteases in the extrinsic and intrinsic pathways, respectively. As shown in Fig. 3*A,* VD_3 induced cleavage of pro-caspase-9, as ascertained by reduced levels of the M_r ~50,000 proform and appearance of a M_r ~35,000 band corresponding to the large subunit of processed caspase-9. The cleavage of pro-caspase-9 was partially blocked by zVAD-fmk, demonstrating the specificity of these results. Treatment of cells with the DNA-damaging agent VP16 served as a control for an apoptotic stimulus known to activate the intrinsic pathway. In contrast to caspase-9, treatment of prostate cancer cells with VD_3 failed to induce proteolytic cleavage of pro-caspase-8. As a control, culturing cells with anti-Fas antibody, CH-11, a known inducer of caspase-8 processing (Fig. 3*A*), stimulated caspase-8 cleavage. In addition to caspase-9, VD_3 also induced cleavage of pro-caspase-3, a downstream effector protease. Active caspase-3 was detected using an antibody that specifically recognizes the cleaved large subunit of the processed protease (Fig. 3*A*).

Caspase activity in VD_3-treated prostate cancer cells was also assessed by enzyme assays, measuring hydrolysis of fluorogenic peptide substrates in cell lysates. As shown in Fig. 3*B,* VD_3 induced increases in protease activity cleaving the caspase-9 substrate Ac-LEHD-AFC and the caspase-3 substrate Ac-DEVD-AFC but not the caspase-8 substrate Ac-IETD-AFC. Treatment of prostate cancer cells with anti-Fas antibody (CH-11) or VP16 served as positive controls for activation of caspase-8 and caspase-9, respectively (Fig. 3*B*).

VD_3 Induces Caspase-independent Release of Cyt-c from Mitochondria. Because Caspase-9 activation commonly results from release of mitochondrial Cyt-c (33), we explored the effects of VD_3 on Cyt-c using subcellular fractionation methods. For these experiments, mitochondria-containing membrane (M) and soluble cytosolic (C) fractions were compared by immunoblotting using anti-Cyt-c antibody. As shown in Fig. 4, nearly all of the Cyt-c was found in M fractions before VD_3 treatment. After culturing prostate cancer cells with VD_3, marked increases in cytosolic Cyt-c

were detected. The release of Cyt-c into the cytosol was not inhibited by zVAD-fmk, indicating a caspase-independent process. Incubating the same blots with antibodies to mitochondrial Hsp60 and cytosolic β-tubulin confirmed successful fractionation of the relevant cellular compartments (Fig. 4). Taken together, these data suggest that VD_3 directly induces release of Cyt-c from mitochondria without requirement for caspases.

Enforced Overexpression of Bcl-2 Protects Prostate Cancer Cells from VD_3-induced Apoptosis. To further explore the whether VD_3 induces apoptosis primarily through the intrinsic pathway, we transiently transfected ALVA-31 cells with a plasmid encoding Bcl-2 protein, an inhibitor of Cyt-c release and suppressor of the intrinsic pathway for caspase activation. In addition, transfectants were generated that express the CrmA protein, a potent inhibitor of caspase-8, which suppresses the extrinsic pathway for cell death (34). Expression of plasmid-derived Bcl-2 and CrmA proteins was verified by immunoblotting. Comparisons were made with control-transfected ALVA-31 cells that received the same plasmid lacking a cDNA insert (Fig. 5, *A* and *B*). Expression efficiency was similar for all transfectants, as determined by cotransfection with a GFP encoding plasmid.

ALVA-31 cells overexpressing Bcl-2 displayed marked resistance to apoptosis induced either by VD_3 or by the DNA-damaging agent VP16 (Fig. 5*C*), which was included as a positive control (35). In contrast, CrmA expression in ALVA-31 cells had comparatively little effect on VD_3-induced apoptosis (Fig. 5*D*). Although reducing the percentage of apoptotic cells, CrmA-mediated protection from VD_3 failed to reach statistical significance, suggesting a relatively minor role for the extrinsic pathway in VD_3-induced apoptosis. In contrast, CrmA potently protected ALVA-31 cells from apoptosis induced by anti-Fas antibody CH11 (Fig. 5*D*), confirming the functionality of this antiapoptotic protein. Altogether, these data lend further support to the contention that VD_3 induces apoptosis predominantly through the intrinsic pathway.

VD_3 Down-Regulates Expression of Antiapoptotic Bcl-2 Family Proteins in Prostate Cancer Cells. Because Bcl-2 family members are critical regulators of mitochondrial release of Cyt-c (8), we assessed the effects of VD_3, cRA, and the combination of these agents on the expression of the Bcl-2 family proteins Bcl-2, Bcl-X_L, Mcl-1, Bax, and Bak by immunoblotting. For these experiments, ALVA-31 cells were cultured for 1–4 days with 0.1 μM VD_3, 1 μM cRA, or the combination of these reagents (note that the combination of 0.1 μM VD_3 and 1 μM cRA showed similar cell growth suppression and apoptotic effects compared with 0.05 μM VD_3 + 0.5 μM cRA; data not shown). Lysates were prepared on sequential days (1–4 days) and analyzed by immunoblotting, using antibodies specific for these Bcl-2-family proteins. At 0.1 μM, a pharmacologically relevant concentration, VD_3 induced time-dependent declines in the steady-state levels of antiapoptotic proteins Bcl-2, Bcl-X_L, and Mcl-1, without substantially changing the levels of proapoptotic proteins, Bax and Bak (Fig. 6). On the basis of quantification of the data by scanning densitometry, reductions in the steady-state levels of Bcl-2, Bcl-X_L, and Mcl-1 began within 1 day of treatment

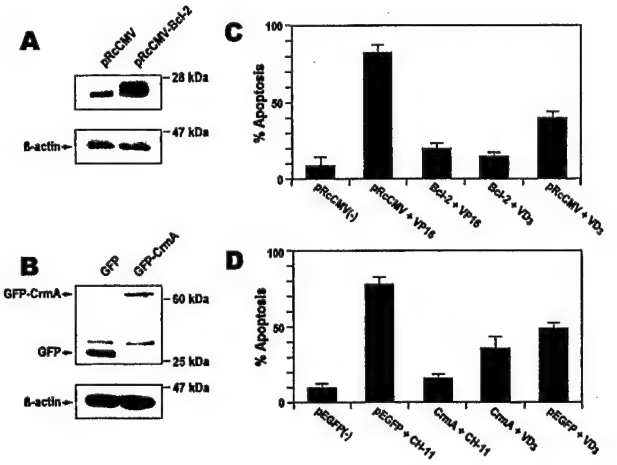

Fig. 5. Overexpression of Bcl-2 suppresses VD_3-induced apoptosis. ALVA-31 cells were transiently transfected with pRcCMV control or pRcCMV-Bcl-2 plasmids (*A*) or with pEGFP ("GFP") or pEGFP-CrmA (*B*). Lysates were prepared from transiently transfected cells treated with vehicle and apoptosis-inducing agents (VD_3 and VP-16) normalized for total protein content (25 μg/lane) and analyzed by SDS-PAGE/immunoblotting using antibodies specific for Bcl-2 (*A*) and GFP (*B*). Blots were also incubated with anti-β-tubulin antibody as a control for loading. *C* and *D*, transfectants of ALVA-31 cells were cultured with or without 0.1 μM VD_3 for 4 days, 100 μM VP16 for 1.5 days, or 100 ng/ml CH11 antibody for 16 h, as indicated, and the percentage of apoptotic cells was determined by DAPI staining (means; *bars*, SD; $n = 3$).

with VD_3, declining to ~20–25% of control by 2–3 days (Fig. 6*C*). cRA (1 μM) was comparatively less potent than VD_3 (0.1 μM) at inducing decreases in the levels of Bcl-2 and Bcl-X_L, although its effects on Mcl-1 expression were similar to VD_3 at the doses tested. The combination of cRA and VD_3 was only slightly more effective than VD_3 alone at reducing expression of antiapoptotic Bcl-2 family proteins, with the clearest difference observed for Bcl-X_L (Fig. 6*C*). These effects of VD_3 and cRA on expression of Bcl-2 family proteins were caspase-independent, as determined by experiments in which ALVA-31 cells were pretreated with zVAD-fmk, demonstrating that VD_3 and cRA reduce levels of these proteins even in the presence of a broad-spectrum caspase inhibitor (data not shown).

VD_3 Reduces Levels of Bag1L Protein. Although VD_3 was found to suppress the expression of several antiapoptotic Bcl-2 family proteins, we explored the possibility that this steroid hormone might additionally have effects on other apoptosis regulators. The human *BAG1* gene encodes at least two Hsp70-binding proteins, including M_r ~50,000 nuclear and M_r ~36,000 cytosolic proteins, which have been implicated in apoptosis suppression and other functions (26, 36). We examined the effects of VD_3, cRA, and the combination of these agents on levels of p36 Bag1 and p50 Bag1L in ALVA-31 prostate cancer cells by immunoblotting, as described above. When applied individually, VD_3 and cRA each profoundly down-regulated levels of p50 Bag1L, having less inhibitory influence on p36 Bag1 (Fig. 6*B*). The combination of VD_3 and cRA resulted in more rapid decline in p50 Bag1L levels compared with treatment of ALVA-31 cells with either agent alone (Fig. 6*C*). Thus, in addition to Bcl-2 family pro-

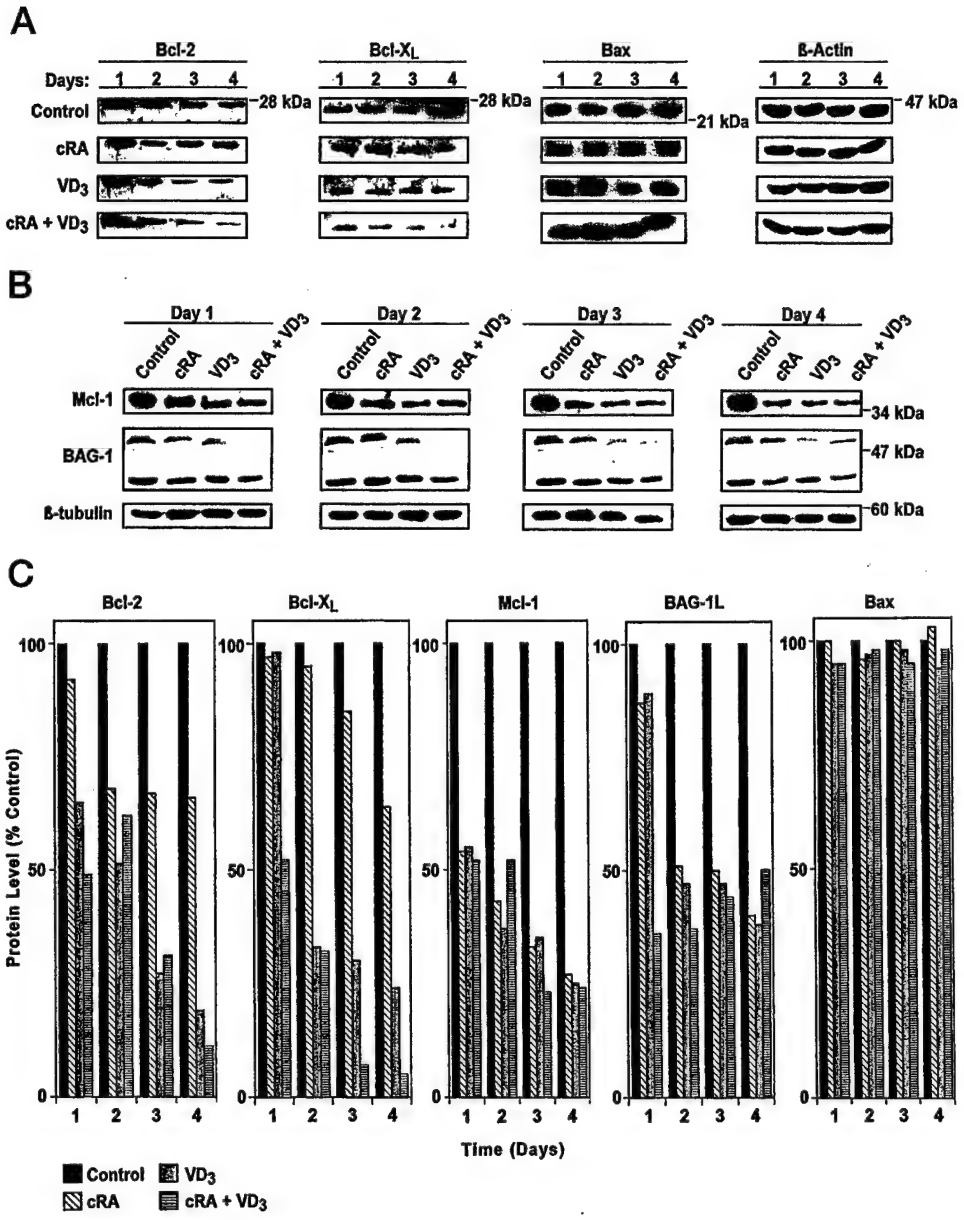

Fig. 6. VD_3 down-regulates expression of antiapoptotic proteins in prostate cancer cell lines. *A*, ALVA cells were cultured for 1–4 days with 0.1 μM VD_3, 1 μM *c*RA, or their combination. Cell lysates were prepared, normalized for total protein content (25 μg/lane), and subjected to SDS-PAGE/immunoblot assay (12% gels) using various antibodies. All data are representative of at least three experiments. *A*, the time course of changes in protein levels was examined for Bcl-2, Bcl-X_L, and Bax, using β-actin as a control. *B*, side-by-side comparisons of effects of VD_3, *c*RA, and the combination of VD_3 and *c*RA were performed at days 1–4, using antibodies recognizing Mcl-1, p50 Bag1L, and p36 Bag1, with β-tubulin serving as a control. *C*, immunoblot data were quantified by scanning densitometry, normalized relative to β-actin or β-tubulin loading controls, and expressed as a percentage relative to diluent-treated (control) cells. Representative data for Bcl-2, Bcl-X_L, Mcl-1, Bag1L, and Bax are presented.

teins, VD_3 also inhibits expression of Bag1L. The reductions in Bag1L levels induced by VD_3 and *c*RA were caspase-independent, as determined by experiments in which ALVA-31 cells were pretreated with zVAD-fmk, demonstrating that VD_3 and *c*RA reduce levels of Bag1L even in the presence of a broad-spectrum caspase inhibitor (data not shown).

VD_3 Reduces Levels of IAP-Family Proteins in VDR-expressing Prostate Cancer Cells. The human IAP-family members XIAP, cIAP1 and cIAP2 are antiapoptotic proteins, which have been demonstrated to directly bind and inhibit certain caspases (11, 37). We analyzed the effects of 0.1 μM VD_3, 1 μM *c*RA, and the combination of VD_3 and *c*RA on levels of XIAP (Fig. 7*A*), cIAP1 (Fig. 7*B*), and cIAP2 (Fig. 7*C*) proteins by immunoblotting in the VDR-expressing prostate cancer cell lines ALVA-31 and LN-CaP. The VDR-insensitive prostate cancer line Du-145 was also tested, as a control. VD_3 reduced levels of XIAP and cIAP1 in both ALVA-31 and LN-CaP but not Du-145 cells. Levels of cIAP2 were also reduced in LN-CaP cells treated with VD_3 but not in the other cell lines tested. Pretreatment of cells with zVAD-fmk demonstrated that VD_3-induced reductions in levels of IAPs were largely, but not entirely, caspase-independent (Fig. 7).

*c*RA had more variable effects on IAP expression, slightly reducing XIAP levels in ALVA-31 and LN-CaP cells, partially depressing levels of cIAP1 in LN-CaP but not ALVA-31, and markedly reducing levels of cIAP2 in LN-CaP but not ALVA-31 cells. IAP expression was not affected by *c*RA treatment of Du-145 cells (Fig. 7). Treatment of ALVA-31 and LN-CaP cells with the combination of VD_3 and *c*RA resulted

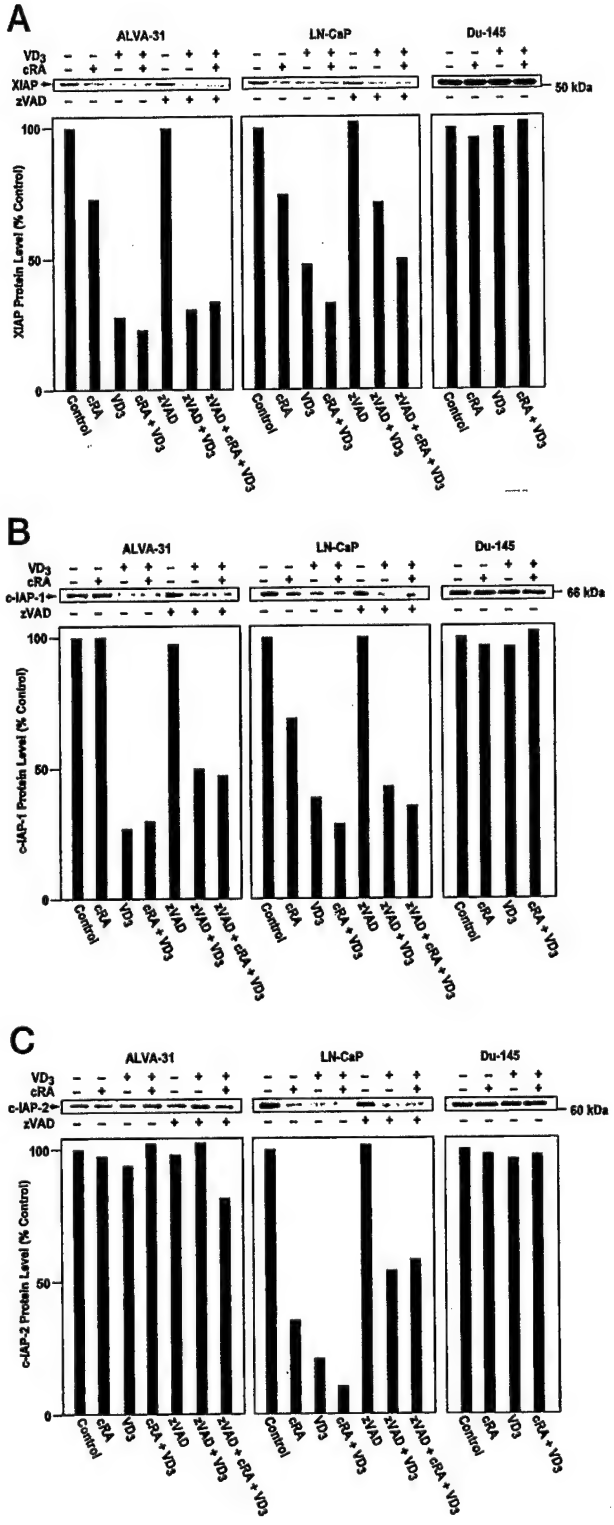

Fig. 7. VD_3 reduces levels of IAP-family proteins in prostate cancer cell lines. Prostate cancer cell lines ALVA-31 (*left*), LN-CaP (*middle*), and Du-145 (*right*) were cultured for 4 days with 0.1 μM VD_3, 1 μM cRA, or their combinations. In some cases, 50 μM caspase inhibitor zVAD-fmk was added to cultures 12 h before VD_3 and cRA. Medium was changed every 2 days, replenishing VD_3, cRA, and zVAD-fmk. Cell lysates were prepared, normalized for total protein content (25 μg/lane), and subjected to SDS-PAGE/immunoblot assay (12% gels) using antibodies recognizing XIAP (*A*), cIAP1 (*B*), or cIAP2 (*C*), followed by antibody detection using an ECL methods with exposure to X-ray film. Immunoblot data (*top*) were quantified by scanning densitometry, expressing results as a percentage relative to diluent-treated (*control*) cells (*bottom*). All data are representative of at least three experiments.

in suppression of IAP-family proteins, similar to VD_3 alone. Again, the suppression of IAP expression by the combination of cRA and VD_3 was partially caspase-independent.

Discussion

The discovery of VDR within the epithelial cells of the prostate almost a decade ago initiated numerous studies to explore the effects of VDR ligands on malignant cells originating from this gland, demonstrating that VD_3 is capable of inhibiting the growth of at least some prostate cancers (1). Recent investigations have provided evidence that this growth inhibition involves both reduced cell division and increased apoptosis (6). Here we confirmed the apoptosis-inducing effects of the naturally occurring VDR ligand, VD_3, on two VDR-expressing prostate cancer cell lines ALVA-31 and LN-CaP and explored the mechanisms involved.

Our data indicate that VD_3 activates the intrinsic pathway for apoptosis in prostate cancer cell lines. The evidence supporting this conclusion includes: (*a*) proteolytic processing of pro-caspase-9 but not pro-caspase-8; (*b*) induction of LEHD (caspase-9) but not IETD (caspase-8) protease activity; (*c*) caspase-independent release of Cyt-c from mitochondria; and (*d*) suppression of VD_3-induced apoptosis by overexpression of Bcl-2 but not CrmA. These findings thus confirm and extend previous studies of the action of VD_3 in human prostate cancer cell lines (6).

The mechanism by which VD_3 induces mitochondrial release of Cyt-c remains to be elucidated. One potential mechanism involves reducing expression of antiapoptotic Bcl-2 family proteins, Bcl-2, Bcl-X_L, and Mcl-1, without affecting levels of proapoptotic proteins, Bax and Bak. Bcl-2 family proteins are central regulators of Cyt-c release from mitochondria, with ratios of anti- and proapoptotic Bcl-2 family members dictating whether Cyt-c remains sequestered in these organelles or is released into the cytosol (reviewed in Ref. 8). Thus, VD_3-mediated down-regulation of the expression of these antiapoptotic Bcl-2 family proteins may precipitate Cyt-c release in prostate cancer cells. Future studies will determine whether VD_3 induces reductions in Bcl-2, Bcl-X_L, and Mcl-1 protein levels through direct transcriptional mechanisms *versus* alternative indirect mechanisms that may involve posttranscriptional steps in gene regulation. In this regard, the delayed time course with which VD_3 triggers reductions in Bcl-2-family proteins tends to suggest an indirect mechanism.

In addition to Bcl-2-family proteins, we observed that VD_3 also reduced levels of other types of proteins known to be involved in apoptosis suppression, including IAP-family members. Although it is possible that VD_3 directly reduces expression of IAP-family gene via VDR-mediated transcriptional mechanisms, the expression of XIAP, cIAP1, and cIAP2 has been reported to be controlled largely through

posttranscriptional mechanisms (38, 39). In this regard, these members of the IAP-family possess an E3-like function because of their ability to bind ubiquitin-conjugating enzymes, inducing their own proteasome-dependent degradation (40). Thus, VD_3 may reduce expression of IAPs by indirect mechanisms. Moreover, more than one mechanism may contribute to the reduced levels of IAPs seen in VD_3-treated prostate cancer cells, given that a caspase-inhibitory compound (zVAD-fmk) partially prevented VD_3-mediated down-regulation of some IAPs in some prostate cancer cell lines.

The caspases that are inhibited by XIAP, cIAP1, and cIAP2 operate in the intrinsic pathway (caspase-9) and at the convergence of the intrinsic and extrinsic pathways (caspase-3 and caspase-7). Thus, the ability of VD_3 to activate the intrinsic pathway could be partly attributable to its effects on IAP expression. However, IAP-family proteins operate downstream of Cyt-c release (11). Thus, although reduced levels of XIAP, cIAP1, and cIAP2 would be expected to lower the threshold of caspase activity needed to execute the apoptotic program, it would not be sufficient to cause Cyt-c release. Consequently, we favor the idea that effects of VD_3 on Bcl-2 family protein are more likely to explain the ability of this steroid hormone to trigger apoptosis of prostate cancer cell.

Interestingly, VD_3 reduced expression of Bag1L, a Hsp70-binding nuclear protein that has been shown to suppress apoptosis when overexpressed in breast cancer cell lines through an unknown mechanism (41). Bag1L has several potential functions, including modulating the transcriptional activity of steroid/retinoid family transcription factors. In this regard, we demonstrated previously that VD_3 induces association of VDR with Bag1L and provided evidence that Bag1L enhances the transcriptional activity of VDR in cells (42). The down-regulation of Bag1L protein levels seen in VD_3-treated cells thus suggests the possibility of a negative feedback mechanism in which reduced levels of Bag1L would be expected to render cells more resistant to VDR ligands. Consequently, the inhibitory effect of VD_3 on prostate cancer cells may be self-limited.

Because VDR binds its cognate response elements in target genes as either a homodimer (VDR/VDR) or heterodimer (VDR/RXR), we contrasted the effects of VD_3 alone and in combination with a RXR ligand, cRA. Although addition of cRA may reduce the amounts of VD_3 required to achieve reductions in antiapoptotic proteins, the net effect of using VD_3 in combination with cRA was not clearly superior to VD_3 alone. However, this issue deserves further investigation, particularly with respect to contrasting various synthetic ligands for VDR and RXR in an effort to identify synergistic combinations that might permit potent anticancer activity with reduced side effects. In this regard, combined treatment of some types of human tumor lines (*e.g.*, NCI-H82, HL-60, and MCF-7) with VDR and RXR ligands has been shown previously to provide superior growth-inhibitory activity compared with either agent individually (43–46). Also, it should be noted that although VD_3 acts through both nuclear VDR-dependent as well as through nongenomic mechanisms, for example causing rapid changes in uptake of Ca^{+2} in the intestine (47), it has been shown clearly that VDR is necessary for the growth-inhibitory actions of this ligand.

Taken together, the data reported here indicate that VD_3 reduces expression of multiple antiapoptotic proteins in sensitive prostate cancer cell lines and that it promotes induction of apoptosis via the mitochondrial (intrinsic) pathway. These findings suggest the possibility of using VDR ligands to reduce thresholds for apoptosis, thus sensitizing prostate cancer cells to the cytotoxic actions of conventional chemotherapeutic drugs and X-irradiation, which also generally induces apoptosis via the intrinsic pathway. An important consideration in applications of VD_3 for prostate cancer treatment is selecting patients whose tumors express VDR and in which VDR is transcriptionally competent, as revealed by the lack of efficacy of VD_3 in Du-145 prostate cancer cells. Thus, VD_3-based therapy for prostate cancer may be most applicable to early-stage tumors. Also, the ability of VD_3 to reduce expression of Bag1L suggests that VD_3 responses will be self-limiting, necessitating that careful consideration is given to the sequencing and timing of combination therapies using VD_3 together with chemotherapy or radiotherapy. These and other issues require further investigation if natural or synthetic ligands of VDR are to be optimally exploited for the treatment of prostate cancer.

Acknowledgments

We thank Drs. H. F. DeLuca and M. R. Uskokovic for VD_3, G. Miller for ALVA-31 cells, and April Sawyer and Rachel Cornell for manuscript preparation. We also thank Drs. K. Welsch, B. Guo, A. Schimmel, M. Naito, F. Stenner-Liewen, M. Renatus, and J. Zapata for valuable discussions and reagents. We acknowledge Eric Watanabe, Juddesign, for excellent graphic art presentations.

References

1. Gross, C., Peehl, D. M., and Feldman, D. Vitamin D and prostate cancer. *In:* D. Feldman, F. H. Glorieux, and W. P. Pike (eds.), Vitamin D, pp. 1125–1200. San Diego: Academic Press, 1997.

2. DeLuca, H. F. The vitamin D story: a collaborative effort of basic science and clinical medicine. FASEB J., *2:* 224–236, 1988.

3. Darwish, H. M., and DeLuca, H. F. Recent advances in the molecular biology of vitamin D action. Prog. Nucleic Acid Res. Mol. Biol., *53:* 321–344, 1996.

4. Glass, C. K. Differential recognition of target genes by nuclear receptor monomers, dimers, and heterodimers. Endocr. Rev., *15:* 391–407, 1994.

5. Blutt, S. E., Allegretto, E. A., Pike, J. W., and Weigel, N. L. 1,25-Dihydroxyvitamin D_3 and 9-*cis*-retinoic acid act synergistically to inhibit the growth of LNCaP prostate cells and cause accumulation of cells in G_1. Endocrinology, *138:* 1431–1437, 1997.

6. Blutt, S. E., McDonnell, T. J., Polek, T. C., and Weigel, N. L. Calcitriol-induced apoptosis in LNCaP cells is blocked by overexpression of Bcl-2. Endocrinology, *141:* 10–17, 2000.

7. Reed, J. C. Apoptosis. *In:* J. N. Abelson and M. I. Simon (eds.), Methods in Enzymology, Vol. 322, pp. 569. San Diego: Academic Press, 2000.

8. Deveraux, Q. L., Schendel, S. L., and Reed, J. C. Antiapoptotic proteins: the Bcl-2 and inhibitor of apoptosis protein families. *In:* J. Narula, V. M. Dixit, and L. W. Miller (eds.), Apoptosis in Cardiovascular Disease, Vol. 19, pp. 57–74. Philadelphia: W. B. Saunders Co., 2001.

9. Deveraux, Q. L., and Reed, J. C. IAP family proteins: suppressors of apoptosis. Genes Dev., *13:* 239–252, 1999.

10. Holcik, M., and Korneluk, R. G. XIAP, the guardian angel. Nat. Rev. Mol. Cell. Biol., *2:* 550–556, 2001.

11. Deveraux, Q. L., Takahashi, R., Salvesen, G. S., and Reed, J. C. X-linked IAP is a direct inhibitor of cell death proteases. Nature (Lond.), *388:* 300–304, 1997.

12. Grossman, D., Kim, P. J., Schechner, J. S., and Altieri, D. C. Inhibition of melanoma tumor growth *in vivo* by survivin targeting. Proc. Natl. Acad. Sci. USA, *98:* 635–640, 2001.

13. Guzey, M., and DeLuca, H. F. A group of deltanoids (vitamin D analogs) regulate cell growth and proliferation in small cell carcinoma. Res. Commun. Mol. Pathol. Pharmacol., *98:* 3–18, 1997.

14. Furr, H. C., Barua, A. B., and Olson, J. A. Analytical methods. *In:* Michael B. Sporn, Anita B. Roberts, and D. S. Goodman (eds.), The Retinoids, Ed. 2, pp. 179–209. New York: Raven Press, 1994.

15. Hedlund, T. E., Duke, R. C., and Miller, G. J. Three-dimensional spheroid cultures of human prostate cancer cell lines. Prostate, *41:* 154–165, 1999.

16. Spector, D. L., Goldman, R. D., and Leinwand, L. A. Analyzing RNA synthesis: nonisotopic labeling. *In:* Cells: A laboratory Manual, Vol. 3, pp. 110–110.10. New York: Cold Spring Harbor Laboratory Press, 1998.

17. Haraguchi, M., Torii, S., Matsuzawa, S., Xie, Z., Kitada, S., Yoshida, H., Mak, T. W., and Reed, J. C. Apoptotic protease activating factor (Apaf-1)-independent cell death suppression by Bcl-2. J. Exp. Med., *191:* 1709–1720, 2000.

18. Wang, H-G., Miyashita, T., Takayama, S., Sato, T., Torigoe, T., Krajewski, S., Tanaka, S., Hovey, L., III, Troppmai, J., Rapp, U. R., and Reed, J. C. Apoptosis regulation by interaction of Bcl-2 protein and Raf-1 kinase. Oncogene, *9:* 2751–2756, 1994.

19. Weislow, O. S., Kiser, R., Fine, D. L., Bader, J., Shoemaker, R. H., and Boyd, M. R. New soluble-formazan assay for HIV-1 cytopathic effects: application to high-flux screening of synthetic and natural products for AIDS-antiviral activity. J. Natl. Cancer Inst., *81:* 577–586, 1989.

20. Darzynkiewicz, Z., Juan, G., Li, X., Gorczyca, W., Murakami, T., and Traganos, F. Cytometry in cell necrobiology: analysis of apoptosis and accidental cell death (necrosis). Cytometry, *27:* 1–20, 1997.

21. Kaufmann, S. H., Mesner, P. W., Jr., Samejima, K., Tone, S., and Earnshaw, W. C. Detection of DNA cleavage in apoptotic cells. *In:* J. C. Reed (ed.), Methods in Enzymology, Vol. 322, pp. 3–15. San Diego: Academic Press, 2000.

22. Harlow, E., and Lane, D. Immunoblotting. Antibodies, pp. 474–506. Cold Spring Harbor, NY: Cold Spring Harbor Laboratory, Inc., 1988.

23. Krajewski, S., Krajewska, M., Shabaik, A., Miyashita, T., Wang, H-G., and Reed, J. C. Immunohistochemical determination of *in vivo* distribution of bax, a dominant inhibitor of Bcl-2. Am. J. Pathol., *145:* 1323–1333, 1994.

24. Krajewski, S., Bodrug, S., Gascoyne, R., Berean, K., Krajewska, M., and Reed, J. C. Immunohistochemical analysis of Mcl-1 and Bcl-2 proteins in normal and neoplastic lymph nodes. Am. J. Pathol., *145:* 515–525, 1994.

25. Krajewski, S., Bodrug, S., Krajewska, M., Shabaik, A., Gascoyne, R., Berean, K., and Reed, J. C. Immunohistochemical analysis of Mcl-1 protein in human tissues: differential regulation of Mcl-1 and Bcl-2 protein production suggests a unique role for Mcl-1 in control of programmed cell death *in vivo*. Am. J. Pathol., *146:* 1309–1319, 1995.

26. Takayama, S., Krajewski, S., Krajewska, M., Kitada, S., Zapata, J. M., Kochel, K., Knee, D., Scudiero, D., Tudor, G., Miller, G. J., Miyashita, T., Yamada, M., and Reed, J. C. Expression and location of Hsp70/Hsc-binding anti-apoptotic protein BAG-1 and its variants in normal tissues and tumor cell lines. Cancer Res., *58:* 3116–3131, 1998.

27. Zhang, H., Huang, Q., Ke, N., Matsuyama, S., Hammock, B., Godzik, A., and Reed, J. C. Drosophila pro-apoptotic bcl-2/bax homologue reveals evolutionary conservation of cell death mechanisms. J. Biol. Chem., *275:* 27303–27306, 2000.

28. Yu, L. H., Kawai-Yamada, M., Naito, M., Watanabe, K., Reed, J. C., and Uchimiya, H. Induction of mammalian cell death by a plant Bax inhibitor. FEBS Lett., *512:* 308–312, 2002.

29. Stenner-Liewen, F., Liewen, H., Zapata, J. M., Pawlowski, K., Godzik, A., and Reed, J. C. CADD, a chlamydia death domain-containing protein that induces apoptosis. J. Biol. Chem., *277:* 9633–9636, 2002.

30. Reed, J. C., Stein, C., Subasinghe, C., Haldar, S., Croce, C. M., Yum, S., and Cohen, J. Antisense-mediated inhibition of *BCL2* proto-oncogene expression and leukemic cell growth and survival: comparisons of phosphodiester and phosphorothioate oligodeoxynucleotides. Cancer Res., *50:* 6565–6570, 1990.

31. Zar, J. H. Two-samples hypotheses. *In:* J. H. Zar (ed.), Biostatistical Analysis, Ed. 2, pp. 122–150. Englewood Cliffs, NJ: Prentice-Hall, Inc., 1984.

32. Whitacre, C. M., and Berger, N. A. Factors affecting topotecan-induced programmed cell death: adhesion protects cells from apoptosis and impairs cleavage of poly(ADP-ribose) polymerase. Cancer Res., *57:* 2157–2163, 1997.

33. Kluck, R. M., Bossy-Wetzel, E., Green, D. R., and Newmeyer, D. D. The release of cytochrome *c* from mitochondria: a primary site for Bcl-2 regulation of apoptosis. Science (Wash. DC), *275:* 1132–1136, 1997.

34. Wagenknecht, B., Schulz, J. B., Gulbins, E., and Weller, M. Crm-A, bcl-2, and NDGA inhibit CD95L-induced apoptosis of malignant glioma cells at the level of caspase-8 processing. Cell Death Differ., *5:* 894–900, 1998.

35. Joza, N., Susin, S. A., Daugas, E., Stanford, W. L., Cho, S. K., Li, C. Y., Sasaki, T., Elia, A. J., Cheng, H-Y. A., Ravagnan, L., Ferri, K. F., Zamzami, N., Wakeham, A., Hakem, R., Yoshida, H., Kong, Y-Y., Mak, T. W., Zúñiga-Pflücker, J. C., Kroemer, G., and Penninger, J. M. Essential role of the mitochondrial apoptosis-inducing factor in programmed cell death. Nature (Lond.), *410:* 549–554, 2001.

36. Knee, D. A., Froesch, B. A., Nuber, U., Takayama, S., and Reed, J. C. Structure-function analysis of Bag1 proteins: effects on androgen receptor transcriptional activity. J. Biol. Chem., *276:* 12718–12724, 2001.

37. Roy, N., Deveraux, Q. L., Takashashi, R., Salvesen, G. S., and Reed, J. C. The c-IAP-1 and c-IAP-2 proteins are direct inhibitors of specific caspases. EMBO J., *16:* 6914–6925, 1997.

38. Tamm, I., Kornblau, S. M., Segall, H., Krajewski, S., Welsh, K., Kitada, S., Scudiero, D. A., Tudor, G., Qui, Y. H., Monks, A., Andreeff, M., and Reed, J. C. Expression and prognostic significance of IAP-family genes in human cancers and myeloid leukemias. Clin. Cancer Res., *6:* 1796–1803, 2000.

39. Holcik, M., Lefebvre, C., Yeh, C., Chow, T., and Korneluk, R. G. A new internal-ribosome-entry-site motif potentiates XIAP-mediated cytoprotection. Nat. Cell Biol., *1:* 190–192, 1999.

40. Yang, Y., Fang, S., Jensen, J. P., Weissman, A. M., and Ashwell, J. D. Ubiquitin protein ligase activity of IAPs and their degradation in proteasomes in response to apoptotic stimuli. Science (Wash. DC), *288:* 874–877, 2000.

41. Kudoh, M., Knee, D. A., Takayama, S., and Reed, J. C. Bag1 proteins regulate growth and survival of ZR-75-1 human breast cancer cells. Cancer Res., *62:* 1904–1909, 2002.

42. Guzey, M., Takayama, S., and Reed, J. C. BAG1L enhances *trans*-activation function of the vitamin D receptor. J. Biol. Chem., *275:* 40749–40756, 2000.

43. Guzey, M., Sattler, C., and DeLuca, H. F. Combinational effects of vitamin D3 and retinoic acid (all *trans* and 0 *cis*) on proliferation, differentiation, and programmed cell death in two small cell lung carcinoma cell lines. Biochem. Biophys. Res. Commun., *249:* 735–744, 1998.

44. Freedman, L. P., and Lemon, B. D. Structural and functional determinants of DNA binding and dimerization by the vitamin D receptor. *In:* D. Feldman, F. H. Glorieux, and W. P. Pike (eds.), Vitamin D, pp. 127–148. San Diego: Academic Press, 1997.

45. Morosetti, R., and Koeffler, H. P. Vitamin D compounds and analogs: effects on normal and abnormal hematopoiesis. *In:* D. Feldman (ed.), Vitamin D, pp. 1155–1166. San Diego: Academic Press, 1997.

46. Colston, K. Vitamin D and breast cancer: therapeutic potential of new vitamin D analogs. *In:* D. Feldman, F. H. Glorieux, and J. W. Pike (eds.), Vitamin D, pp. 1107–1123. San Diego: Academic Press, 1997.

47. Brasitus, T. A., and Sitrin, M. D. Chemoprevention of colon cancer by vitamin D_3 and its metabolites/analogs. *In:* D. Feldman, F. H. Glorieux, and W. P. Pike (eds.), Vitamin D, pp. 1141–1154. San Diego: Academic Press, 1997.

Structural analysis of BAG1 cochaperone and its interactions with Hsc70 heat shock protein

Klára Briknarová[1,2], Shinichi Takayama[1,2], Lars Brive[1], Marnie L. Havert[1], Deborah A. Knee[1], Jesus Velasco[1], Sachiko Homma[1], Edelmira Cabezas[1], Joan Stuart[1], David W. Hoyt[3], Arnold C. Satterthwait[1], Miguel Llinás[4], John C. Reed[1] and Kathryn R. Ely[1]

[1]The Burnham Institute, La Jolla, California 92037, USA. [2]These two authors contributed equally to this work. [3]EMSL, Pacific Northwest National Laboratory, Richland, Washington 99352, USA. [4]Department of Chemistry, Carnegie Mellon University, Pittsburgh, Pennsylvania 15213, USA.

BAG-family proteins share a conserved protein interaction region, called the 'BAG domain', which binds and regulates Hsp70/Hsc70 molecular chaperones. This family of cochaperones functionally regulates signal transducing proteins and transcription factors important for cell stress responses, apoptosis, proliferation, cell migration and hormone action. Aberrant overexpression of the founding member of this family, BAG1, occurs in human cancers. In this study, a structure-based approach was used to identify interacting residues in a BAG1–Hsc70 complex. An Hsc70-binding fragment of BAG1 was shown by multidimensional NMR methods to consist of an antiparallel three-helix bundle. NMR chemical shift experiments marked surface residues on the second (α2) and third (α3) helices in the BAG domain that are involved in chaperone binding. Structural predictions were confirmed by site-directed mutagenesis of these residues, resulting in loss of binding of BAG1 to Hsc70 *in vitro* and in cells. Molecular docking of BAG1 to Hsc70 and mutagenesis of Hsc70 marked the molecular surface of the ATPase domain necessary for interaction with BAG1. The results provide a structural basis for understanding the mechanism by which BAG proteins link molecular chaperones and cell signaling pathways.

Both *in vitro* and *in vivo*[1–3], the BAG domain of BAG1 suppresses refolding of peptide substrates by the molecular chaperone Hsc70. This suppression apparently uncouples ATP-hydrolysis from peptide release[4] and acts as an antagonist of the cochaperone protein Hsc70 interacting protein[2,5] (Hip). BAG-family proteins are conserved throughout evolution, with homologs[5] found in humans, mice, *Drosophila, Caenorhabditis elegans, Schizosaccharomyces pombe, Saccharomyces cerevisiae* and plants. The human members of this family include BAG1, BAG2, BAG3 (CAIR-1/Bis), BAG4 (SODD), BAG5 and BAG6 (BAT3/Scythe)[5–10]. In addition to the BAG domain near the C-terminal end of the molecules, BAG proteins also contain diverse N-terminal regions that target cellular locations and interact with other proteins involved in numerous cellular processes[11,12]. It is speculated that BAG proteins serve as bridging molecules that recruit Hsc70 to specific target proteins, thus creating a novel mechanism to alter cell signaling by conformational change rather than post-translational modification[5–8,10].

Structure of BAG domain

NMR experiments indicate that the C-terminal region of BAG1 is highly helical (Fig. 1*a*), consistent with the results of circular dichroism (CD) analysis and secondary structure prediction[13].

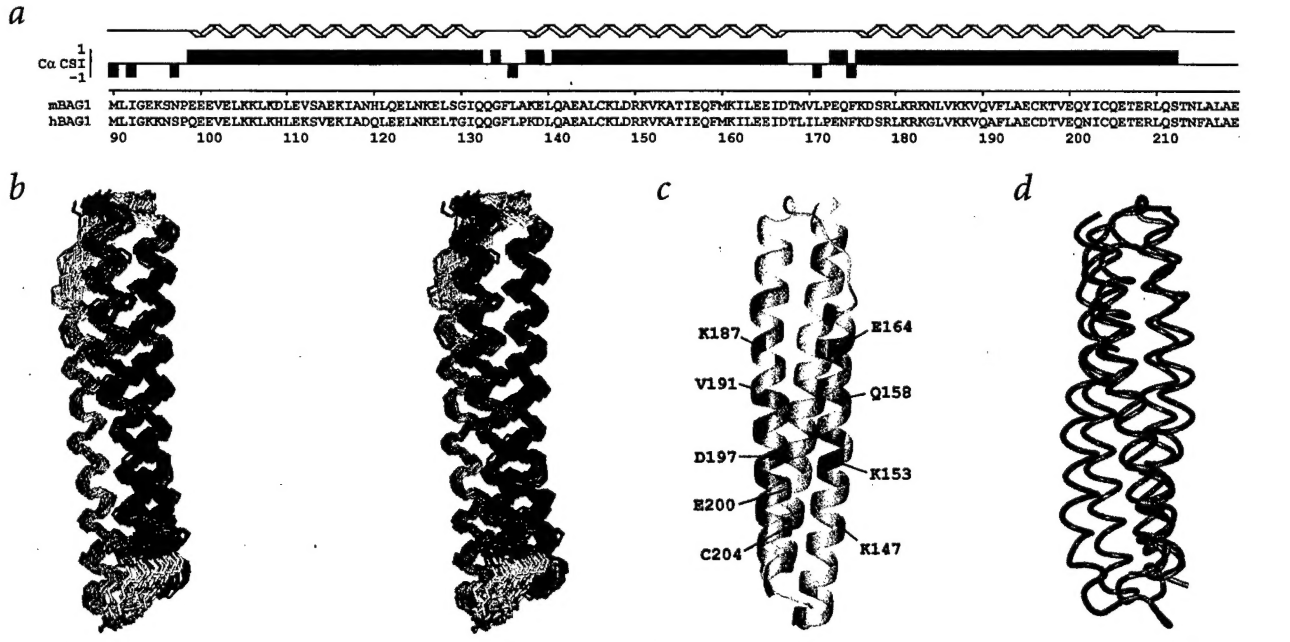

Fig. 1 C-terminal region of BAG1 is a three-helix bundle. ***a***, Cα chemical shift index[33] (CSI) of residues 90–219 of murine BAG1 (mBAG1). The sequence of the murine BAG1 fragment used in this study is indicated to scale below the CSI data and aligned with human BAG1L. The α-helices are defined schematically at the top of the figure. ***b***, Stereo image of superimposed backbone traces of a family of 25 final structures of BAG1 residues 99–210. The first helix (α1) is colored blue, the second one (α2) green and the third one (α3) orange; the connecting loops are white. The images were generated with the program MOLMOL[34]. ***c***, Ribbon representation of BAG1 residues 99–210 colored according to ^{1}H- and ^{15}N-chemical shift changes of the individual residues upon binding of Hsc70 peptide (Asn 256–Cys 267). The color intensity is proportional to the change. Gray indicates residues for which no data are available. Some of the residues with the most pronounced changes are labeled. The model depicted here is rotated 180° relative to the orientation in (*b*). ***d***, Comparison of BAG1 with syntaxin (view as in (*a*)). Tube models of the cα atoms of residues 101–212 of BAG1 (orange) and residues 27–146 of syntaxin (blue; PBD code 1BR0)[23] are superimposed. Note the similar configuration of helices in these two antiparallel three-helix bundles.

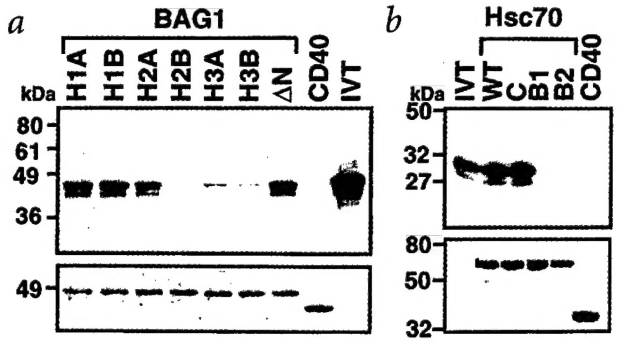

Fig. 2 Mutational analysis of BAG1 binding to Hsc70. ***a***, GST fusion proteins representing wild type BAG1 (WT; residues 90–219) or mutants were tested. Mutants were made by substituting Ala for surface residues in the central region of the elongated BAG1 molecule at residues on adjacent turns of each α-helix. The mutations were: H1A (E115A, K116A, N119A); H1B (E123A, K126A); H2A (D149A, R150A); H2B (E157A, K161A); H3A (Q190A); and H3B (D197A, Q201A). Proteins were immobilized on glutathione-Sepharose beads and tested for *in vitro* binding to *in vitro* translated (IVT) ^{35}S-L-Met-labeled Hsc70 ATPase domain (residues 67–377). GST-CD40 (cytoplasmic domain) was included as a negative control. Samples were analyzed by SDS-PAGE and autoradiography to detect bound Hsc70-ATPase (upper panel) and with Coomassie blue staining to verify loading of equivalent amounts of GST-fusion proteins (lower panel). IVT ^{35}S-Hsc70-ATPase was also loaded directly in the gel for comparisons of the amount of input *versus* bound Hsc70 ATPase. ***b***, GST-fusion proteins representing wild type Hsc70 (WT; residues 1–377) or mutant Hsc70 molecules with substitutions at sites predicted to bind BAG1 were tested. The mutations were: B1 (R258A, R262A), B2 (E283A, D285A) and C (E318A, R322A). The proteins were immobilized on glutathione-Sepharose beads and mixed with *in vitro* translated ^{35}S-L-Met-labeled mouse BAG1. The assay to detect bound BAG1 was performed and monitored as described for (*a*).

The structure of the BAG1 fragment studied here comprises three distinct helical regions — α1 (residues Glu 99–Gln 132), α2 (residues Lys 138–Asp 167) and α3 (residues Lys 176–Leu 210) — arranged in an antiparallel bundle (Fig. 1). Sequence similarities and secondary structure predictions[5,10] suggest that most BAG family proteins may contain a similar three-helix structure.

Interactions of BAG1 with Hsc70

We predicted regions of direct contact between BAG1 and the ATPase domain (residues 1–377) of Hsc70 (ref. 13) based on homology with a complex of GrpE and the ATPase domain of DnaK (the bacterial counterpart of Hsc70)[14]. To test this model experimentally, synthetic peptides representing two helices (residues Ala 54–Pro 63 and Asn 256–Cys 267), which flank the predicted binding crevice in Hsc70, were used in NMR-monitored titrations of BAG1. The latter peptide, Asn 256–Cys 267, induced pronounced chemical shift changes in the central region of α2 and α3 of BAG1 (Fig. 1*c*). These results demonstrated that residues interacting with Hsc70 lie on adjacent turns of α2 and α3 and are located on the same face of the conserved BAG domain.

Sites for mutagenesis in BAG1 were selected based on the results of these chemical shift experiments and used to evaluate the role of residues at predicted interacting surfaces between the BAG domain and Hsc70. In contrast to wild type protein, mutant BAG molecules with Ala substituted at residues Glu 157 and Lys 161 in α2 and Gln 190, Asp 197 and Gln 201 in α3 failed to bind Hsc70 ATPase domain in yeast two hybrid (data not shown) and *in vitro* binding assays (Fig. 2). These mutant molecules retained wild type folding patterns, as verified by CD (data not shown). Consistent with the model, mutant proteins with Ala substituted in the central region of α1 at residues Glu 115, Lys 116, Asn 119 or Lys 126 retained the ability to bind to Hsc70. The contact surfaces suggested by mutagenesis correlate well with those predicted by the chemical shifts (Fig. 1*c*). Thus, a region of BAG1 that is essential for binding to the ATPase domain of Hsc70 has been defined.

To test the predicted molecular surface of the ATPase domain of Hsc70 contacting BAG1, the BAG domain was docked interactively to the atomic model of Hsc70 (ref. 15). Our previous studies defined the minimal BAG1-binding region (residues 186–377) of Hsc70 (ref. 1). This region lacks the N-terminal lobe of the bi-lobed ATPase domain. Docking strategies optimized geometric and electrostatic charge complementarity of the central part of the electronegative BAG domain with the C-terminal lobe of the ATPase domain. Residues on the surface of the ATPase domain oriented to contact critical residues in the BAG domain were selected as sites for Ala substitution mutagenesis, including Arg 258, Arg 262, Glu 283 and Asp 285. Unlike the wild type ATPase domain, all of these mutants failed to bind BAG1 when tested in yeast two hybrid (data not shown) and *in vitro* binding assays (Fig. 2). In contrast, substitution of Ala for residues Glu 318 and Arg 322 on the opposite face of this lobe did not inhibit interaction with BAG1. These results define a surface region on Hsc70 that is the site for binding BAG1. This surface differs from that predicted by homology modeling[13] because the contact surface involves only one lobe of the ATPase domain.

The BAG1 and Hsc70 recognition surfaces predicted by these studies are shown in Fig. 3. The interacting region in Hsc70 is located on one face of the C-terminal lobe adjacent to a deep crevice in the bi-lobed ATPase domain. ATP binds at the bottom of this crevice[15,16]. Members of the Hsc70/Hsp70 heat shock family interact with linear peptide folding intermediates. This interaction is mediated by cycles of ATP binding and hydrolysis followed by ADP/ATP exchange and peptide release. The prokaryotic homologue of BAG1, GrpE, binds to both lobes of

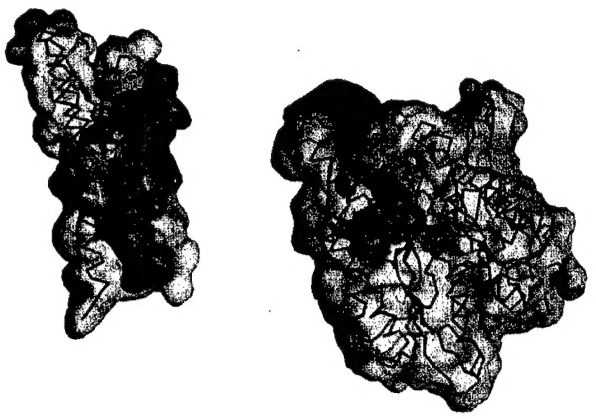

Fig. 3 Contact regions of the BAG1–Hsc70 ATPase complex. The proteins are represented by red Cα traces and transparent surfaces of BAG1 on the left and Hsc70 ATPase domain[15] on the right. An ADP molecule that binds in the cleft between the two lobes of the ATPase domain is shown in red as van der Waal's spheres. The complex has been 'opened up' by a 180° rotation of BAG1 to reveal the contact surfaces predicted from mutagenesis and molecular docking. The sites of mutation that abolish binding are colored yellow and adjacent contact sites suggested from molecular docking are colored cyan. This image was produced with the program SPOCK[35].

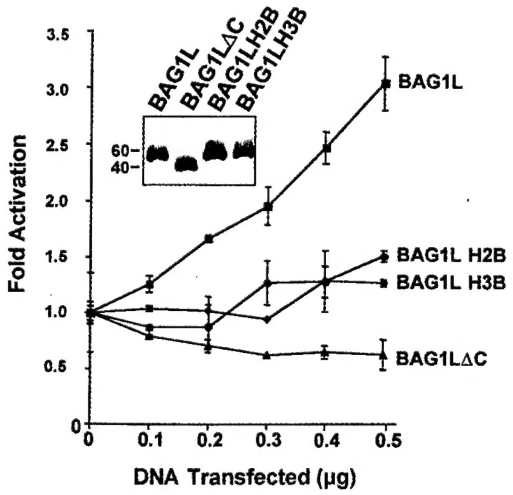

Fig. 4 BAG domain is necessary for transactivation of AR by BAG1L. Mutant BAG1L proteins containing Ala substitutions within the BAG domain that ablated Hsc70 binding *in vitro* and a BAG1L truncation mutant lacking α3 of the BAG domain (ΔC) were tested. Mutant proteins are H2B (E157A, K161A in α2) and H3B (D197A, Q201A in α3). (These sites are numbered 283, 287, 323 and 327 in human BAG1L). Cos-7 cells were transfected with fixed amounts of pSG5-AR, pLCl, pCMV-βGal and increasing amounts of pcDNA3-BAG1L, wild type and mutants. Cell extracts were prepared and assayed for CAT and β-galactosidase activity at 40 h after transfection. Data are expressed as fold transactivation relative to cells transfected with reporter gene alone (mean ± S.E.; n = 2).

the Hsp70 homolog DnaK ATPase domain[14,17] and stimulates dissociation of ADP from DnaK by inducing a conformational change in the nucleotide-binding cleft, including the N-terminal lobe of the domain[14]. BAG1 is also known to promote dissociation of ADP[2], but the mechanism may differ and remains to be elucidated. In contrast to GrpE, our results suggest that contact with the N-terminal lobe of the ATPase domain may not be critical for binding of BAG1.

Analysis of the BAG1–Hsc70 contacts *in vivo*

The significance of the structural analyses was tested in intact cells, comparing the bioactivity of wild type and mutant BAG1 proteins. At least four isoforms of BAG1 are produced in many cells, including BAG1 and a longer isoform BAG1L. The unique N-terminal region of BAG1L contains both SV40 large T-like and nucleoplasmin-like candidate nuclear localization signals, which target BAG1L to the nucleus[5]. BAG1L has been shown to form complexes with and coactivate steroid hormone receptors[18–22], such as androgen receptor[11] (AR), in a manner requiring the BAG domain-containing C-terminal region of BAG1. We therefore engineered the same mutations described above for BAG1 into plasmids encoding the BAG1L protein and tested them for the ability to enhance the transcriptional activity of AR. As shown in Fig. 4, wild type BAG1L caused a concentration-dependent increase in AR-mediated transactivation of a reporter gene promoter containing androgen response elements (AREs)[11]. However, mutant BAG1L proteins containing the same Ala substitutions within the BAG domain that ablated Hsc70 binding demonstrated diminished capacity to affect AR transactivation in these assays. Immunoblot analysis confirmed that the differences in activity of wild type and mutant BAG1L proteins were not attributable to differences in levels of expression. We conclude therefore that the contact residues required for interaction of BAG1 with Hsc70 are critical for the function of this protein in cells.

Table 1 Structural statistics for BAG1

Ensemble	
R.m.s. deviation from experimental restraints[1]	
NOE distance restraints (Å)	0.030 ± 0.001
Dihedral angle restraints (°)	0.42 ± 0.03
R.m.s. deviation from idealized geometry	
Bonds (Å)	0.0031 ±0 .0002
Angles (°)	0.46 ± 0.01
Impropers (°)	0.36 ± 0.01
R.m.s. deviation from mean coordinates[2]	
Backbone atoms (N, Cα, C) (Å)	1.1 ± 0.4
Heavy atoms (Å)	1.6 ± 0.3
Ramachandran plot[2]	
Most favored regions (%)	94.2
Additional allowed regions (%)	4.4
Generously allowed regions (%)	1.0
Disallowed regions (%)	0.4

[1]No NOE distance and dihedral angle restraint was violated by more than 0.5 Å or 5°, respectively, in any of the structures.
[2]Residues 99–210; mean coordinates were obtained by averaging coordinates of the 25 calculated structures, which were first superposed using backbone atoms (N, Cα, C) of residues 99–210.

Structural similarity of BAG1 and syntaxin

BAG-family members bind to a variety of intracellular proteins and regulate diverse cellular processes including cell division, survival and migration. Members of this family link cell signaling to molecular chaperones, altering cellular pathways by changing protein conformation. Using the BAG1 structure, the database of known three-dimensional structures was searched with the program DALI[23] for similar folding patterns. A striking similarity (see Fig. 1*d*) was noted with the syntaxin protein[24,25]. Syntaxins are members of a large family of related proteins that are key components in protein trafficking. The N-terminal region of syntaxin is an independently folded antiparallel three-helix bundle that participates in protein–protein interactions. A hydrophobic groove between helices 2 and 3 on the surface of syntaxin lined by conserved residues can accommodate interactions with another helix in a distal portion of the molecule. This helix is 'swapped' when the molecule associates with SNARE complexes at the plasma membrane[25]. The structural similarities with BAG1 suggest that BAG domains may participate in similar protein–protein interactions, adapting to molecular exchange of α-helices. Future studies may reveal molecular interfaces in BAG-binding proteins that are complementary with BAG domains, and which may modulate Hsc70/BAG1 interactions.

Note added in proof: While this manuscript was under review, a study of the BAG1-interacting surface of Hsc70 ATPase domain using peptide libraries was reported[26]. Also, the crystal structure of BAG1 in complex with nucleotide-free Hsc70 ATPase domain was published[27]. BAG1 residues that interact with the ATPase domain in the crystal structure are located on α2 and α3, as suggested by chemical shift experiments in the present study. The contact surfaces colored here in Fig. 3 include most of the residues seen at the interface in the crystal structure, with the exception of residues in the N-terminal lobe of the ATPase domain. For direct comparison with the crystal structure, the reader should add 55 to the BAG1 sequence number used in our NMR study.

Methods

NMR spectroscopy. A recombinant fragment containing residues 90–219 of murine BAG1 was purified essentially as described for a longer construct[13]. NMR samples contained 1–2 mM ^{15}N-, $^{13}C/^{15}N$- or $^{2}H/^{15}N$-labeled protein in 10 mM potassium phosphate buffer, pH 7.2, 25 mM KCl, 1 mM DTT and 1 mM EDTA in 90% H_2O/10% D_2O. Spectra were acquired at 37 °C on a Bruker 500MHz and Varian 500, 600 and 750 MHz spectrometers. The data were processed and analyzed with Felix 98.0 (Molecular Simulations, Inc.). ^{1}H, ^{15}N and ^{13}C assignments were established based on CBCA(CO)NH, HNCACB, HNCO, CBCACOHA, C(CO)NH, H(CCO)NH, HCCH-TOCSY (HB)CB(CGCD)HD, $^{13}C/^{15}N$-edited NOESY, 4D ^{15}N-edited NOESY and HNCACB optimized for Asn and Gln NH_2 groups. Distance restraints were obtained from 3D ^{15}N-edited NOESY and 3D $^{13}C/^{15}N$-edited NOESY. ϕ and ψ dihedral angle restraints were generated with TALOS[28]. Structures were calculated with the torsion angle dynamics simulated annealing protocol implemented in CNS 1.0 (ref. 29) using restraints for 1,567 interproton distances (98 long range, $5 \leq |i - j|$, 267 medium range, $2 \leq |i - j| \leq 4$, 363 sequential and 839 intraresidual), 168 hydrogen bond distances, and 88 ϕ and 86 ψ dihedral angles. Statistics for 25 final structures are summarized in Table 1.

Chemical shift experiments and computer modeling. Helix-nucleated peptides representing helical regions of the ATPase domain of human Hsc70 predicted to bind to BAG1 were synthesized using a protocol described in ref. 30. Helix-nucleation was introduced to stabilize the helical nature of the synthetic peptides, corresponding with the known conformation in the protein[15,16]. The CD spectra for the nucleated peptides were consistent with enhanced helicity[30] relative to control linear peptides. ^{1}H-^{15}N HSQC spectra were recorded for ^{15}N-labeled BAG1 solutions containing varying concentrations of peptide. Most pronounced resonance shifts of BAG1 amides were noted and mapped onto the structure. To model the binding surfaces in a BAG1–Hsc70 complex, docking of BAG1 to Hsc70 ATPase domain (PDB accession number 1NGA)[15] was performed manually to visually optimize geometric fit and intermolecular distance between contact residues identified from the HSQC experiments and surface residues on the ATPase domain. Docking was directed to contact regions predicted from homology modeling[13].

Plasmids. Mutations in BAG1 were generated by two-step PCR-based mutagenesis using a full length murine BAG1 cDNA (SN 245–9) (ref. 31) as template. Products were purified by QiaQuick gel extraction kit (Qiagen), subcloned into the TOPO TA vector (Invitrogen) and sequenced. The fragments were subcloned into either pGEX4T-1 for expression as mutant GST-fusion proteins or into pJG4-5 for yeast two-hybrid assays. Mutations in Hsc70 were made by the same methods, using a cDNA encoding the ATPase domain[1].

Protein interaction assays. For yeast two hybrid assays[32], the yeast EGY48 strain was cotransformed with pJG4-5 plasmids encoding wild type or mutant BAG1/B42 transactivation domain fusion proteins, pGilda plasmids encoding Hsc70 ATPase/LexA DNA-binding domain fusion proteins and a β-galactosidase reporter gene (pSH18-34 or pRB1840).

For *in vitro* binding assays, DH5α cells were transformed with pGEX4T-1 plasmids encoding wild type or mutant GST-BAG1 fusion proteins. After induction at room temperature with 0.1 mM IPTG, cells were lysed by sonication, and expressed proteins were isolated from lysates by affinity purification on glutathione-Sepharose (Pharmacia). *In vitro* translated ^{35}S-methionine labeled Hsc70 ATPase domain[1] (1 μl) was mixed with 5 μg immobilized mutant GST-BAG1 fusion proteins, along with negative controls. Alternatively, GST-Hsc70 ATPase domain was produced and immobilized on glutathione-Sepharose and then mixed with *in vitro*-translated ^{35}S-BAG1 or negative control proteins. After 1 h incubation at 4 °C, beads were washed extensively and then subjected to SDS-PAGE electrophoresis to detect bound protein.

Reporter gene assays. Cos-7 cells (3×10^4 cells/well in 12-well plates) were transfected as described[11] with fixed amounts of 0.06 μg of pSG5-AR, 0.5 μg of pLCl, 0.04 μg of pCMV-βGal and increasing amounts of pcDNA3-BAG1L, wild type and mutant plasmids. Total DNA was maintained at 1.1 μg by the addition of empty plasmid. After 30 hrs, cells were stimulated with 1 nM R1881 for 10 h. Cell extracts were prepared and assayed for CAT and β-galactosidase activity at 40 h after transfection, expressing data as a ratio of CAT:β-galactosidase.

Coordinates. The coordinates have been deposited in the Protein Data Bank with accession code 1I6Z.

Acknowledgments

This research was performed in part at the Environmental Molecular Sciences Laboratory (a national scientific user facility sponsored by the U.S. DOE Office of Biological and Environmental Research) located at Pacific Northwest National Laboratory, operated by Battelle for the DOE. The authors are grateful to the staff at the HFMR facility at EMSL for useful discussions. We also thank K. Baker for protein purification and characterization, X. Jia for assistance with the Varian 500 MHz spectrometer and P. Crescenti for manuscript preparation. This work was funded by the National Institutes of Health NCI, NIHLB, USAMRDC Breast Cancer Program, the University of California Breast Cancer Research Program, the State of California Cancer Research Program, the Susan G. Komen Breast Cancer Foundation, the Human Frontier Science Program and CaPCURE.

Correspondence should be addressed to K.R.E. *email: ely@burnham.org*

Received 30 November, 2000; accepted 2 March, 2001.

1. Takayama, S. *et al. EMBO J.* **16**, 4887–4896 (1997).
2. Höhfeld, J. & Jentsch, S. *EMBO J.* **16**, 6209–6216 (1997).
3. Nollen, E.A.A., Brunsting, J.F., Song, J., Kampinga, H.H. & Morimoto, R.I. *Mol. Cell. Biol.* **20**, 1083–1088 (2000).
4. Bimston, D. *et al. EMBO J.* **17**, 6871–6878 (1998).
5. Takayama, S., Zhihua, X. & Reed, J.C. *J. Biol. Chem.* **274**, 781–786 (1999).
6. Doong, H. *et al. Oncogene* **19**, 4385–4395 (2000).
7. Lee, J. H. *et al. Oncogene* **18**, 6183–6190 (1999).
8. Jiang, Y., Woronicz, J. D., Liu, W. & Goeddel, D.V. *Science* **283**, 543–546 (1999).
9. Thress, K., Song, J., Morimoto, R.I. & Kornbluth, L. *EMBO J.* **20**,1033–1041 (2001).
10. Tschopp, J, Martinon, F. & Hofmann, K. *Curr. Biol. R* **9**, 381–384 (1999).
11. Froesch, B.A., Takayama, S. & Reed, J.C. *J. Biol. Chem.* **273**, 11660–11666 (1998).
12. Crocoll, A., Schneikert, J., Hubner, S., Martin, E. & Cato, A. C. *Kidney Int.* **57**, 1265–1269 (2000).
13. Stuart, J.K. *et al. J. Biol. Chem.* **273**, 22506–22514 (1998).
14. Harrison, C.J., Hayer-Hartl, M., Di Liberto, M., Hartl, F.-U. & Kuriyan, J. *Science* **276**, 431–435 (1997).
15. Flaherty, K.M., Wilbanks, S.M., DeLuca-Flaherty, C. & McKay, D.B. *J. Biol. Chem.* **269**, 12899–12907 (1994).
16. Flaherty, K.M., DeLuca-Flaherty, C. & McKay, D.B. *Nature* **346**, 623–628 (1990).
17. Liberrek, K., Marszalek, J., Ang, D., Georgopoulos, C. & Zylicz, M. *Proc. Natl. Acad. Sci. USA* **88**, 2874–2878 (1991).
18. Zeiner, M. & Gehring, U. *Proc. Natl. Acad. Sci. USA* **92**, 11465–11469 (1995).
19. Liu, R. *et al. J. Biol. Chem.* **273**, 16985–16992 (1998).
20. Schneikert, J., Hübner, S., Martin, E. & Cato, A.C.B. *J. Cell Biol.* **146**, 929–940 (1999).
21. Knee, D.A., Froesch, B.A., Nuber, U., Takayama, S. & Reed, J.C. *J. Biol. Chem.* **in the press** (2001).
22. Schneikert, J. *et al. EMBO J.* **19**, 6508–6516 (2000).
23. Holm, L. & Sander, C. *J. Mol. Biol.* **233**, 123–138 (1993).
24. Fernandez, I. *et al. Cell* **94**, 841–849 (1998).
25. Misura, K.M.S., Scheller, R.H. & Weis, W.I. *Nature* **404**, 355–362 (2000).
26. Petersen, G., Hahn, C. & Gehring. *J. Biol. Chem.* **in the press** (2001).
27. Sondermann, H. *et al. Science* **291**, 1553–1557 (2001).
28. Cornilescu, G., Delaglio, F. & Bax, A. *J. Biomol. NMR* **13**, 289–302 (1999).
29. Brünger, A.T. *et al. Acta. Crystallogr. D* **54**, 905–921 (1998).
30. Cabezas, E. & Satterthwait, A.C. *J. Am. Chem. Soc.* **121**, 3862–3875 (1999).
31. Takayama, S. *et al. Cell* **80**, 279–284 (1995).
32. Golemis, E.A., Gyuris, J. & Brent, R. In *Current protocols in molecular biology* (eds, Asbubel, F.M. & Struhl, K. J.) 1–17 (Wiley & Sons, Inc. New York; 1994).
33. Wishart, D.S. & Sykes B.D. *J. Biomol. NMR* **4**, 171–180 (1994).
34. Koradi, R., Billeter, M. & Wüthrich, K. *J. Mol. Graph.* **14**, 51–55 (1996).
35. Christopher, J.A. *The structural properties observation and calculation kit* (The Center for Macromolecular Design, Texas A&M University, College Station, Texas; 1998).